A COMPARISON OF THERMAL BEHAVIOR OF SELECTED BIOMASS IN THAILAND FOR EFFECTIVE ENERGY UTILIZATION UNDER THERMOGRAVIMETRIC ANALYSIS

MR. WITCHAYA PRUKSAKIT
ID: 55300700526

A THESIS SUBMITTED AS A PART OF THE REQUIREMENTS
FOR THE DEGREE OF MASTER OF ENGINEERING
IN ENERGY TECHNOLOGY AND MANAGEMENT

THE JOINT GRADUATE SCHOOL OF ENERGY AND ENVIRONMENT
AT KING MONGKUT'S UNIVERSITY OF TECHNOLOGY THONBURI

2 ND SEMESTER 2013

A Comparison of Thermal Behavior of Selected Biomass in Thailand for Effective Energy Utilization under Thermogravimetric Analysis

Mr. Witchaya Pruksakit
ID: 55300700526

A Thesis Submitted as a Part of the Requirements
for the Degree of Master of Engineering
in Energy Technology and Management

The Joint Graduate School of Energy and Environment
at King Mongkut's University of Technology Thonburi

2nd Semester 2013

Thesis Committee

(Asst.Prof.Dr. Suthum Patumsawad)	Advisor
(Assoc.Prof.Dr. Suneerat Fukuda)	Member
(Dr. Boonrod Sajjakulnukit)	Member
(Assoc.Prof.Dr. Suvit Tia)	External examiner

Thesis Title: A Comparison of Thermal Behavior of Selected Biomass in Thailand for Effective Energy Utilization under Thermogravimetric Analysis.

Student's name, organization and telephone/fax numbers/email

Mr. Witchaya Pruksakit
The Joint Graduate School of Energy and Environment (JGSEE)
King Mongkut's University of Technology Thonburi (KMUTT)
126 PrachaUthit Rd., Bangmod, Tungkru, Bangkok 10140 Thailand
Telephone: 0-84872-0372
Email: witchaya.pruksakit@hotmail.com

Supervisor's name, organization and telephone/fax numbers/email

Asst. Prof. Dr. Suthum Patumsawad
Department of Mechanical and Aerospace Engineering
King Mongkut's University of Technology North Bangkok (KMUTNB)
1518Pracharat 1 Road, Wongsawang, Bangsue,Bangkok 10800 Thailand
Telephone: 02-913-2500 Ext.8322, 8303
Email: stt@kmutnb.ac.th

Topic: A Comparison of Thermal Behavior of Selected Biomass in Thailand for Effective Energy Utilization under Thermogravimetric Analysis.

Name of student: Mr. Witchaya Pruksakit **Student ID:** 55300700526
Name of Supervisor: Asst. Prof. Dr. Suthum Patumsawad

ABSTRACT

Due to the decrease of primary energy sources especially fossil fuels, and concerns about CO_2 emissions, biomass is currently being widely used for renewable energy sources. However, uncertainty of biomass characteristic plays significant problem in technology development and operation design.

Generally, biomass has high oxygen and low sulfur contain in chemical composition. Heating value of biomass of biomass vary for 10-23 MJ/kg depend on type of biomass. During thermal process, biomass release high volatile matter when compare with coal. Biomass has high chlorine content which depends on local of plant case high corrosion problem at high temperature. Differences in alkaline/alkaline earth deposit in biomass which case of slagging and fouling problem can be primary assessment by slagging index. Other thing that should be concerned when used biomass for thermal conversion process is degradation behavior of biomass. Different type of biomass contain different chemical structure deposition is major effect for degradation behavior of biomass.

In this thesis, Thai biomass properties (i.e. HHV, ultimate analysis, proximate analysis etc.), thermal behavior of biomass and kinetic of reaction under TGA (pyrolysis and combustion) are present that will support decision making in terms of energy conversion technology selection and operating condition setting.

ACKNOWLEDGEMENTS

I would like to express my sincere thanks to my thesis advisor, Asst.Prof.Dr. Suthum Patumsawad for his kindness, and assistance throughout the course of this research.

I am very grateful to the member of my thesis committee, Assoc.Prof.Dr. Suneerat Fukuda, Dr. Boonrod Sajjakulnukit and the external examiner, Assoc.Prof.Dr. Suvit Tia for invaluable suggestions.

Much appreciation to the Joint Graduate School of Energy and Environment, King Mongkut's University of Technology Thonburi for the scholarship and financial supports.

Finally, I would like to give special thanks to my parents and my friends for all their support throughout the period of this research.

CONTENTS

CONTENTS (Cont')

CONTENTS (Cont')

LIST OF TABLES

LIST OF FIGURE

LIST OF FIGURE

NOMENCLATURE

A	Pre-exponential factor
ASTM	American Society for Testing and Materials
α	Fraction of starting material consumed $\alpha = \frac{m_0 - m}{m_0 - m_f}$
DTG	Derivative thermogravimetry
ρ	Density
E	Activation energy, kJ/mol
ER or ϕ	Equivalence ratio
Φ	Heating rate, ^{o}C/min
ΔH	Enthalpy change, MJ/kmol
k	Rate constant of reaction
n	Order of reaction
min	Minute
m_0	Initial mass of sample
m_f	Final mass of sample
R	Ideal gas constant.
s	Second
t	Time, s
T	Temperature, K (Kelvin = ^{o}C + 273)
TG	Thermogravimetry
%wt	Percent by weight

CHAPTER 1
INTRODUCTION

1.1 Rationale

Nowadays, due to the expansion of energy consumption and its increasing trend, in contrast to fossil fuel which is the primary energy source for power generation, has decreased continuously. Moreover, the aspects of environment and global warming have been concerned recently past. The concept of renewable energy has played a significant role and has been increasing wide spread such as solar energy for thermal process, wind energy and hydro energy for power generation. One of them that used widely is biomass which has long been known. The following Fig 1.1 shows the main ways of energy exploitation of biomass.

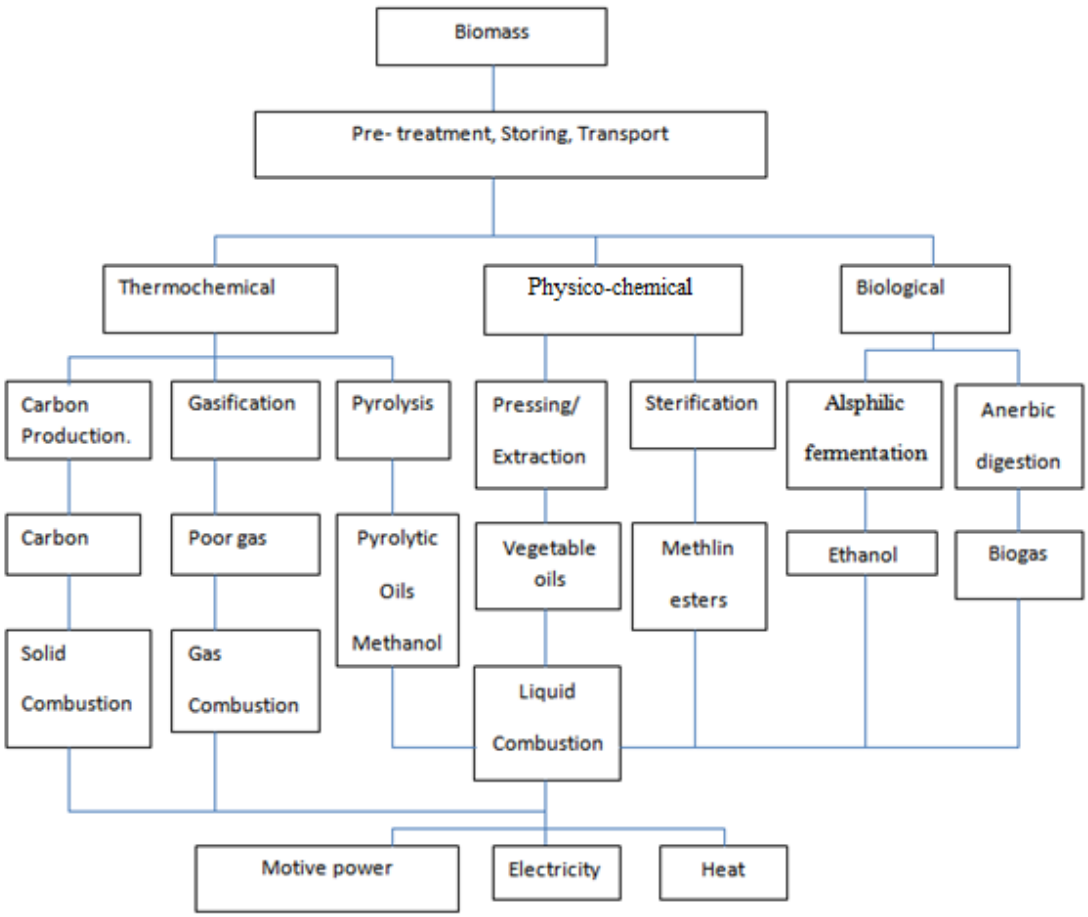

Figure 1.1 Main ways of energetic exploitation of biomass.[1]

The main advantages that attract to use biomass for renewable energy are, firstly, it can provide various forms of energy (heat, electricity, transport fuels). Secondly, it is the largest renewable energy source that used for today and lastly it can reduce carbon emission when comparing to fossil fuel. In Thailand, solid fuels from biomass are widely used in field of thermochemical process for power generation. However, there are some limitations and obstacles in the development of biomass technologies for power generation. For example, it has varied of compositions and heating value in biomass. Each type of biomass has its own chemical composition, chemical structure and heating values (10-23 MJ/kg fuels). [2-4]

In additional chemical composition and heating value, thermal degradation process (drying, devolatilezation and char oxidation) of solid fuels play significant effect for energy utilization from biomass.

Sutiratana [5] performed an overview of the biomass utilization in Thailand and discussed the problem of biomass energy utilization in Thailand. One of limitation for biomass technology developed is lack of information in available new and renewable source of energy (NRSE) technology and applications.

As mentioned above, it shows some knowledge of various types of biomass under thermal degradation in many conditions. It is one of critical to develop and improve power generation technology to the target of optimum efficiency, economy and environmental protection.

1.2 Research Objectives

Various type of biomass required different suitable operational conditions for efficiency energy utilization of biofuels. Chemical composition, element deposition heating value degradation behavior etc. are database to common used set operation condition. The aims of this research follow as:

- Study thermal behavior of biomass under pyrolysis and combustion process by TGA.

- Establish a database of Thai biomass fuels or feedstock.

1.3 Scope of Work

- Study thermal behavior of Thai agricultural residuals under pyrolysis and oxidation process under TGA.

- Apply kinetic parameters to describe thermal behavior of biomass during thermal process.

1.3.3 Collect properties of Thai biomass which common used in field of energy conversion.

1.4 Thesis Outline

The detailed descriptions of biomass characteristics, TGA experiment and kinetic of reaction are combined and summarized in the following chapters. Chapter 2 describes biomass properties and thermal conversion of biomass. Chapter 3 describes theory of TGA and principle of kinetic of reaction from TGA. Chapter 4 describes methodology in this thesis. Chapter 5 discuss about Thai biomass properties and primary assessment of biomass for energy utilization. Chapter 6 summarize thermal behaviors of biomass at low heating rate and kinetic of reaction. Conclusion and future of this work are showed in Chapter 7.

CHAPTER 2
BIOMASS PROPERTIES AND THERMAL CONVERSION

The design and operation of biomass combustion systems rely substantially on several biomass characteristics, namely, heating value, moisture, ash content, density and elemental composition.[3] The high moisture and ash contents in biomass fuels can cause ignition and combustion problems. Ash deposition in biomass causes of fireside corrosion, fouling and slagging problems, because of the lower heating values of biomass accompanied by flame stability problems.[2] The uses of each biomass fuel type appear different issues. The problems require proper management to the process used. In this chapter present biomass properties such as proximate analysis, ultimate analysis, heating value etc. and thermal conversion process of biomass.

2.1 Biomass properties

Various types of biomass have different properties and characteristics such as heating value, moisture content, ash content, etc. ASTM standard for analytical biomass properties are shown in Table 2.1

Table 2.1 Method of biomass fuel analysis [6]

Property	Analytical method
Heating value	ASTM D2015
Particle size distribution	ASTM E828
Bulk density	ASTM E873
Proximate composition	
Moisture	ASTM E871
Ash	ASTM E830 (575^{o}C)
Volatiles	ASTM D1102 (600 ^{o}C)
Fixed carbon	ASTM E872/E897 (by difference)
Ultimate elemental	
C,H	ASTM E777
N	ASTM E778
S	ASTM E775
Cl	ASTM E776

2.1.1 Proximate analysis

The proximate analysis is a determination of fixed carbon, volatile matter, and ash content of the sample. The carbon content determined through this method is not the actual carbon content, but only the nonvolatile part of carbon content, as some of the carbon present in biomass also escapes along with the volatiles. [7]

The volatile matter content in biomass (d.b.) varies in the interval of 48–86%.

The fixed carbon content (d.b.) in biomass varies in the interval of 1–38%.

The ash yield (d.b.) determined at 550–600 ^{o}C in air for biomass varies in the interval of 0.1–46%. [8]

2.1.2 Ultimate analysis

The ultimate analysis provides the composition of elemental carbon, hydrogen, oxygen, nitrogen and sulfur for a combustible sample. [7]

- Carbon (C). The C content in biomass varies in the interval of 42–71% (db.)
- Oxygen (O). The O content in biomass is mostly calculated by difference and varies in the interval of 16–49% (db.)
- Hydrogen (H). The H content in biomass varies in the interval of 3–11% (db.)
- Nitrogen (N). The N content in biomass varies in the interval of 0.1–12% (db.)
- Sulphur (S). The S content in biomass varies in the interval of 0.01–2.3% (db.)
- Chlorine (Cl). The Cl content in biomass varies in the interval of 0.01–0.9% (db.) [8]

2.1.3 Moisture content in biomass.

Water content in biomass as measured varies in the interval of 3% up to 200 % on a dry basis depending on the species of biomass. Water contain in Biomass can be classify into two types [9]: Bond water and free water.

Bound water is found in the cell wall and is believed to be hydrogen bounded to the hydroxyl groups of primarily the cellulose and hemi-cellulose, and to a lesser extent, also to hydroxyl groups of lignin.

Free water exists as liquid in the lumens or voids of biomass. No hydrogen bonding therefore is held only by weak capillary forces. Free water can not affect to swelling or physical properties change because call wall are already saturated.

During thermal conversion process water content is important because it can leave the system as either vapor or liquid phase. Wet biomass needs longer residence time within the furnace, case of incomplete combustion (in combustion process) and can lead to the

creation of tar or creosote for eventual blockages or fire. High moisture content case of low heating value which required high biomass value for feed into bed case of cost for storage and transportation increased.

2.1.4 Ash

Ash is the impurities or non-combustion content in biomass. Fouling, slagging and fireside corrosion are associated with ash effect during a thermal process. Fouling is defined as fly ash quenched in heat recovery when temperature below malting point. Slagging defined as ash malt at surface of furnace and heat-transfer surface. Ash forming matters in biomass fuels can be grouped into four types [10]:

(1) Water soluble salts,

(2) Elements associated with the inorganic materials of the biomass,

(3) Minerals included in the fuel structure,

(4) Inorganic material added to biomass from extraneous sources.

Element concentrations in biomass consist Si, Al, Fe, Ca, Mg, Mn, Na, K, P, S and Cl. Bryers (1995), [11] overview about ash-forming in biomass. Sulfer (S) contain in biomass by two different forms. Once is sulfate and another one is organic sulfur. Chlorine (Cl) contain in biomass in chlorine ion form. Concentration of chlorine depends on soil condition rather than physiology of plant. Phosphorus (P) Contain in biomass in oxidized from or incorporate in organic structure. Silicon (Si) in biomass appears as a hydrate oxide usually in an amorphous form. Potassium (K) occur as a univalent ion ($^{+}$K). Calcium (Ca) occurs in the axoplasm and can be exchangeable form the cell walls. Aluminum (Al) concentrations in biomass exceed 300 ppm on dry basis. Iron (Fe) is common concentrate in leaves.

Ash release and formation can be creating operational problems in a combustion system such as [10]:

(1) formation of slag and aggregates caused by fused or partly fused ash at high temperature in combustion appliances,

(2) fouling and slagging deposits on heat exchange components surfaces due to condensation of alkali salts and binding of fine ash particles carried by the flue gas,

(3) gas and deposits induced fireside corrosion and accelerated metal wastage of furnace and boiler components,

(4) reduced performance of flue gas cleaning equipment due to formation of aerosols and fine particulate matters.

2.1.4.1 Ash behavior during thermal process

During combustion process, ash forming matters may occur including [10]:

(1) release and volatilization of inorganic species from burning fuel and char particles,

(2) interaction of inorganic elements with formation of salts (e.g. chlorides, sulphates, hydroxides and phosphates) in liquid and gas phases,

(3) interactions between solid phase particles and released volatile inorganic species,

(4) fusion or partial fusion of low melting ash components (i.e. alkali silicates) with formation of a molten phase,

(5) sintering of unburned char residues and inert solid ash residues due to presence of molten phase.

For biomass, potassium is the major alkali element of concern. By contrast, sodium is the most troublesome alkali component for most coal-fired systems. Potassium and calcium are important in the formation of sulfate deposits on boiler surfaces. Pure in silica are low rick slagging and fouling problem because high melting point. Silica in combination with alkali and alkaline earth metals, however, especially with the readily volatilized forms of potassium present in biomass, can lead to the formation of low melting point compounds which readily slag and foul at normal biomass boiler furnace temperatures. Chlorine can be an important facilitator in fouling, leading to the condensation of alkali chlorides on heat transfer surfaces in the boiler, and promoting the development of alkali sulfates. Chlorine may be an important element in the vaporization of alkali species, leading to the formation of more severe deposits. Sodium and aluminum, which are not normally found in inherently high concentrations, may be introduced as soil or through prior processing operations and may also influence the fouling behavior. Sulfur is also a major player in ash deposition. Sulfur, in essentially all of its forms, quantitatively oxidizes during combustion. Some of it then reacts with alkali materials to form sulfates. Alkali sulfates are unstable at typical combustion temperatures of 900 ^{o}C. These sulfates are found condensed on fly ash or deposited on watenvalls parallel to the flow of gas. For most biomass fuels, the elements silicon, potassium, calcium, chlorine, sulfur, and to some extent, phosphorus, appear to be the principal elements involved in the fouling of boiler surfaces. [12]

Shao et al. (2012) [13] reviewed biomass characteristics on ash deposition during combustion. Biomass contains high potassium (K) but lower sulfur compare with coal. In herbaceous plants such as straw have high chlorine (Cl) concentrations very common. The element in the form of water soluble inorganic salts easily volatilized during the combustion, leading to high mobility for alkali materials. The highly active alkali/alkaline metals and chlorine contents may easily form vapor phase chloride compounds/ions and easy to volatilization to the vapor phase chloride compounds/ions because of low melting point (< 800 ^{o}C) of these chloride compounds. Silicates deposition in biomass could melt at 800–900 ^{o}C. The produced alkali silicates and mixed alkali and/or calcium chlorides/sulfates tend to deposit on reactor walls or heat exchangers surfaces, causing fouling/corrosion even at a low fusion temperature (<700 °C).

Sonobe and Worasuwannarak (2008) [14] performed Kinetic analyses of biomass pyrolysis using the distributed activation energy model. The results showed catalytic effects of alkali and alkaline earth metals during the pyrolysis play a major role in the variation of activation energy among the different biomass species.

Vamvuka et al. (2006) [15] investigated effect of mineral matter on the physical and combustion under TGA. They conclude mineral matter such as calcium, magnesium, potassium and silicon minerals acted as inert materials, inhibiting the pyrolysis and combustion rates of the samples.

2.1.4.2 Melting and tendencies of biomass fuel ashes

Groups of Melting and tendencies of biomass ashes can be classified as follows [12];

- High silica and alkalis rich ashes, with low melting temperatures.
- Low silica and high calcium ashes, with high melting temperatures.
- Phosphorous-rich biomass/waste fuels. Ash melting behavior of phosphorous rich solid fuels is very complex and depends on the concentrations of other elements. Depending on the fuel ash chemistry the low melting K-rich phosphates and higher melting K-Ca/Mg phosphates can be formed.

2.1.4.3 Slagging/Fouling Predictive Methods

There are two main ways to estimate ash forming tendencies during a thermal process. First is the direct determination of melting temperature from laboratory furnace. This method observe ash sample change its shape when temperature increase. Standard

involve this method is ASTM D1857, DIN 15730, ISO 54. This method can be used for find significant temperature point follow as [16]:

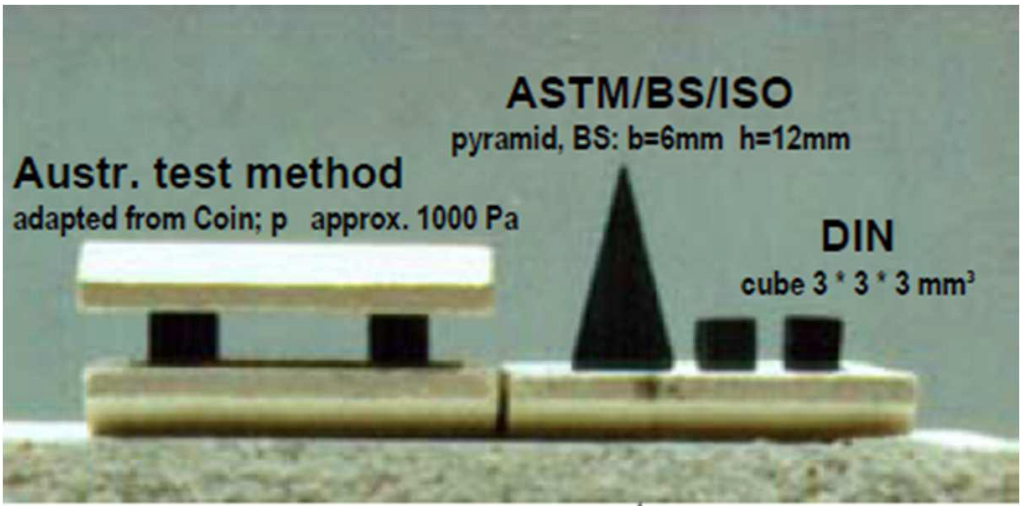

Figure 2.1 Ash fusion characteristic temperatures defined based on the sample geometry change during the heating process. [17]

The Shrinkage Starting Temperature (SST) is the temperature at which the test piece first starts to shrink.

Initial Deformation Temperature (IT) is temperature where tips of test pieces show the first signs of rounding due to melting.

Softening Temperature (ST) is the temperature where the height of the test piece is Specification, although it is commonly reported.

Hemisphere Temperature (HT) is the temperature where the test piece has melted sufficiently to form a hemisphere.

Flow Temperature (FT) is the temperature where the test piece has effectively melted and is spread over the supporting tile.

Slagging index which involve temperature above, following equation:

$$R_s = \frac{(4 \times IT) + HT}{5}$$

Fuels with a slagging index less than 1150 ^{o}C have a severe slagging potential, while value greater than 1340 ^{o}C indicate weak slagging potential.

Limitations of this method are uncertainties in determining of initial temperature deformation of ash, operation condition (i.e. heating rate, heat flux etc.) in laboratory are dissimilar of condition in boiler and leak information in ash composition. [16]

Second method used major element deposition to predict ash behavior. Ash indices are used for apply preliminary assessment for predict ash behavior, initial develop from coals, and have high accuracy in their prediction. However, due to different in ash composition of biomass, their result is contrast.

Gulyurtlu et al, (2008) [18] investigated slagging indices for predict slagging and fouling tendency of biomass co-firing with coal. Polish coal with straw pellets and the Cerejon coal with wood pellets and olive cake were chosen in this study. Their results showed B/A and B/A_{+P} , it is possible to verify that the slagging potential increase with the quantity of biomass used. $R_{B/A}$ is not appropriate for biomass, as was verified experimentally. During straw pellets combustion, the agglomeration was found to occur, although the index gave low probability of this occurrence. BAI is very coherent with the results obtained experimentally. S_R is not applicable and F_u appears to have some applicability. These results are supported by Munir et al (2010), [19] Cotton stalk, Shea meal, wood chips and Russian coal were used in their work. Slagging indices were applied for prediction ash forming tendency of co-firing of biomass and coal. They conclude that no correlation available which can determine the slagging indices for biomass unequivocally.

Alkaline index (AI) has become popular in recent years as a threshold indicator for fouling and slagging. The alkaline index developed by the coal industrial involves calculating the weight in alkali oxides ($K_2O + Na_2O$) per heat unit, kg/GJ and was applied to assent rate solid fuels for slagging or fouling. The calculation is made by

$$AI = \frac{0.1x\left[(\%ash)x(\%alkali \quad in \quad ash)\right]}{HHV(MJ/kg)} = \frac{kg \quad alkali}{GJ}$$

An index range of 0-0.17 kg/GJ is low slagging risk: 0.17-0.34 kg/GJ indicates the material will probably slag and over 0.34 kg/GJ is rick slagging formation. For Biomass, alkali index is incomplete as a descriptor of fouling behavior, however, and is useful principally as a general guide.[6]

Different in composition of biomass case of less accuracy prediction when apply slagging/fouling indices. For biomass fuels, common index is based on ratio of (Na+K)/(2S+Cl) elements present in the fuel. If this ratio is lower than 1.0, this index presence of enough S and Cl to form alkaline sulphates and chlorides. [20]

Another one is ratio of silica and alumina to alkali metals in ash (Si+Al)/(Na+K) allowing the assessment of the potential of the silica/alumina based ashes or additives for

capturing alkali metals. However, slagging/fouling tendency cannot depend of ash composition alone. Operation condition and boiler design play significant for ash behavior.

Table 2.2 Slagging/fouling indices.

Indices	Equation	Description
Slagging (basic to acidic compounds ratio) index	$\frac{B}{A}=\left(\frac{Fe_2O_3+CaO+Na_2O+K_2O+MgO}{SiO_2+Al_2O_3+TiO_2}\right)$	B/A < 0.5, low slagging inclination 0.5<B/A<1.0, medium B/A = 1.00, high B/A≥ 1.75, severe
Slagging index plus phosphorous	$\frac{B}{A_{+P}}=\left(\frac{Fe_2O_3+CaO+Na_2O+K_2O+MgO+P_2O_5}{SiO_2+Al_2O_3+TiO_2}\right)$	B/A_{+p} < 0.5, low slagging inclination 0.5< B/A_{+p} <1.0, medium B/A_{+p} = 1.00, high $B/A_{+p} \geq$ 1.75, severe
Simplified B/A	$R_{(B/A)}=\left(\frac{Fe_2O_3+CaO+MgO}{SiO_2+Al_2O_3}\right)$	0.75 < $R_{(B/A)}$ low slagging
Bed agglomeration index (Fluidize bed reactor)	$BAI=\left(\frac{Fe_2O_3}{K_2O+Na_2O}\right)$	Bed agglomeration occurs when BAI values become lower than 0.15
Slagging (Babcock) index	$R_s=\left(\frac{B}{A}\times S\right)$ Where S = % of sulfur on dry basis	R_s < 0.6 , low slagging R_s = 0.6 – 2.0, medium R_s = 2.0-2.6, high R_s > 2.6, extremely high
Fouling index	$F_u=\left(\frac{B}{A}\right)\times\left(Na_2O+K_2O\right)$	$F_u \leq$ 0.6, low fouling F_u = 0.6-40 , high fouling F_u > 40 , extremely high
Slag viscosity index	$S_R=\left(\frac{SiO_2}{SiO_2+MgO+CaO+Fe_2O_3}\right)\times 100$	S_R > 72, low slagging 72 ≥S_R ≥ 65, medium $S_R \leq$ 65 high slagging

2.1.5 Major biomass structure components

Biomass is a heterogeneous substance. The Main chemical structure contained in biomass are cellulose, hemi-cellulose, and lignin. Each pseudo-component has individual thermal behavior case of different in overall thermal behavior of biomass.

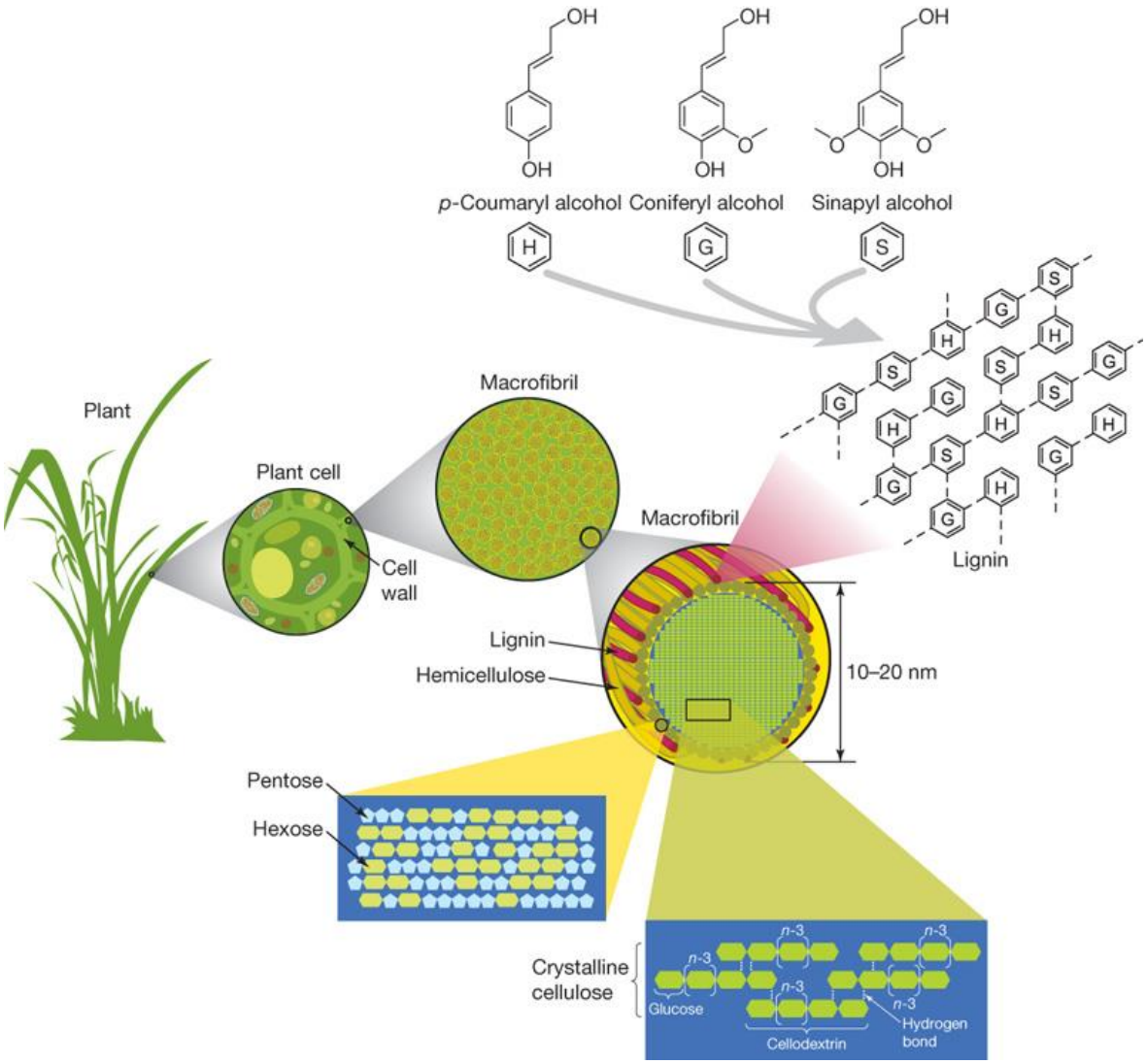

Figure 2.2 Structure of lignocellulose. [21]

Celluloses or Alpha cellulose is a polysaccharide having the generic formula $(C_6H_{10}O_5)_n$ an average molecular weight range of 300,000 to 500,000.

Hemi-celluloses are complex polysaccharides that occur in association with cellulose in the cell walls. Many have the generic formula $(C_5H_8O_4)_n$.

Lignins are highly branched, substituted, mononuclear aromatic polymers in the cell walls of certain biomass, especially woody species, and are often bound to adjacent cellulose fibers to form what has been called a lignocellulosic complex.

The lapid and protein fractions of plant biomass are normally much less on a percentage basis than the carbohydeate components. Protines are polymer composed of natural amino acids that are bounded together peptide linkages. Lapids are eaters of the triol, glycerol and long chain fatty acids. The fatty acids are any of variety of monobasis fatty acids such as palmitic and oleic acids. The esters are formed in a large variety of oilseed crops, green plants and some microalgae.

Other classes of organic materials, such as alkaloids, pigments, resin, sterols, terpenes, terpenoids, waxes and many samples organic compounds are present in various biomass species, but they are usually present in very small amounts. [4]

As general rule, the major organic components on a moisture and ash-free basis in biomass are about 10-25 wt.% of lignin, 20-40 wt.% of hemicelluloses and 40-60 wt.% of celluloses on dry basis.[22]

Cheng et al. (2012) [23] studied the thermal behaviors of three major components in lignocellulosic biomass. Cellulose start volatile decomposes at 258 ^{o}C after that at 305 ^{o}C is decompose of high-energy bond during pyrolysis process. Combustion of cellulose showed 2 stage degradation first stage occur at temperature rang 226-335 ^{o}C which descript volatile matter combustion and second stage occur at 335-482 ^{o}C descript char combustion.

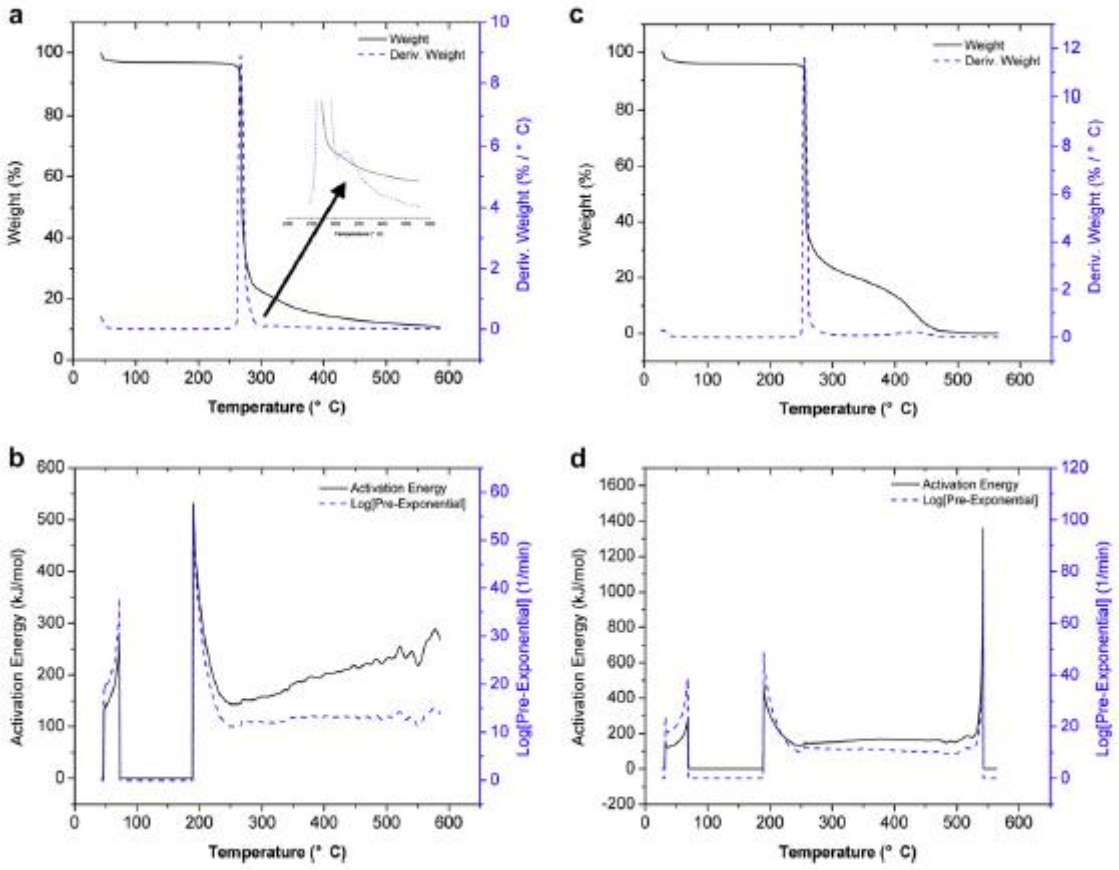

Figure 2.3 Modulated TGA results of microcrystalline cellulose (MCC): a) TG and DTG curves of MCC pyrolysis: b) Distribution of activation energy and pre-exponential factor of MCC pyrolysis: c) TG and DTG curves of MCC combustion: d) Distribution of activation energy and pre-exponential factor of MCC combustion. [23]

Hemi-cellulose degradation starts at 149 ^{o}C and high degradation rate occurs at 149-315 ^{o}C during the pyrolysis process. In combustion process hemi-cellulose start decomposition at 147 ^{o}C. Main thermal degradation occurred at 220 ^{o}C with C-O-C bonds ruptured and some pyranose C-C bonds broken. After that, degradation of chain fragments occurred at high temperature.

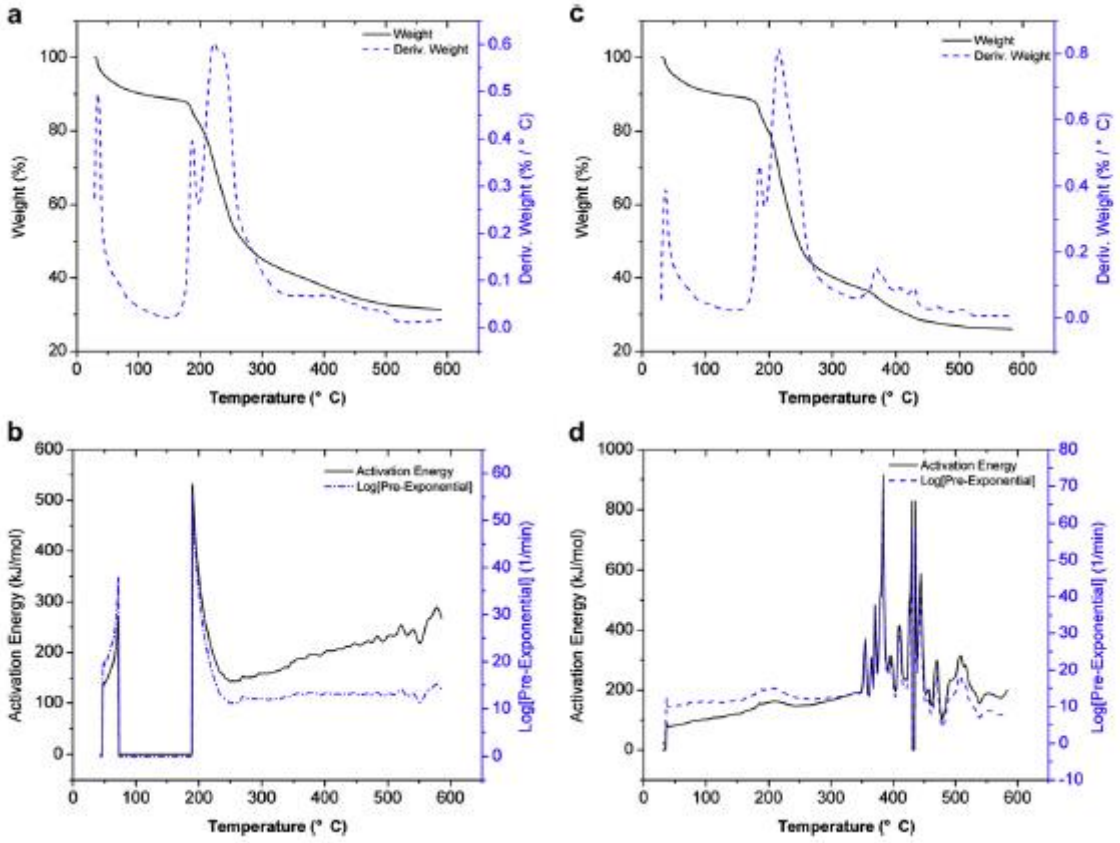

Figure 2.4 Modulated TGA results of birchwood xylan (Hemi-cellulose): (a) TG and DTG curves of xylan pyrolysis; (b) Distribution of activation energy and pre-exponential factor of xylan pyrolysis; (c) TG and DTG curves of xylan combustion: (d) Distribution of activation energy and pre-exponential factor of xylan combusion. [23]

Degradation of lignin pyrolysis start at 186 ^{o}C and main mass degradation occur wide temperature range 186-413 ^{o}C. In combustion process, lignin decomposes very different from pyrolysis. Minor degradation of lignin occur at 287-306 ^{o}C and major decomposition occurred at 306-449 ^{o}C.

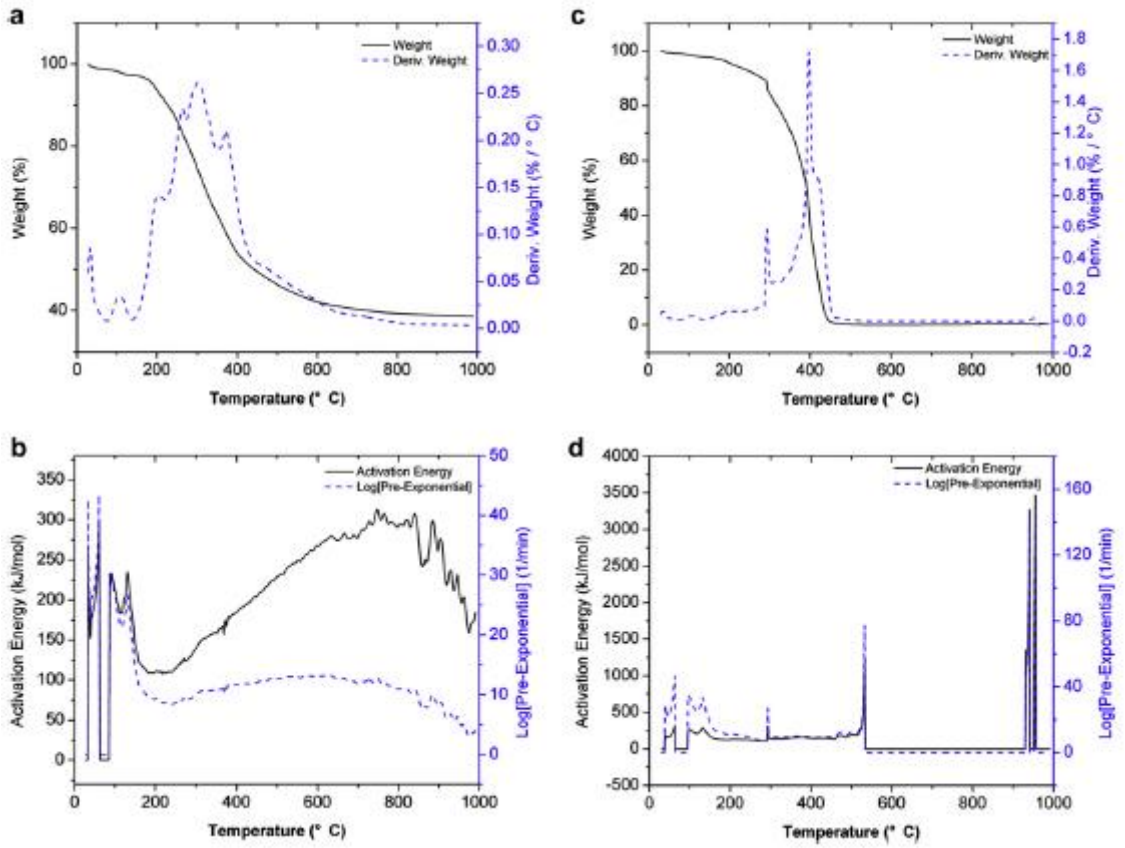

Figure 2.5 Modulated TGA results of Organosolv lignin: (a) TG and DTG curves of lignin pyrolysis; (b) Distribution of activation energy and pre-exponential factor of lignin pyrolysis; (c) TG and DTG curves of lignin combustion; (d) Distribution of activation energy and pre-exponential factor of lignin combustion. [23]

2.1.6 Densities

Density is an important design parameter for any biomass conversion system. For biomass, we can define three characteristic densities: true, apparent, and bulk.

2.1.6.1 True density

True density is the weight per unit volume occupied by the solid constituent of biomass. Total weight is divided by actual volume of the solid content to give its true density.

$$\rho_{true} = \frac{total\ mass of\ biomass}{solid\ volume\ in\ biomass}$$

2.1.6.2 Apparent density

Apparent density is based on the apparent or external volume of the biomass. This includes its pore volume (or that of its cell cavities). For a regularly shaped biomass, mechanical means such as micrometers can be used to measure the different sides of a particle to obtain its apparent volume. An alternative is use of volume displacement in water. The apparent density considers the internal pores of a biomass particle but not the interstitial volume between biomass particles packed together.

$$\rho_{apparent} = \frac{\text{total mass of biomass}}{\text{apparent valume of biomass including solids and internal pores}}$$

Apparent density is most commonly used for design calculations because it is the easiest to measure, and it gives the actual volume occupied by a particle in a system.

2.1.6.3 Bulk density

Bulk density is based on the overall space occupied by an amount or a group of biomass particles:

$$\rho_{bulk} = \frac{\text{total mass of biomass particles or stack}}{\text{bulk volume occupied by biomass particles or stack}}$$

Bulk volume includes interstitial volume between the particles, and as such, it depends on how the biomass is packed. [24]

2.1.7 Heating values

Heating values is defined as total heat released during the combustion process when the unit mass of fuel oxidizes with pure oxygen.

$$C + O_2 \rightarrow CO_2$$
$$H_2 + 0.5O_2 \rightarrow H_2O$$
$$S + O_2 \rightarrow SO_2$$

High heating values (HHV): total energy release during combustion process when water in flue gas (product from combustion process) condenses into liquid form.

$$H_2 + 0.5O_2 \rightarrow H_2O_{(g)} \rightarrow H_2O_{(l)} + \text{Heat}$$

Low heating values (LHV): total energy release.

$$LHV = HHV - m_w h_{fg}$$

where m_w = mass of water vapor in products of combustion per unit mass of fuels

h_{fg} = latent heat of vaporization of water vapor at its partial pressure in the combustion products. (h_{fg} = 2.44 MJ/kg at 25 ^oC). [25]

$$H_2 + 0.5O_2 \quad \rightarrow \quad H_2O_{(g)}$$

The lower heating value is less than the higher value by the latent energy of water vaporization. Wet biomass, moisture in the fuel will reduce both heating values, because there is less dry fuel per unit mass wet fuel and lower hating value and reduce from heat to vaporize moisture into the vapor phase. [26]

$$HHV_{Wet\ \ basis} = HHV_{Dry\ \ basis} \times [1 - M] \qquad \text{and,}$$

$$LHV_{Wet\ \ basis} = \left[HHV_{Dry\ \ basis} - h_{fg} \left[\left(\frac{M}{1 - M} \right) + 0.09H \right] \right] \times [1 - M]$$

where M = moisture content in wet basis,

H = Percent of hydrogen content in biomass (dry basis).

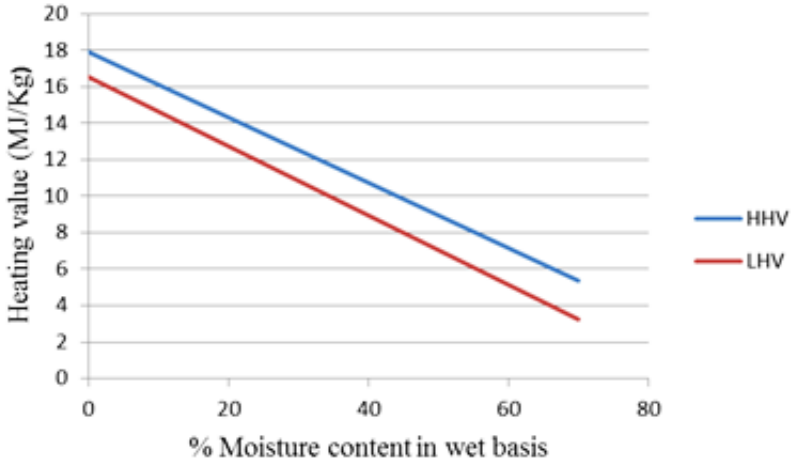

Figure 2.6 Comparison between LHV and HHV of bagasse at different percentages of moisture content**.**

2.1.8 Stoichiometry of combustion

The stoichiometry of combustion is defined as the minimum of air/oxygen required for the complete combustion process. Carbon (C), Hydrogen (H), and Sulfur (S) are converted into carbon dioxide (CO_2), water (H_2O) and sulfur dioxide (SO_2).

- Equivalence ratio (ER, φ)

Equivalence ratio defines as mass ratio of air to fuel divide as mass ration of air to fuel at stoichiometry.

$$\text{ER} = \frac{(m_{air} / m_{fuel})}{(m_{air} / m_{fuel})_{stoi}}.$$

ER = 1; Stoichiometric of combustion.

ER > 1; Excess air/Fuel – lean mixtures.

ER< 1; Fuel – rich. [25]

2.2 Thermal conversion of biomass

In Thailand, the main technology available to apply to used biomass for energy utilization is the thermochemical process (pyrolysis, gasification, and combustion).

2.2.1 Biomass Pyrolysis

Pyrolysis processes are the thermal degradation of carbonaceous material in the absence of oxygen (Equivalence ration (ER) ≈ 0 – 0.1), at atmospheric pressure and temperature ranging from 300-600 ^{o}C. Generally pyrolysis process can be classified into two types. Firstly, it is slow pyrolysis which biomass is heating to temperature around 400 ^{o}C at slow heating rate. The main products from this process are Char (solid) and light gas (CO, CO_2, CH_4 ,etc.).

Secondly, we know as fast pyrolysis which material was heated at very fast heating rate (1000-10,000 ^{o}C/s) to temperature around 500 -1000 ^{o}C. Main products are Bio-oil (from biomass) and gaseous (which quickly remove and quenched into liquid form).

Torrefaction is the pyrolysis process in which biomass is heated to temperature around 200-320 ^{o}C. This method used to pre-treatment for biomass to improve heating value of biomass. Moisture contents, some part of lignin and hemi-cellulose (main –pseudo component) were removed from this process. 50-70 % of original weight decrease and heating value up to 30 % compare with original biomass.

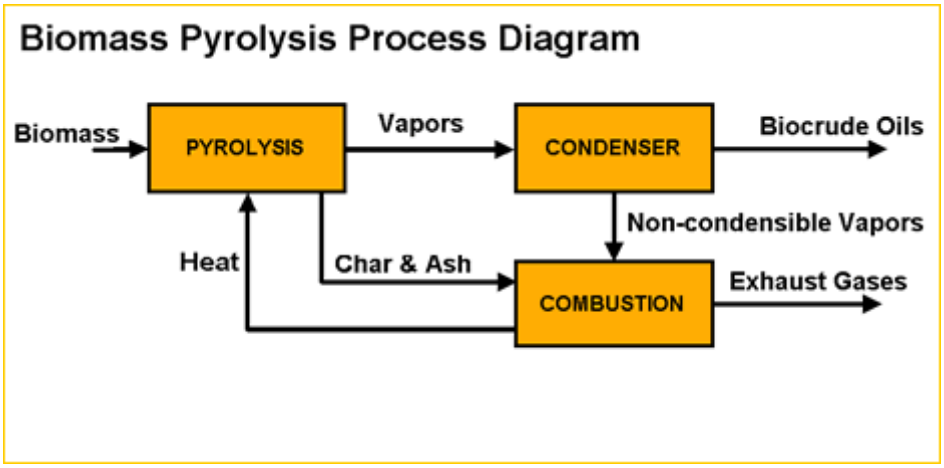

Figure 2.7 Pyrolysis diagram [27]

2.2.2 Biomass Gasification

Gasification is defined as the thermal conversion process of carbonaceous material to combustible gases with low oxygen or air (Equivalence ration (ER) ≈ 0.2-0.33). Combustible gases from this process can be used reliably for heating, industrial process application electricity generation and liquid fuels production. Producer gas from this process consists carbon monoxide, hydrogen (H_2), carbon dioxide (CO_2), methane (CH_4) and other light gases plus nitrogen (N_2).

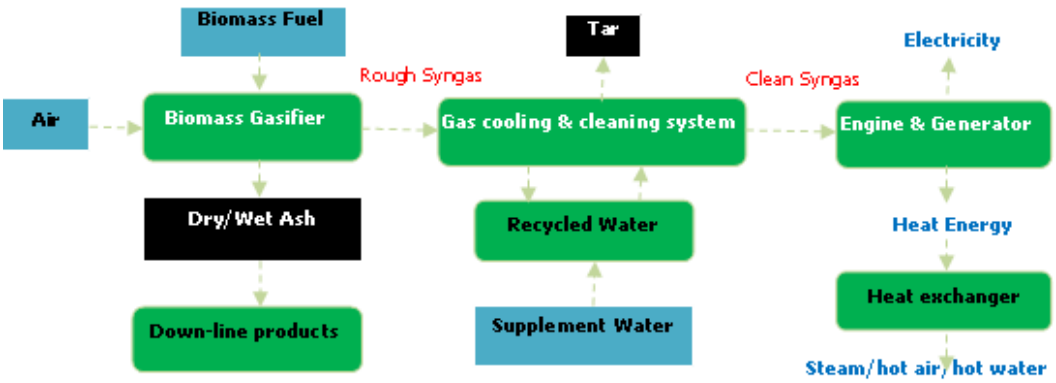

Figure 2.8 Biomass gasification diagram [28]

The gasification compound with the 4 steps of the thermal process is as follows:

- Heating and drying

First step of gasification is heating and drying with 20-50 wt% of moisture content in biomass was removed. This process starts at 100 ^{o}C to 300 ^{o}C. Particle size of feed stock

is directly effect for this process, heating and drying begins on outer surface to center of biomass. Lagging temperature between center and outer surface of large particle effect to uncompleted drying process before feed into reactor.

- Pyrolysis

This process occurs at temperature ranging around 225 ^{o}C and finished at 400-500 ^{o}C. This process include with produced water, permanent gases (CO, CO_2, H_2 and light hydrocarbon), tarry vapors (those that condense upon cooling) and char formation. 80 wt% of biomass are converted into vapors and gases.

- Gas-Solid Reactions

Process of gas – solid reactions occur during pyrolysis process with char (solid phase) react with oxygen, steam admitted to the gasifier, gas and vapors released during pyrolysis. Chemical reactions of this process as follow:

Carbon-oxygen reaction

$$C + \tfrac{1}{2} O_2 \leftrightarrow CO \quad \Delta H_R = -110.5 \text{ MJ/kmol}$$

Boudouard reaction

$$C + CO_2 \leftrightarrow 2CO \quad \Delta H_R = 172.4 \text{ MJ/kmol}$$

Carbon – water reaction

$$C + H_2O \leftrightarrow H_2 + CO \quad \Delta H_R = 131.3 \text{ MJ/kmol}$$

Hydrogenation reaction

$$C + 2H_2 \leftrightarrow CH_4 \quad \Delta H_R = -74.8 \text{ MJ/kmol}$$

For equilibrium chemical reaction, all carbon in char would be converted to gaseous products. In practice, the contact time between char and gaseous reactants at evaluates temperature is usually insufficient to achieve equilibrium reaction effect to the result that up to 10 wt% of the biomass appears as char in the gasification product.

- Gas-phase Reaction

Volatiles released during the pyrolysis process remain at high temperature, and react with water. The final products are methane (CH_4) and hydrogen (H_2). The chemical reaction is as follows:

Water-gas shift reaction

$$CO + H_2O \leftrightarrow H_2 + CO_2 \quad \Delta H_R = -41.1 \text{ MJ/kmol}$$

Methanation

$$CO + 3H_2 \leftrightarrow CH_4 + H_2O \quad \Delta H_R = -206.1 \text{ MJ/kmol}$$

The water-gas shift reaction is important in increasing the H_2 content of syngas, while the methanation reaction can strongly influence the CH_4 content of syngas.

2.2.3 Biomass Combustion

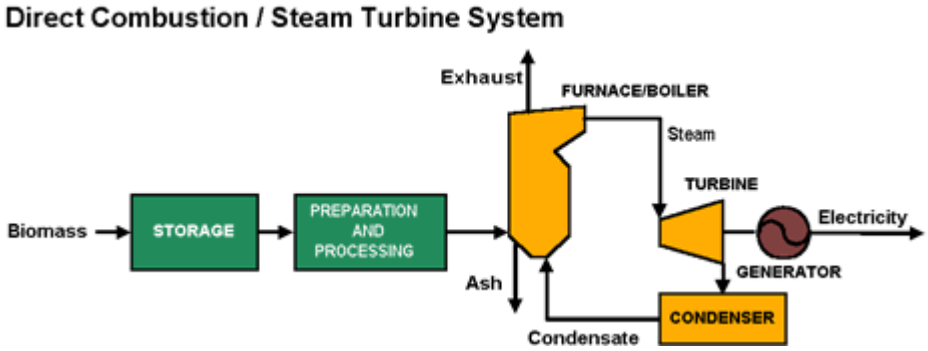

Figure 2.9 Direct combustion system, processed biomass is the boiler fuel that produces steam to operate a steam turbine and generator to make electricity [29]

Combustion is the simplest method to convert chemical energy stored in fuels (burnable material) into heat by exothermic oxidation process. The main objective of good combustion is as follows:

- Temperature high enough to ignite.
- Turbulence mixing between fuel and oxygen.
- Time for complete combustion.

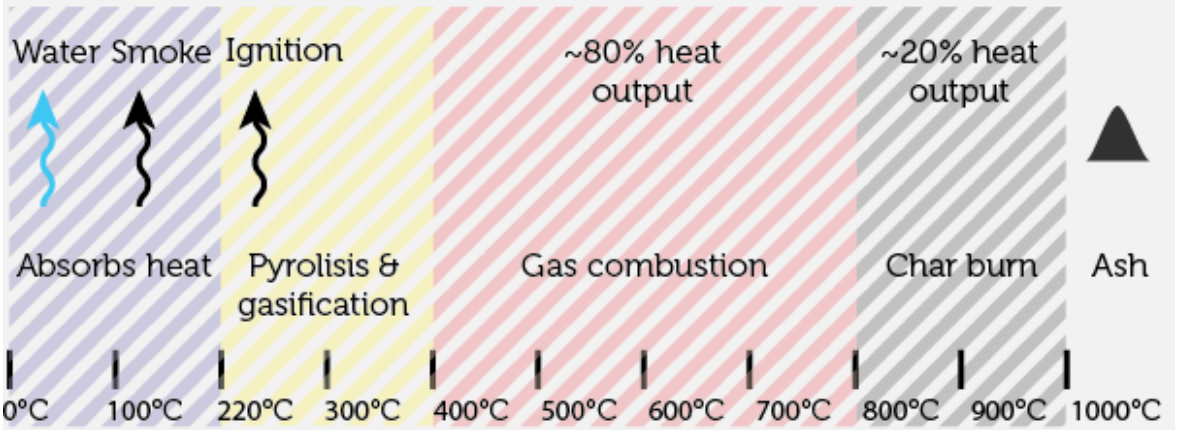

Figure 2.10 Biomass combustion diagram [30]

The simplest step to describe the combustion process of biomass is follows as:

- Heat up and drying

- Devolatilization (pyrolysis) to release volatile matter (VM) and producing char.
- Gashouse products diffuse to surface of particle and react with oxygen (combustion of volatiles).
- Oxygen diffuses to particle surface and gaps inside particles.
- Combustion of char.

In biomass combustion process, the value of equivalence ratio (ER) is around 1.2-1.5 to avoid incomplete combustion. [31]

CHAPTER 3
THERMOGRAVIMETRIC ANALYSIS (TGA) AND KINETIC OF REACTION

This chapter presents the working principle of TGA which is divided into two parts. First part involves principle working of TGA including with graph type, limitation and thermal behavior of biomass from TGA. Second part descript kinetic of reaction from TGA both isoconvention and model fitting method.

3.1 Thermogravimetric Analysis (TGA)

Thermogravimetric analysis (TGA) is the techniques that widely used to study the thermal behavior of samples in both solid and liquid phase. The data that get from TGA is mass degradation versus time or temperature and can be divided into two types of techniques. First is Isothermal thermogravimetric with mass change at constant temperature ($\Delta T=0$) which generally use for study thermal stability, kinetic rate of decomposition reaction, absorption or desorption of sample. Second is dynamic thermogravimetry with sample mass was recorded relate with time/temperature at constant heating rate (φ = Constant) at fixed heating rate. [32]

Figure 3.1 Thermogravimetric Analyzer

Brown (1988) [32] performed possible interpretations as follows:

Type (i) curves. The sample undergoes no decomposition with the loss of volatile products over the temperature range shown. No information is obtained, however, on whether solid phase transition, melting, polymerization or other reaction involving no volatile products have occurred.

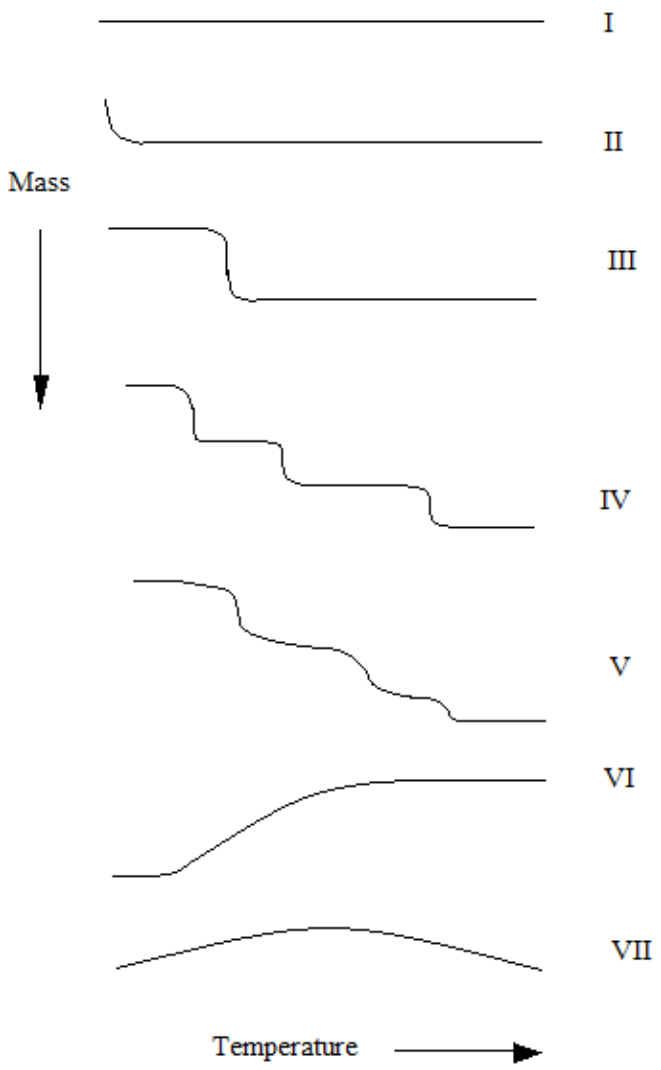

Figure 3.2 Main types of thermogravimetric (TG) curves. [32]

Type (ii) curves. The rapid initial mass loss observed is characteristic of desorption or drying. It could arise when working at reduced pressure from effects such as thermomolecular flow or convection.

Type (iii) curves. These represent the decomposition of the sample in a single stage. The curve may be used to define the limits of stability of the reactant, to determine the stoichiometry of the reaction, and to investigate the kinetics of reaction.

Type (iv) curves. These indicate multi-stage decomposition with relatively stable intermediates. Again, the temperature limits of stability of the reactant and of the intermediates can be determined form the curve, together with the more complicated stoichiometry of reaction.

Type (v) curves. These also represent multi-stage decomposition, but in this example stable intermediates are not formed and little information on all but the stoichiometry of the overall reaction can be obtained. It is important to check the effect of heating rate on the resolution of such curves. At low heating rates, type (v) curves may tend to resemble type (iv) curves more closely, while at high heating rates both type (iv) and type (v) curves may resemble type (iii) curves and hence the detail of the complex decomposition is lost.

Type (vi) curves. These show a gain in mass as a result of the reaction of the sample with the surrounding atmosphere. Atypical example would be the oxidation of a metal sample.

Type (vii) curves. These are not often encountered, e.g. the product of an oxidation reaction decomposes again at higher temperatures.

In 1965 the first international conference on thermal Analysis (ICTA) established a committee on standardization charged with the task of studying how and where standardization might further the value of thermal analysis. To accompany TG record, information should be prepared [7]:

1. Identification of all substances (sample, reference, diluent) by a definitive name, an empirical formula, or an equivalent compositional data list.
2. A statement of the sources of all substances, details of their histories, pretreatments and chemical purities so far as these are known.
3. Measurement of average rate of linear temperature change over the temperature range involving the phenomena of interest.
4. Identification of the sample atmosphere by pressure, composition, and purity whether the atmosphere is static self-generated or dynamic through or over the sample. Where applicable, the ambient atmospheric pressure and humidity should be

specified. If the pressure is other than atmospheric, full details of the control methods should be given.

5. A statement of the dimensions, geometry, and materials of the sample holder, the method of loading the sample holder, and the method of loading sample, where applicable.

6. Identification of the abscissa scale in terms of time or of temperature at a specified location. Time or temperature should be plotted to increase from left to right.

7. A statement of the methods used to identify intermediates or final products.

8. Faithful reproduction of the original records.

9. Wherever possible, each thermal effect should be identified and supplementary supporting evidence stated.

10. Identification of the thermobalance, including the location of the temperature measuring thermocouple.

11. A statement of the sample weight and weight scale for the ordinate. Weight loss should be plotted as a downward trend, and deviations from this practice should be clearly marked. Additional scales may be used for the ordinate where desired.

12. If derivative thermogravimetry is employed, the method of obtaining the derivative should be indicated and the units of the ordinate specified.

3.2 Thermogravimetric Analysis of Biomass

Many researchers apply TGA to the thermal behavior of biomass, which can include variable conditions, such as atmospheric environment, heating rate, particle size etc., either pure or co-firing/pyrolysis with fossil fuels.

H.B. Vuthaluru (2003), [33] performed Thermogravimetric studies of thermal behavior of coal/biomass blends during co-pyrolysis. Coal from Western Australia was chosen to pyrolyzed with wood west, wheat straw, peat and municipal solid waste (MSW). The kinetics of thermal decomposition base on order of reaction was chosen in their work. TG curves showed an initial decrease in the weight of samples between 100 and 150 ^{o}C due to release of moisture remaining in the samples. Thermal degradation of pure coal showed single step degradation. Biomass showed two stage degradation and co-pyrolysis showed three stage degradation. For co-pyrolysis, first stage degradation like degradation of biomass, second and third stage like co-degradation of biomass and coal. The data

indicated fuel undergo co-pyrolysis are independent thermal conversion without chemical interactions between them and can be predicted thermal behavior from those of parent fuels.

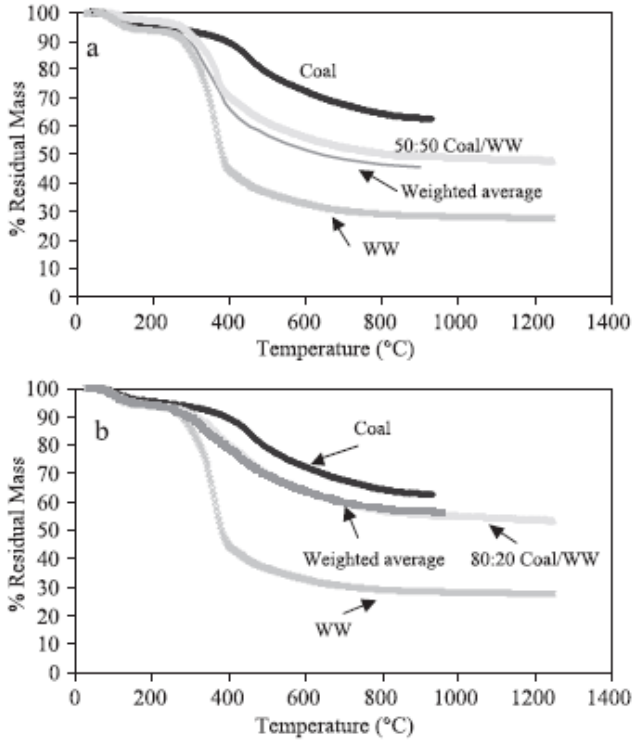

Figure 3.3 Comparison residual mass with weight average values for typical coal/ wood waste blends. (a) 50:50 of coal and wood; (b) 20:80. of coal and wood [33]

Reveendran et al. (1996) [34] studied the thermal behavior of biomass during pyrolysis by TGA and packed-bed pyrolyzer. The results showed each kind of biomass has a characteristic pyrolysis behavior which is explained based on its individual components characteristics. Studied on isolated biomass components as well as synthetic biomass showed that interactions among the components are not of as much significance as the composition of the biomass. Zonation of thermal degradation as follow:

Zone I:	< 100 ^{o}C	Drying zone.
Zone II:	100 – 250 ^{o}C	Extractives start decomposing.
Zone III:	250-350 ^{o}C	Predominantly hemicellulose decomposition.
Zone IV:	350-500 ^{o}C	Mainly cellulose and lignin decomposition.
Zone V:	>500 ^{o}C	Mainly lignin decomposition

Skreiberg et al. (2011) [22] investigated the thermal behavior of selected biomass fuels and mixtures as wood, coffee waste and glossy paper. The results presented each single fuel had pyrolysis and combustion characteristics based of its own main pseudo-components. The pyrolysis and combustion characteristics of selected fuel mixers and the gas composition analysis were showed quantitative and qualitative summative behavior based on single fuels.

Yang et al. (2007), [35] was studied the characteristics of hemicellulose, cellulose and lignin pyrolysis. Cellulose is in powers fibruous form, lignin is alkali lignin in brown powders and hemi-cellulose is xylan were chosen for studied characteristics under thermogravimetric analyzer (TGA) with differential scanning calorimetry (DSC) detector and a pack bed. And gas products from TGA were out line measured using Fourier transform infrared (FTIR) spectroscopy. The results showed pyrolysis of hemi-cellulose and cellulose occurred quickly, with the weight loss of hemi-cellulose mainly happened at 220-315 ^{o}C and that of cellulose at 315-400 ^{o}C. However, lignin was more difficult to decompose, as its weight loss happened in a wide temperature range (160-900 ^{o}C) and generated solid residue was very high (~40 wt.%).

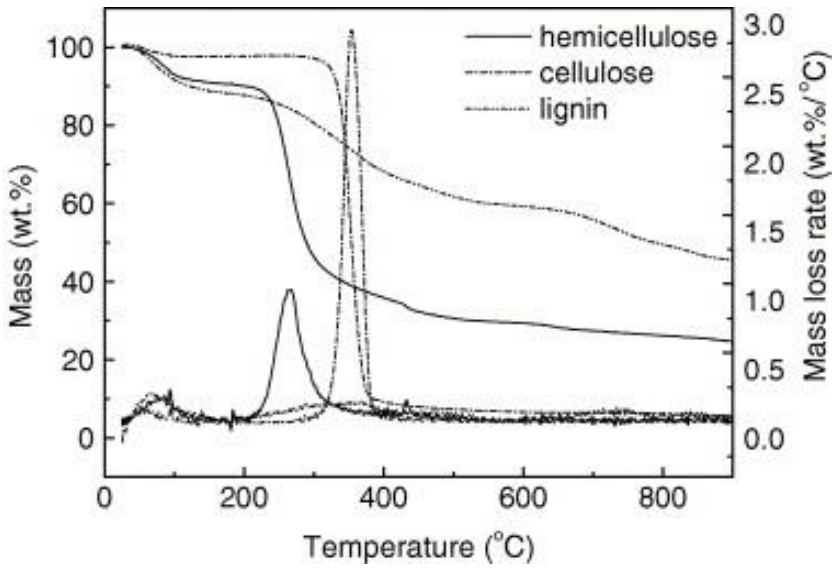

Figure 3.4 Pyrolysis curves of hemicellulose, cellulose and lignin in TGA. [35]

Roman et al. (1981) [36] investigated the devolatilization of feedlot manure at different particle sizes and variable heating rates. Their data indicated at atmospheric pressure and in pure nitrogen environment. It showed devolatilization begins around 200

^{o}C and is almost completed around 500 ^{o}C. Moreover, the devolatilization of manure decreased and the char produced increased with increasing particle size. The temperature at which the maximum rate of devolatilization occurred was mainly affected by the heating rate.

3.3 Kinetic of Reaction from TGA.

Chemical kinetics is the study of chemical reactions with respect to reaction rate, formation of substance, etc. The study of motion (fast or slow) of chemical reactions is called kinetics.

A kinetic study by thermogravimetry involves measurement of α, is defined as $\alpha = \frac{m_0 - m}{m_0 - m_f}$ where m_0 is the initial mass and m_f the mass of the sample when reaction complete or equivalent definitions in term amounts of gas evolved or heat absorbed or evolve, of either as a function of time or temperature. [32]

The majority of kinetic methods used in the area of thermal analysis consider the rate to be a function of onlytwo variables, T and α

$$\frac{d\alpha}{dt} = k(T) f(\alpha)$$

The dependence of the process rate on temperature is represented by the rate constant, k(T), and the dependence on the extent of conversion by the reaction model, f(α). This equation describes the rate of a single-step process. The extent of conversion, α, is determined experimentally as a fraction of the overall change in a physical property that accompanies a process. If a process is accompanied by mass loss, the extent of conversion is evaluated as a fraction of the total mass loss in the process.

The temperature dependence of the process rate is typically parameterized through the Arrhenius equation

$$k(T) = Ae^{-E/RT}$$

For reversible reactions, the rate of reaction will depend on the partial pressure of the gaseous product. The rate equation should thus include allowance for this, in terms of some function h(p)

$$\frac{d\alpha}{dt} = Ae^{-E/RT} f(\alpha) h(P)$$

The pressure dependence, h(P) is ignored in most of kinetic computational methods used in the area of thermal analysis. It should be remembered that the pressure may have a profound effect on the kinetic process. [34]

For dynamic measurements (φ = constant), the usual approach is to write

$$\frac{d\alpha}{dt} = \frac{d\alpha}{dT} \times \frac{dT}{dt} = \frac{d\alpha}{dT} \times \varphi$$

where φ is the heating rate. The heating usually maintained constant.

The conversion dependence of the process rate can be expressed by using a wide variety of reaction models, f(α), some of which are presented in Table 3.1

That is, they may have a very limited (if any) applicability when interpreting the reaction kinetics that do not involve any solid phase. It is always useful to make sure whether a solid substance would react in the solid state when heated. On heating, before a reaction starts a solid crystalline substance can melt or a solid amorphous substance can undergo the glass transition so that in either case the reaction would take place in the liquid phase. At any rate, one should be advised to use the reaction models appropriate to the process being studied.

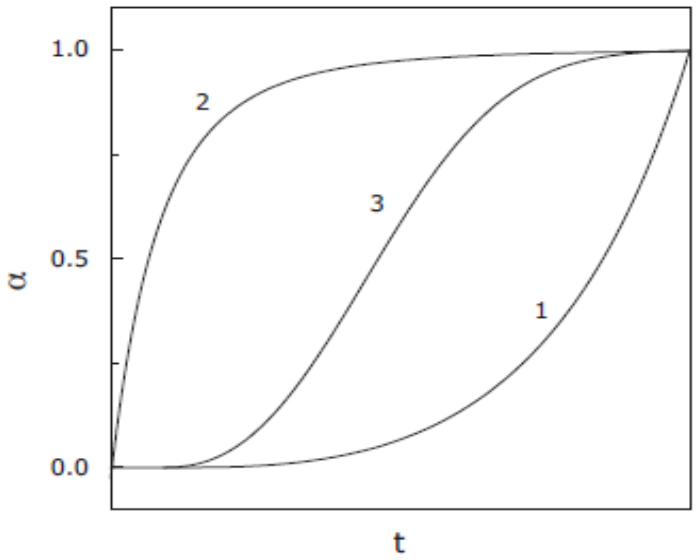

Figure. 3.5 Characteristic α vs. time (t) "reaction profiles" for (1) accelerating, (2) decelerating, and (3) sigmoidal models. [37]

Although there are a significant number of reaction models, they all can be reduced to three major types: accelerating, decelerating, and sigmoidal (sometimes also called

autocatalytic). Accelerating models represent processes whose rate increases continuously with increasing the extent of conversion and reaches its maximum at the end of the process.

Models of this type can be exemplified by a power–law model:

$$f(\alpha) = n\alpha^{(n-1)/n}$$

where n is a constant. Models of the decelerating type represent processes whose rate has maximum at the beginning of the process and decreases continuously as the extent of conversion increases. The most common example here is a reaction-order model:

$$f(\alpha) = (1-\alpha)^{n}$$

where n is the reaction order. Diffusion models (Table 3.1) are another class of decelerating models. Sigmoidal models represent processes whose initial and final stages demonstrate respectively the accelerating and decelerating behavior so that the process rate reaches its maximum at some intermediate values of the extent of conversion. The Avrami–Erofeev models:

$$f(\alpha) = n(1-\alpha)[-\ln(1-\alpha)]^{(n-1)/n}$$

provide a typical example of the sigmoidal kinetics. Only those kinetic methods that are capable of treating all three types of the conversion dependencies can be recommended as reliable methods.

Kinetic analysis can have either a practical or theoretical purpose. A major practical purpose is the prediction of process rates and material lifetimes. The predictions are reliable only when sound kinetic analysis methods are used. The theoretical purpose of kinetic analysis is interpretation of experimentally determined kinetic triplets. Each of the components of a kinetic triplet is associated with some fundamental theoretical concept. E_a is associated with energy barrier, A with the frequency of vibrations of the activated complex, and $f(\alpha)$ with the reaction mechanism. [37]

3.3.1 Model fitting method

The model fitting method is a method that calculates the kinetic parameters by assuming reaction models. Some kinetic models are showed in Table 3. First recommendation for this method is all parameter bases on single heating rate. Second for model fitting is to identify an appropriate model. If this not done correctly, the kinetic parameters will be meaningless.[34] An advantage of this method is can be apply for multi-step reaction model by divide range of reaction. Mainly kinetic model which applies in fields of biomass study is first or n order of reaction.

$$f(\alpha) = (1-\alpha)^n \qquad \text{where } (n \neq 1), \text{ or}$$

$$f(\alpha) = (1-\alpha) \qquad \text{where } (n = 1).$$

This method allows to calculated kinetic model base on single heating and is known to be notoriously unreliable.

3.3.2 Isoconvension method (Model-free method)

The isoconvension method is a method that allows calculating activation energy (E) without assuming a reaction model (e.g. Ozawa-Flynn-wall, Kissinger). This method base on assumption α = constant, f(α) is also constant at any heating rate. For this methods, its required series of 3-5 runs at different heating rate or a series of runs at different constant temperature. However, Isoconvension methods allow calculating only activation energy. It's diffuse for calculate pre-exponential and reaction model from Isoconvension method but can be calculate by assume single step of reaction. Recommendation for find pre-exponential and reaction model by assuming a single step of the reaction, the activation energy does not vary significantly with the extent conversion. [37]

3.3.3 Phenomenological models

3.3.3.1 Single reaction model

The single step model is the simplest kinetic model which assumes that the decomposition rate of the pyrolysis process depends on an arbitrary reaction order. The reaction scheme can be represented as;

$$\text{Raw material} \xrightarrow{k} \text{Char} + \text{Volatiles}$$

where *k* is the rate constant of the reaction following the Arrhenius law.

3.3.3.2 Two-Step Consecutive-Reaction Model

Guo and Lua two-step consecutive-reaction model proposed a reaction model based on the consideration that all cellulosic components of biomass, namely lignin, cellulose and hemicellulose, will decompose first into intermediates and then to the final solid char and volatiles. For example, cellulose converts to intemediates of anhydrocellulose and levoglucosan, while hemicellulose decomposes to furanoses and furans and the intermediates of lignin are condensed aromatic and phenolic compounds.The kinetic rate of biomass based on this model can thus be represented as

$$\text{Raw material} \xrightarrow{k_1} \text{Intermediate} + \text{Volatile (I)}$$

$$\text{Intermediate} \xrightarrow{k_2} \text{Char} + \text{Volatile (II)}$$

where $k_1$and $k_2$are reaction rate constants of the first and second steps of reaction, respectively.

Two-step consecutive reaction model with provision of stoichiometric coefficients proposed adding the stoichiometric coefficients of the reactions, x and y, in the reaction schemes of the original two-step consecutive model. That is,

$$\text{Raw material} \xrightarrow{k_1} \text{x} \bullet \text{Intermediate} + \text{Volatile (I)}$$

$$\text{Intermediate} \xrightarrow{k_2} \text{y} \bullet \text{Char} + \text{Volatile (II)}$$

The assumptions are a pure kinetic controlled process, no secondary reactions among the gaseous products and the pyrolysis reactions following first-order reaction for the first step and nth order for the second step, respectively.

Table 3.1 Broad classification of solid–state rate expressions.[32]

Model	$f(\alpha)$	$g(\alpha)=\int_0^{\alpha}\frac{d\alpha}{f(\alpha)}$
Acceleratory α-time curves		
P2 power law	$2\alpha^{1/2}$	$\alpha^{1/2}$
P3 Power law	$3\alpha^{2/3}$	$\alpha^{1/3}$
P4 Power law	$4\alpha^{3/4}$	$\alpha^{1/4}$
P2/3 Power law	$2/3\alpha^{-1/2}$	$\alpha^{3/2}$
Sigmoid α-time curves		
A2 Avrami-Erife'ev	$2\times(1-\alpha)\times[-\ln(1-\alpha)]^{1/2}$	$[-\ln(1-\alpha)]^{1/2}$
A3 Avrami-Erife'ev	$3\times(1-\alpha)\times[-\ln(1-\alpha)]^{2/3}$	$[-\ln(1-\alpha)]^{1/3}$
A4 Avrami-Erife'ev	$4\times(1-\alpha)\times[-\ln(1-\alpha)]^{3/4}$	$[-\ln(1-\alpha)]^{1/4}$
B1 Prout-Tompkins	$\alpha(1-\alpha)$	$\ln[\frac{\alpha}{1-\alpha}]$
Deceleratory α-time curves		
Based on geometrical models		
R2 Contracting area	$2(1-\alpha)^{1/2}$	$1-(1-\alpha)^{1/2}$
R3 Contracting volume	$3(1-\alpha)^{2/3}$	$1-(1-\beta)^{2/3}$
Based on diffusion mechanisms		
D1 One-dimensional	$1/2\alpha$	α^2
D2Two-dimensional	$[-\ln(1-\alpha)]^{-1}$	$(1-\alpha)\ln(1-\alpha)+\alpha$
D3Three-dimensional	$\frac{3}{2}\times(1-\alpha)^{2/3}\times[1-(1-\alpha)^{1/3}]^{-1}$	$[1-(1-\alpha)^{1/3}]^2$
D4 Ginstling-Brounshtein	$\frac{3}{2}\times[(1-\alpha)^{-1/3}-1]^{-1}$	$(1-\frac{2\alpha}{3})-(1-\alpha)^{2/3}$
Base on 'order of reaction'		
F1 First order	$1-\alpha$	$-\ln(1-\alpha)$
F_n n order	$(1-\alpha)^n$	$\left[\frac{1}{1-\alpha}\right]^n$

3.3.3.3 Independent Parallel Reactions Model

This model assumes that a raw material consists of multiple components, e.g. two component, M1 and M2. The reaction is controlled by kinetic process only and there are no secondary reactions among the gaseous products and char.

$$M1 \xrightarrow{k_1} \text{Volatile + char}$$

$$M2 \xrightarrow{k_2} \text{Volatile + char}$$

where k_1 and k_2 represent the rate constant of reaction occurring from the first and the second fractions, respectively.

Weerachanchai et al. (2010), [38] compared pyrolysis the kinetic models for TGA of biomass. Five models (One-step global model assuming first order reaction, One-step global model assuming n^{st} order reaction, Two-step consecutive reaction model based on Guo and Lua (2001) concept, Two-step consecutive reaction model with provision of stoichiometric coefficients and Two parallel reactions model) based on three pyrolysis schemes consisting of one-step global reaction, two-step consecutive-reactions and two parallel reactions were tested in their research. The results showed, on model fitting, the best fitting was observed for the two parallel reactions model. The one-step global model assuming n^{th} order reaction and the two-step consecutive reaction model with provision of stoichiometric coefficient gave satisfactory prediction. However, the one-step global model assuming, first order reaction and the two-step consecutive-reaction model of Guo and Lua showed relatively large deviation between predicted and experimental results.

Kok and Özgür (2013) [39] studied the kinetics of reactions of three types of biomass (miscanthus, poplar wood, and rice husk) and five different heating rate (5, 10, 15, 25, and 50 ^{o}C/min). Three different isoconventional methods were applied in their research. They recommended the results from kinetic analysis were difficult to report specific activation energy of solid fuel combustion reactions since each kinetic method may give different results. Solid fuels are not homogenous and the results are sensitive to experimental conditions, material characteristics and the kinetic used in the calculation.

CHAPTER 4
METHODOLOGY

The methodology in this thesis is divided into two main parts. First part is collected Thai biomass properties for support data base. Second, thermal behavior of biomass pyrolysis and combustion are studied by TGA.

4.1 Raw Material Analysis

4.1.1 Proximate analysis.

The proximate components (volatile matter, fixed carbon and Ash contain) of biomass were analyzed by a thermogravimetric analyzer. (Pyris 1 TGA, Perkin Elmer). 6 mg of biomass sample was place into pan. The sample was heat from ambient temperature up to 110 ^{o}C and hold for 10 min to release water content in biomass under 50 ml/min nitrogen supply. Dry sample was heat from 110 ^{o}C up to 900 ^{o}C after that switch to supply air and hold for 10 min at final step. The weight loss during 110 ^{o}C to 900 ^{o}C was calculated to obtain percentage of volatile matter. And residual mass at last step present percentage of ash content. Fixed carbon can be calculated by 100 percent minus percentage of volatile matter and ash content.

4.1.2 Ultimate analysis

Chemical elements (C, H, N and S) contained in the biomass were an analyze by elemental analyzer (Thermo Finnigan, Flash EA 1112) and oxygen (O) content was calculated by 100% minus percentage of other compositions.

4.1.3 High heating value (HHV)

High heating values (HHV) of the biomass samples were obtained from a bomb calorimeter. 100 mg of dry sample was test by Gallenkamp Bomb Calorimeters.

Correlations between HHV of biomass characteristic were collected and present in this work. The average absolute error of each correlation was calculated from:

$$\text{Average absolute error (AE)} = \frac{1}{\text{n}}\sum_{i=n}^{i}\left|\frac{HHV_E - HHV_M}{HHV_M}\right| x100\%$$

where n is the number of samples

HHV_E is estimated value of HHV

HHV_M is measured value of HHV

4.2 TGA Experiment

4.2.1 Thermal behavior of biomass

Bagasse, corn cob, empty fruit brunch, leucaena and rice straw were chosen to study the thermal behavior of biomass. Selected samples were grinding to reduce particle size (< 2mm).

4.2.1.1 Biomass pyrolysis

A 6 mg of bagasse, corn cob, empty fruit brunch, leucaena and rice straw were placed into pan. The sample was heat from ambient temperature up to 110 ^oC and hold for 10 min to release water content in biomass under 50 ml/min nitrogen supply. Dry sample was heat from 110 ^oC up to 900 ^oC at heating rate 10 ^oC/min.

Bagasse, leucaena and rice straw were test at same condition but change heating rate (5, 15 ^oC/min) to study heating rate effect of biomass degradation. After that, the data from experiment were used to determine kinetic parameter.

4.2.1.2 Biomass combustion

6 mg of bagasse, corn cob, empty fruit brunch, leucaena and rice straw were placed into a pan. The sample was heat from ambient temperature up to 110 ^oC and hold for 10 min to release water content in biomass under 50 ml/min of air (20% O_2, 80 % N_2) supply after that samples were heat from 110 ^oC up to 700 ^oC at heating rate 10 ^oC/min.

Bagasse, leucaena dnd rice straw were test at same condition but change heating rate (5, 15 ^oC/min). The data from experiment were used to study thermal behavior of biomass and determine kinetic parameter.

4.2.2 Kinetic of reaction analysis

In this work, both the model fitting method (one step global reaction model and independent reaction model, combustion model) method and the model fitting method (Ozawa-Flynn-wall method) were applied to study the kinetic of the reaction of the selected sample.

4.2.2.1 Model fitting method

4.2.2.1.1 One-step global reaction model

The one-step global reaction model is based on the first order of reaction applied to calculated the kinetic of the reaction of the selected biomass at both pyrolysis and combustion processes at heating rate 10 ^{o}C/min.

$$\frac{d\alpha}{dT} = \frac{A}{\phi} e^{-E/RT}(1-\alpha) \qquad \text{or}$$

$$\frac{d\alpha}{dt} x \frac{1}{(1-\alpha)} = Ae^{-E/RT}$$

By take natural log into Eq 1., the equation simplifies to:

$$\ln\left[\frac{d\alpha}{dT} x \frac{1}{(1-\alpha)}\right] = \ln\left(\frac{A}{\phi}\right) - \frac{E}{RT}$$

Follow from linear equation y= mx + c by assume pre exponential factor (A) is constant. Plot the left-hand part of Eq 2. versus 1/T. Activation energy (E) can be receive from slope and ln(A/φ) is an intercept y.

4.2.2.1.2 Independent parallel reaction model of biomass pyrolysis

The independent parallel reaction is based on the first order of the reaction model applied to finding kinetic parameters of biomass pyrolysis. Rate of conversion for N reaction can be described by:

$$-\frac{dm}{dt} = \sum_i c_i \frac{d\alpha}{dt} \qquad \text{where i = 1,2 .. N}$$

and conversion of each component is given by:

$$\alpha_i = \frac{m_{.0,i} - m_i}{m_{0,i} - m_{final,i}}$$

where $m_{0,i}$, m_i, and $m_{final,i}$ are initial mass, actual sample mass and final mass of component i, respectively. The components are all assumed to decompose individually according to:

$$\frac{d\alpha_i}{dt} = A_i e^{-E/RT}(1-\alpha_i)$$

Coefficient c_i express the contribution of the partial processes to the overall mass loss [9]:

$$c_i = m_{0,i} - m_{final,i}$$

4.2.2.1.3 Biomass combustion models (Barneto et al. (2010) [40])

$$S_H \xrightarrow{1} R_H + V_{H1}$$

$$S_C \xrightarrow{2} R_C + V_{C1}$$

$$R_{H+C} \xrightarrow{3O_2} V_{HC2}$$

$$S_L \xrightarrow{4} V_{L1}$$

$$S_L \rightarrow R_L \xrightarrow{5O_2} V_{L1}$$

Figure 4.1 Combustion diagram [40]

This model assumes the first stage degradation of biomass is an independent parallel reaction model but some new reactions have been added. For the holocellulosic (hemi-cellulose and cellulose) fraction two consecutive reactions are assumed. Product form first stage (parallel reaction) is char and volatile. The second reaction implies holocellulose char combustion in the presence of oxygen. For lignin fraction, best results have been obtained assuming two competitive reactions between volatization and char lignin combustion. From both assumptions two different in char is present. Morphological and porosimetric characteristics of each char types are different case of provoking differences in their combustions. the production of two different chars helps to explain the complex peak produced by char combustion. Degradation of each pseudo component were present in Fig 4.1. S_i, R_i and V_i represent the solid content of the initial fraction (holocellulose and lignin), chars and volatiles, respectively. Equations that describe biomass combustion are:

$$\frac{dV_{H1}}{dt} = k_{H1} V_{\infty H1} \left(1 - \frac{V_H}{V\infty_{H1}}\right)^{n_{H1}}$$

$$\frac{dV_{C1}}{dt} = k_{C1} V_{\infty C1} \left(1 - \frac{V_C}{V_{\infty C1}}\right)^{n_{C1}}$$

$$\frac{dV_{HC2}}{dt} = k_{HC2} V_{\infty HC2} \left(\frac{V_{H+C}}{V_{\infty H+C1}} - \frac{V_{HC2}}{V_{\infty HC2}}\right)^{n_{HC2}}$$

$$\frac{dV_{L1}}{dt} = k_{L1} V_{\infty L1} \left(1 - \frac{V_{L2}}{V_{\infty L1}}\right)^{n_{L1}}$$

$$\frac{dV_{L2}}{dt} = k_{L2} V_{\infty L2} \left(1 - \frac{V_{L2}}{V_{\infty L2}}\right)^{n_{L2}}$$

Where kinetic constants k_i are expressed by the Arrhenius equation, and in this work, all reaction orders are assume to be equal to 1 (n=1).

4.2.2.2 Free model fitting method

The Ozawa-Flynn-wall model (ASTM E1641) [41] was applied to study the kinetics of reactions of biomass. This method allows calculating activation energy (E) of each conversion. Standard equation of this method follows as:

$$\log(\phi) = \log\left(\frac{AE_\alpha}{Rg(\alpha)}\right) - 2.315 - 0.457\frac{E_\alpha}{RT_\alpha}$$

where T = temperature (K) at constant conversion.

Plotting log(φ) versus 1/T at different heating rate. Slope represent $0.457(E_\alpha/RT_\alpha)$ and pre-exponential base on first order of reaction follow from ASTM 1641.

CHAPTER 5
BIOMASS CHARACTERISTICS AND PROPERTIES RELATIONS

This chapter presents the biomass characteristics and properties relations by focusing on Thai biomass, such as proximate analysis, ultimate analysis, heating value, chemical structure, and element analysis. Biomass data collections as present in this work (Appendix A) are received from both experiment and other worked. Aims of this chapter is introduce biomass properties relation and establish a database of Thai biomass fuels that will support primary decision making in terms of energy conversion technology selection and operating conditions setting.

5.1 Proximate of Biomass

Biomass is high volatile matter (> 60 % dry basis) with high mass degradation at low temperatures and case of low heating values compare with fossil fuel. Percentage of ash content in biomass are vary between below 1% and can be up to higher than 30 % on dry basis as showed in Fig. 5.1.

In this figure, the biomass group is clearly separated from fossil fuels which have high fixed carbon and relation between composition and heating value were present. Increase of percentage of ash tends to increase of heating value. From Fig 5.2 (a) showed increases of 1% of ash reduce heating value approximately 0.17 MJ/kg dry basis. Similarly estimation values which report by Jenkins, B.M. (1989), [42] he present increases of 1% of ash in composition reduce the heating approximately 0.2 MJ/kg dry basis. In contrast to ash content, fixed carbon showed increase 1% elevating the heating value by approximately 0.2 MJ/kg (dry basis) as shown in Fig 5.2 (b).

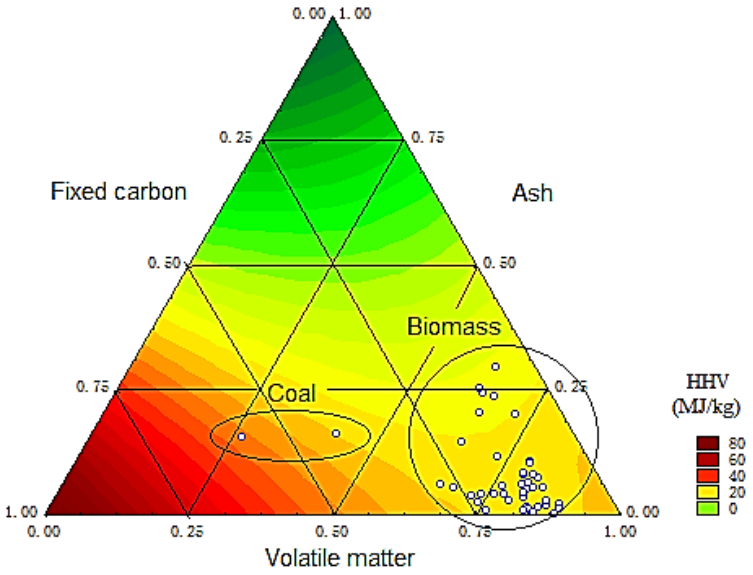

Figure 5.1 Triangle of proximate analysis of biomass

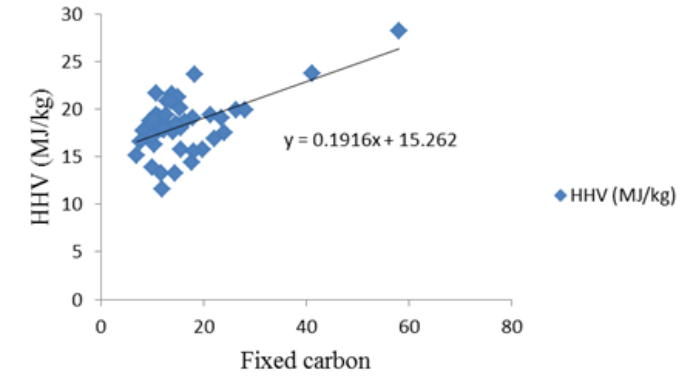

(a)

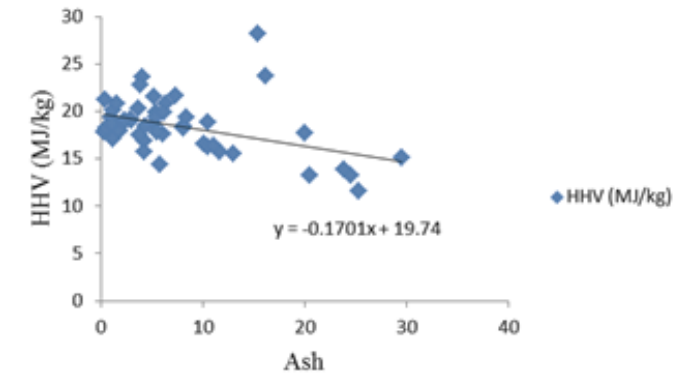

(b)

Figure 5.2 Proximate analysis composition of solid fuels versus HHV: (a) fixed carbon, (b) ash

As mentioned above, the composition of biomass from proximate analysis can be used to predict heating values. Some equations are used to calculation heating value from proximate analysis are shown in Table 5.1. In this table, correlation which develops from Sheng and Azevedo (2005) [43] showed highest accuracy (AE = 8.84 %) and error from proximate and HHV correlation are approximately 10 %. Low levels correlation between proximate analysis and HHV because it provides only the empirical composition of biomass. [43]

5.2 Ultimate analysis

Biomass is a low sulfur solid fuel and benefits when applied to biomass for thermal conversion equipment. Fossil fuels show low oxygen concentration (10 - 40 % d.a.f.) in composition and separate from biomass group which high oxygen content (40-50 % from lignocellulose structure) as shown in Fig 5.3. Carbon content of biomass is varied between (40-50 % d.a.f.). Both of biomass and coal contain hydrogen around 3-6 %. Other composition such as nitrogen and chorine contain in biomass below 5 %.

The qantities of main elemental composition in biomass have high correlation with heating value. 1% increased of carbon in composition showed increased of heating value approximately 0.34 MJ/kg (d.a.f.). This value is close to result that found by Jenkins, B.M. (1989), [42] he discuss that each 1% increase in carbon elevating the heating value by approximately 0.39 MJ/kg (d.a.f.). While oxygen content in biomass is directly reduce heating value as show in Fig 5.4 (b). Each 1% increased of oxygen translates roughly into a decrease of 0.36 MJ/kg (d.a.f.) because oxygen is not a reactive element.

Due to correlation as mentioned earlier, many researchers try to predict heating value form ultimate analysis and some correlation were shown in Table 5.1. From this table, correlation which propose by Sheng and Azevedo (2005) [43] has highest accuracy and correlation which propose by Demirbas (1997) [2]. However, HHV with calculate from ultimate analysis have high accuracy compare with other correlations.

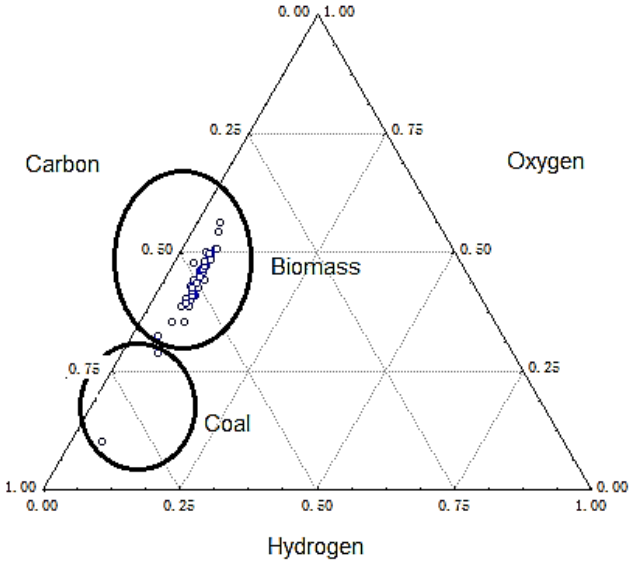

Figure 5.3 Compare chemical composition (Carbon, Hydrogen and Oxygen) contain in biomass

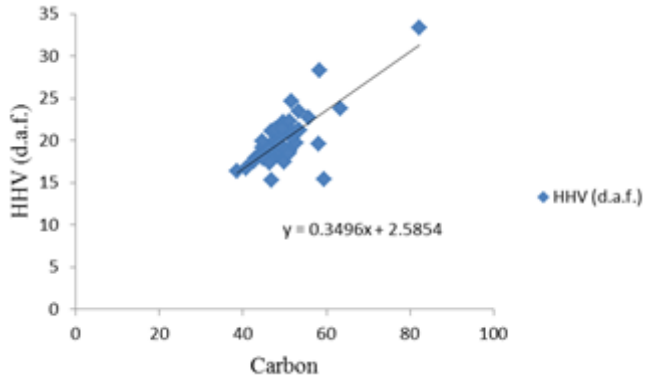

(a)

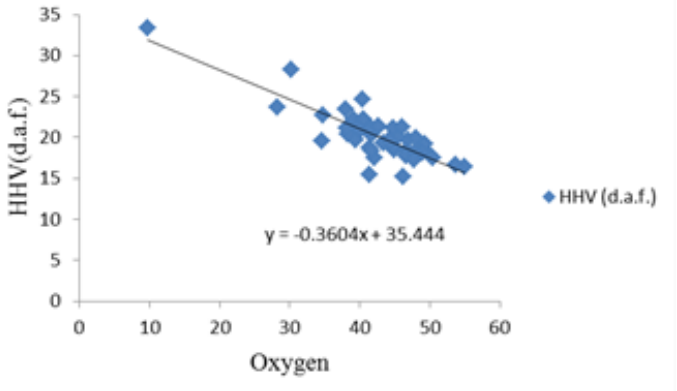

(b)

Figure 5.4 Ultimate analysis composition of solid fuels versus HHV: (a) carbon, (b) oxygen

5.3 Chemical structure

Cellulose, hemi-cellulose, and lignin are the main chemical structures contained in biomass. Different in chemical structure in various type of biomass show different degradation behavior. Cellulose and hemi-cellulose have high oxygen content (generic formula $(C_5H_8O_4)_n$ for hemi-cellulose and $(C_6H_{10}O_5)_n$ for cellulose) and correlate high volatile degradation at low temperature. Formula of lignin generally is complex aromatic hetero-polymers (C-C bond) which high lignin content tent to high fixed carbon as showed in Fig 5.5. Relation between main-pseudo components and high heating value were present in Fig 5.6.Various in chemical formula of each pseudo – components present different in energy contain (nearly 18.6 MJ/kg for cellulose and hemi-cellulose and 23.3–25.6 MJ/kg for lignin).[43]

Although chemical composition can be used for predict heating value of biomass as showed in Table 5.1, high error from these methods were present (> 11 %). The variation of the biomass components properties as well as the biomass chemical composition case of poor quality in correlation when apply chemical structure from predict heating value.[43]

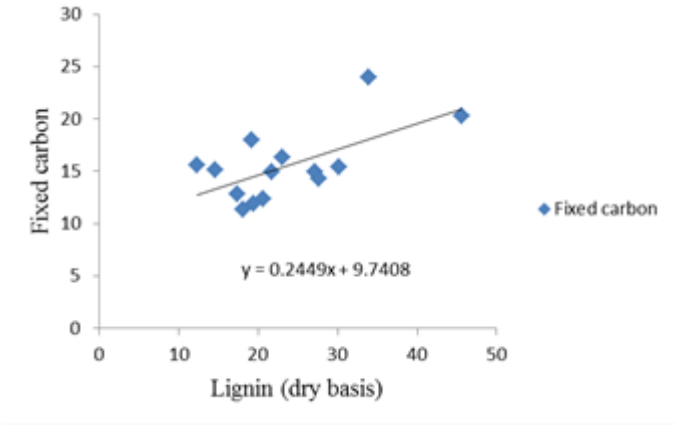

Figure 5.5 Lignin in biomass versus fixed carbon

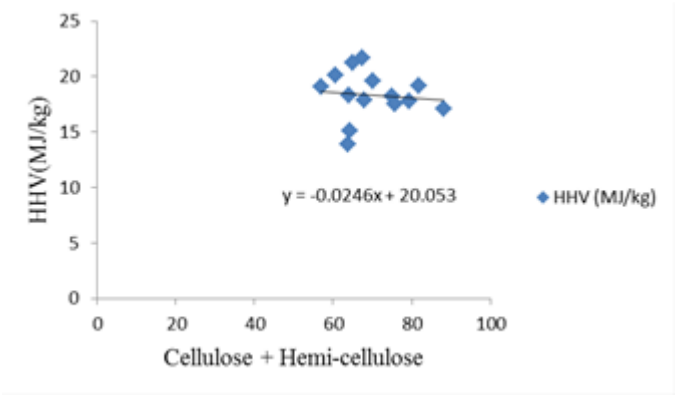

(a)

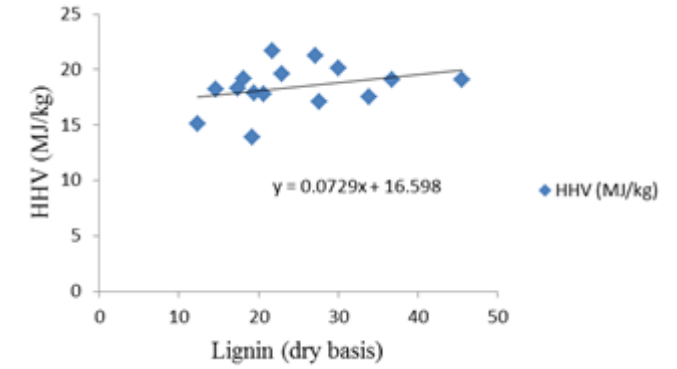

(b)

Figure 5.6 Chemical composition in biomass versus HHV: (a) holocellulose, (b) lignin

Table 5.1 HHV correlations and their evaluations[a]

Name of author	Correlation (HHV, MJ/kg)	Absolutely error	Ref.
Base on proximate analysis			
Jimennez and Gonzalez	HHV = -10.81408 + 0.3133(VM+FC)	10.10	[44]
Changdong Sheng and J.L.T. Azevedo	HHV = 19.914 – 0.2324 Ash	8.84	[43]
Demirbas	HHV = (0.196 x FC) + 14.119	12.25	[2]
Demirbas	HHV = (0.312 x FC) + (0.1534 x VM)	11.70	[2]
Cordero et al.	HHV = (0.3543 x FC) + (0.1707 x VM)	10.10	[45]
Changdong Sheng and J.L.T. Azevedo	HHV = -3.0368 + (0.2218 x VM) + (0.2601 x FC)	9.25	[43]
Nhuchhen and Salam	HHV = 19.2880 - (0.2135x(VM/FC))+ (0.0234x(FC/ASH))-(1.9584 x(ASH/VM))	9.86	[46]
Nhuchhen and Salam	HHV= 20.7999 –(0.3214x(VM/FC)) + (0.0051x$(VM/FC)^2$) - ((11.2277x$(Ash/VM)^3$) + (4.4953x $(Ash/VM)^2$) – (0.7223x$(ASH/VM)^3$) + (0.0383x$(Ash/VM)^4$) + (0.0076x(FC/Ash))	10.41	[46]
Base on ultimate analysis			
Tillman	HHV = (0.4373 x C) – 1.6701	7.07	[47]
Changdong Sheng and J.L.T. Azevedo	HHV = (0.3259 x C) +3.4597	6.48	[43]
Boie	HHV = (0.3516 x C) + (1.16225 x H) – (0.1109 x O) + (0.0628 x N) + (0.10465 x S)	8.74	[48]
IGT	HHV = (0.341 x C) + (1.323 x H) – (0.12 x O) – (0.12 x N) + (0.0686 x S) - (0.0153 x Ash)	9.20	[49]
Graboski and Bain	HHV = (0.328 x C) + (1.4306 x H) – (0.0237 x N) – (0.0929 x S) - ((1-Ash/100) x (40.11 H/C)) + 0.3466	7.82	[50]
Channiwala and Parikh	HHV = (0.3491 x C) + (1.1783 x H) + (0.1005 x S) – (0.1034 x O) - (0.0151 x N) – (0.0211 x Ash)	8.82	[51]
Demirbas	HHV = (0.335 x C) + (1.423 x H) – (0.154 x O) – (0.145 x N)	11.82	[2]
Jenkins	HHV = - 0.763 + (0.301 x C) + (0.525 x H) + (0.064 x O)	6.99	[52]
Based on chemical composition[b]			
Shafizadeh and Degroot	HHV = (0.1739 x Ce) + (0.2663 x L) + (0.3219 x E)	11.68	[53]
Jimennez and Gonzalez	HHV = [1-Ash/(100 - Ash)] x (0.1739Ce + 0.2663L + 0.3219E)	11.22	[44]
Demirbas[c]	HHV = 0.0889L + 16.8218	12.64	[54]

[a]Biomass composition, VM, FC, Ash, C, H, O, N, S are weight percent on dry biomass basis.

[b]Ce, L, E are weight percent of cellulose (including cellulose and hemicellulose), lignin and extractives on dry biomass basis, respectively.

[c]HHV and L in this equation are on dry ash free and extractable-free bases.

5.4 Ash deposition

Uncertainties of ash composition were found in biomass. Low sulfur content is biomass characteristic that is different from fossil fuels. However, herbaceous plants have high chorine content (i.e. 0.58 dry basis of rice straw). Ash content in biomass can be case of slagging, fouling and high temperature corrosion at fireside in boiler/furnace.

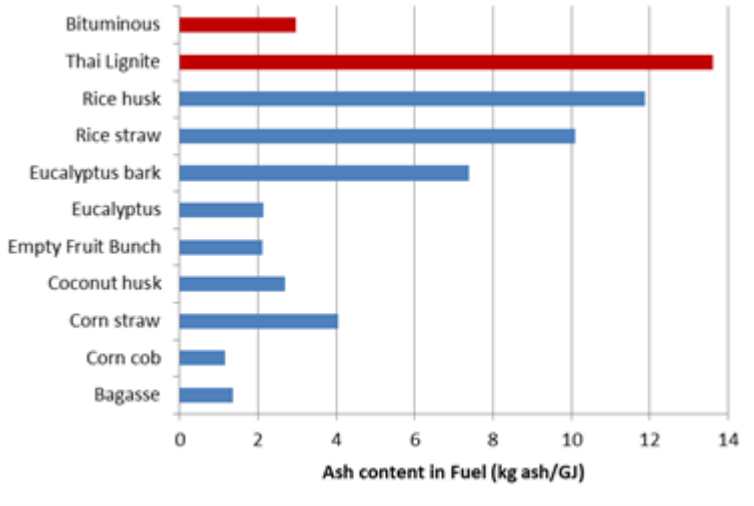

Figure 5.7 Ash content of some solid fuel.

In Fig 5.7, Thai lignite showed highest ash content and corncob showed lowest ash content when compare ash deposition per heat unit input (kg ash/GJ). Ash deposition in fuel per heat unit of eucalyptus, empty fruit bunch, coconut husk, corn cob and bagasse are lower than bituminous which high grade fossil fuel. Rice husk, rice straw, eucalyptus bark, corn straw and Thai have high ash content and tent to high risk of ash problem. However, for high accuracy prediction of slagging, fouling and high temperature corrosion have to consider mineral deposition, chlorine and sulfur content in biomass.

For predict ash behavior, ash indices were present in this work. In Table 5.2 showed ash indices of some solid fuels. Bituminous showed low risk slagging tendency. Thai lignite showed high risk slagging tendency however, BAI index of Thai lignite is in green area which mean it low rick Bed agglomeration in fluidize bed. For biomass Eucalyptus bark and Empty fruit bunch showed high risk slagging tendency. Mainly ash indices of rice husk which highest ash content showed low risk slagging tendency. However BAI index and alkaline index showed extremely rick bed agglomeration and

slagging tendency. This results can be explained by each index consider in different element composition. Used of multiple indices will make the assessment more accurate.

Table 5.2 Slagging indices of some biomass

low risk high risk extremely risk

Type	B/A	B/A_{+P}	$R_{B/A}$	BAI	F_u	S_R	AI (GJ/kg)
Bagasse	0.40	0.44	0.34	2.86	1.98	67.99	0.08
Corn cob	1.42	1.55	0.15	0.03	68.11	86.77	0.55
Corn straw	0.72	0.77	0.39	0.14	13.52	70.08	0.76
Coconut husk	-	-	1.07	0.17	-	21.20	0.03
Empty Fruit Bunch	-	-	2.061	0.07	-	30.35	1.17
Eucalyptus	-	-	1.024	0.17	-	47.96	0.06
Eucalyptus bark	6.10	6.28	5.31	0.10	68.04	12.58	0.82
Rice straw	0.25	0.27	0.07	0.06	3.30	93.01	1.34
Rice husk	0.07	0.08	0.03	0.09	0.32	97.50	0.52
Thai Lignite	0.99	0.99	0.93	5.44	2.67	46.54	0.37
Bituminous	0.15	0.15	0.14	5.97	0.16	80.29	0.03

- Data collection not available for calculation

CHAPTER 6
THERMAL BEHAVIOR OF BIOMASS

This chapter present the thermal degradation behavior of some biomass for both pyrolysis and combustion by TGA. One step global reaction model, independent reaction model, biomass combustion model and Ozawa-Flynn-Wall method were chosen to find kinetic parameter in the work.

6.1 Thermal Behavior of Biomass Pyrolysis

Five types of Thai biomass (Bagasse, Corn cob, Empty fruit brunch, leucaena, and rice straw) were tested by TGA at heating rate 10 ^{o}C/min under nitrogen atmosphere. TG-curve and DTG-curve of samples were shown in Fig 6.1, residual mass of sample during temperature range between room temperature to 110 ^{O}C was neglect able by assume mass degradation are mass lose from moisture release and no reaction occur at this temperature range [33, 34]. It can be classify thermal behavior of dry sample into two main stages. First stage, which high mass degradation rate, is main volatilization of hemi-cellulose and cellulose and second stage is main degradation of lignin. [22, 34, 55] Di Blasi, (2007) [56] discuss about thermal behavior of biomass pyrolysis. Although for each zone a main contributor can be identified as hemicellulose, cellulose and lignin. It is impossible to avoid overlap between the different components in the measured TG-curves. The simultaneous participation of the other components cannot be avoided with an extent that depends on the biomass characteristics and the severity of the conversion conditions and cannot apply degradation behavior of single component to explain degradation of biomass directly because of chemical and physical alterations introduces in the separation procedure of each component. Each type of biomass has unique degradation behaviors as shown in Fig 6.1 for biomass pyrolysis and Fig. 6.4 for biomass combustion. Physical texture (the distribution of hemicellulose, cellulose, lignin, and minerals in biomass) and chemical structures (e.g. functional groups and chemical bonds) have to consider simultaneously when study thermal behavior of biomass. [14]

Compare thermal behavior of biomass pyrolysis when increased at different heating rate were shown in Fig 6.2 (a), the result showed each step degradation of biomass sample

tend to broader in temperature range and degradation rate (-dm/dt) increase when heating rate increased. This phenomena can be explain by each type of biomass contain individual pseudo component and each component has individual decomposition behavior which mass degradation of each stage required different temperature range in the pyrolysis process. At high heating rate, the combination peak of mass degradation may be occurring. It can be explain by heat and mass limitation. With increase heating rate, the temperature in furnace space can be little higher as the temperature of particle and the rate of decomposition are higher than release of volatile. While at same temperature region, higher heating rate has shot reaction time and sample required more time for decomposition case of shift maximum rate curve to higher temperature. Effect from heat transfer limitation, temperature gradients at particle surface can be a bit higher than corn temperature, case of different in mass decomposition process. [57, 58] Although increasing heating rate keeps the reaction occurring at a higher temperature but the time required for degradation is substantially reduced, as shown in Fig 6.2 (b).

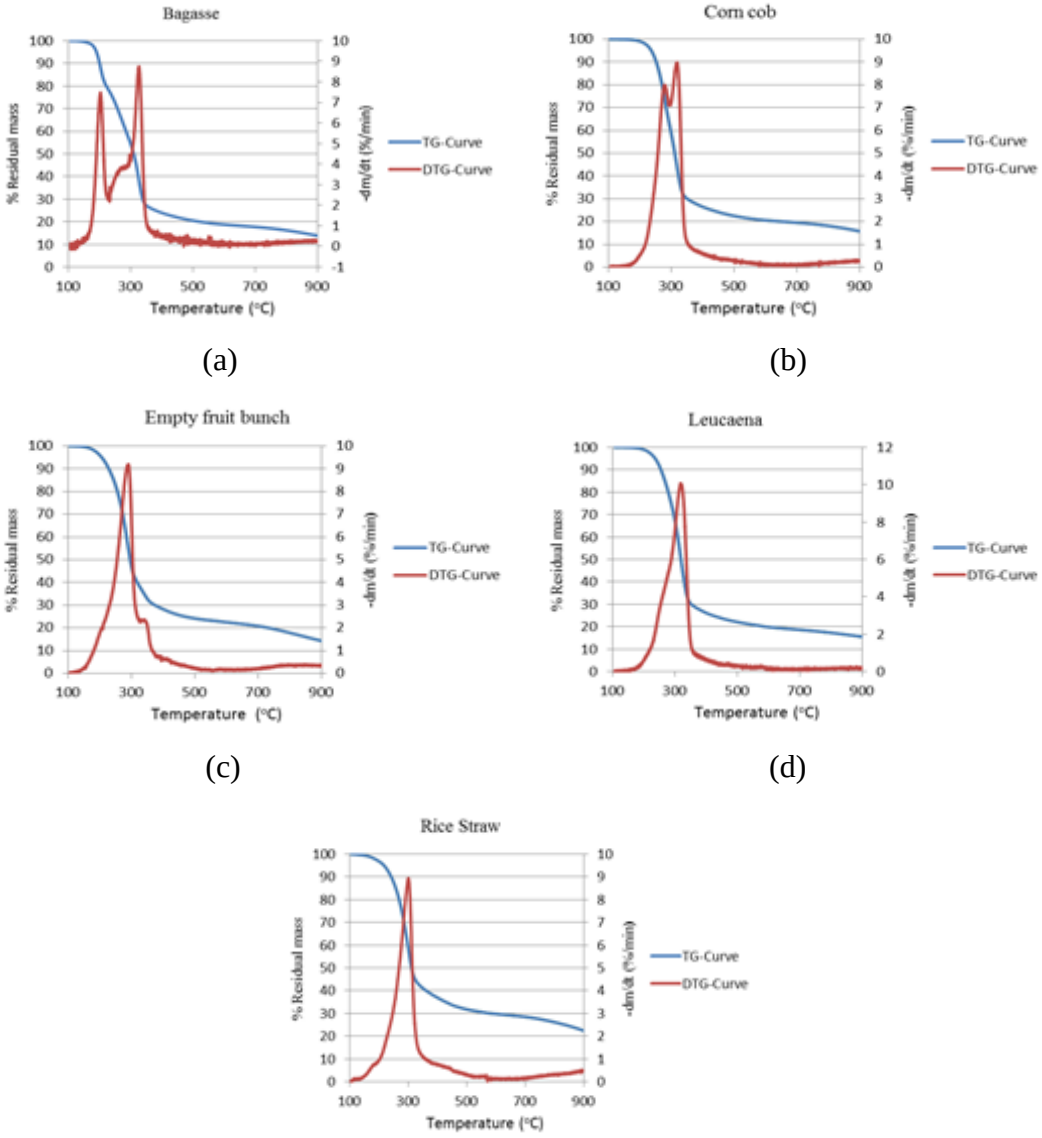

Figure 6.1 TG-DTG curves of biomass pyrolysis at heating rate 10 ^{o}C/min; (a) Bagasse, (b) Corn cob, (c) Empty fruit bunch, (d) Leucaena , (e) Rice straw

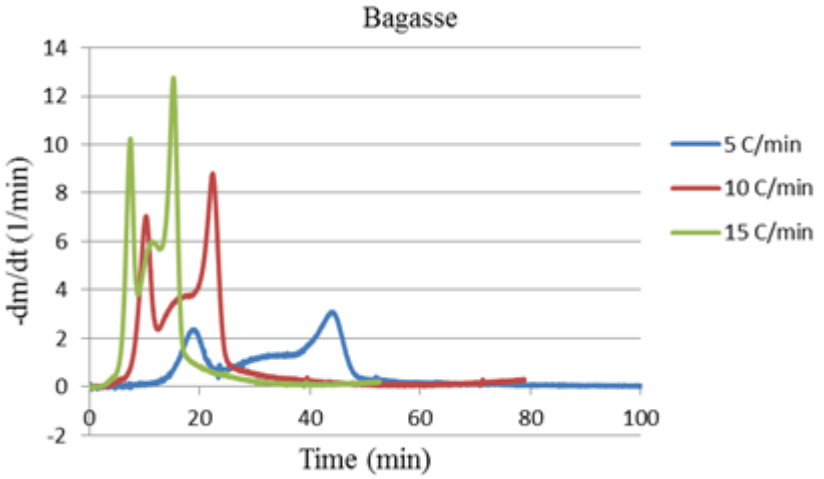

(a)

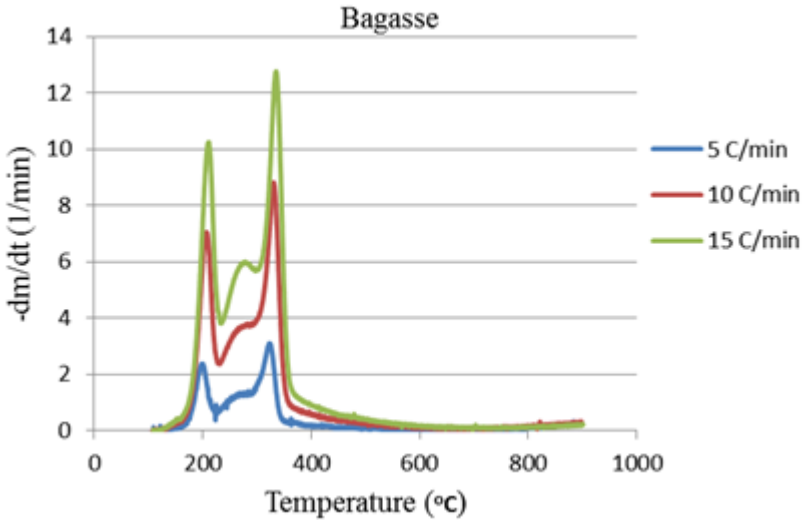

(b)

Figure 6.2 Compare thermal behavior of bagasse pyrolysis at different heating rates: (a) DTG-curve in function of time, (b) DTG-curve in function of temperature.

In Fig 6.3, the first stage of biomass volatilization occurs in a temperature range around 120-350 ^{o}C after that is the decomposition of lignin and char formation. Bagasse is first stat decomposition and highest mass degradation in first stage, rice straw is lowest mass loss and DTG-curve show only single peak in first stage and highest derivative peak is degradation at first stage of leucaena. In second stage, Rice straw showed first start decomposition, leucaena has lowest percentage of mass degradation in this stage and empty fruit bunch has highest percentage of mass loss in this stage. Empty fruit bunch required longest residual time in volatilization stage. Different in pseudo composition in

biomass plays a significant effect in residual time because each pseudo component occur at specific degradation temperature and require time to heat sample into reaction temperature.

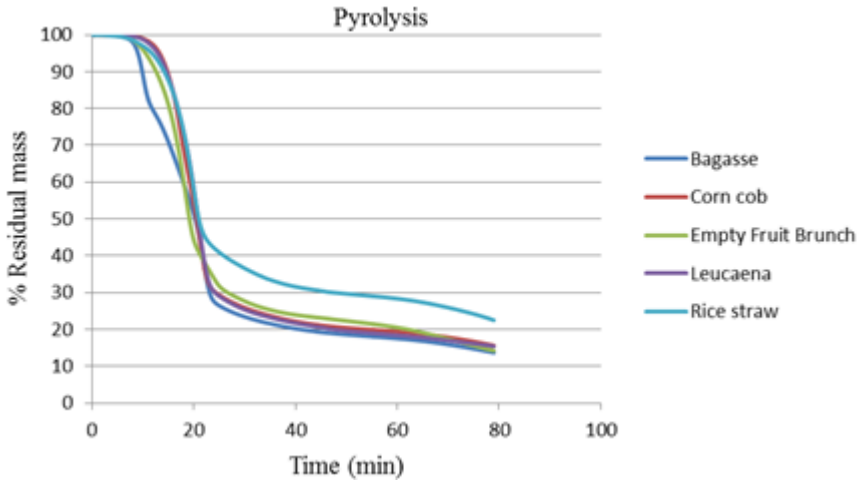

(a)

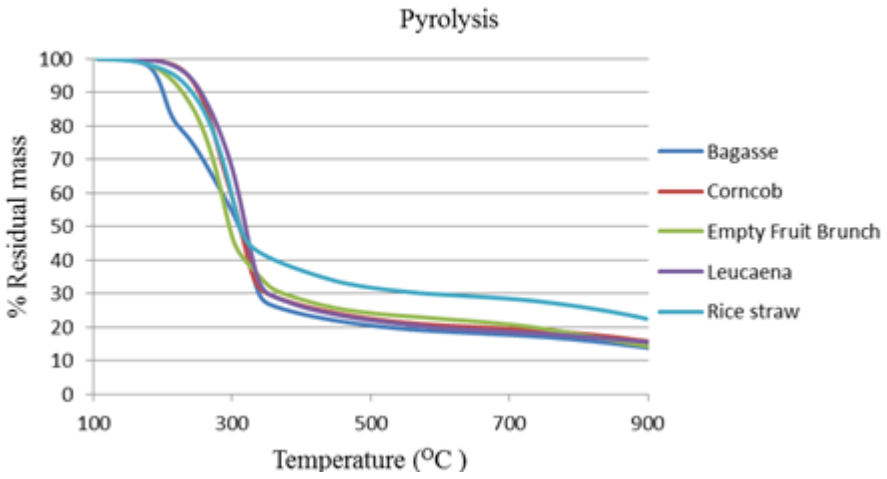

(b)

Figure 6.3 Compare thermal behavior of biomass samples pyrolysis at heating rates 10°C/min: (a) TG-curve in function of time, (b) TG-curve in function of temperature.

Table 6.1 Degradation stages of sample pyrolysis at heating rate 10 ^{o}C/min

Type	First stage		Second stage		DTG Peak 1		DTG Peak 2	
	Temp. range (^{o}C)	% Mass loss	Temp. range (^{o}C)	% Mass loss	Temp. Peak	-dm/dt (%/min)	Temp. Peak	-dm/dt (%/min)
Bagasse	121-348	72.25	348-900	14.07	203.56	7.48	326	8.71
Corn cob	132-350	69.82	350-900	14.56	275.86	7.80	314.84	8.82
Empty fruit bunch	125-365	69.22	365-900	16.58	284.61	8.98	333.18	2.32
Leucaena	150-360	70.82	360-900	13.80	317.57	10.07	-	-
Rice straw	128-340	57.72	340-900	15.07	301.14	8.94	-	-

6.2 Thermal Behavior of Biomass Combustion

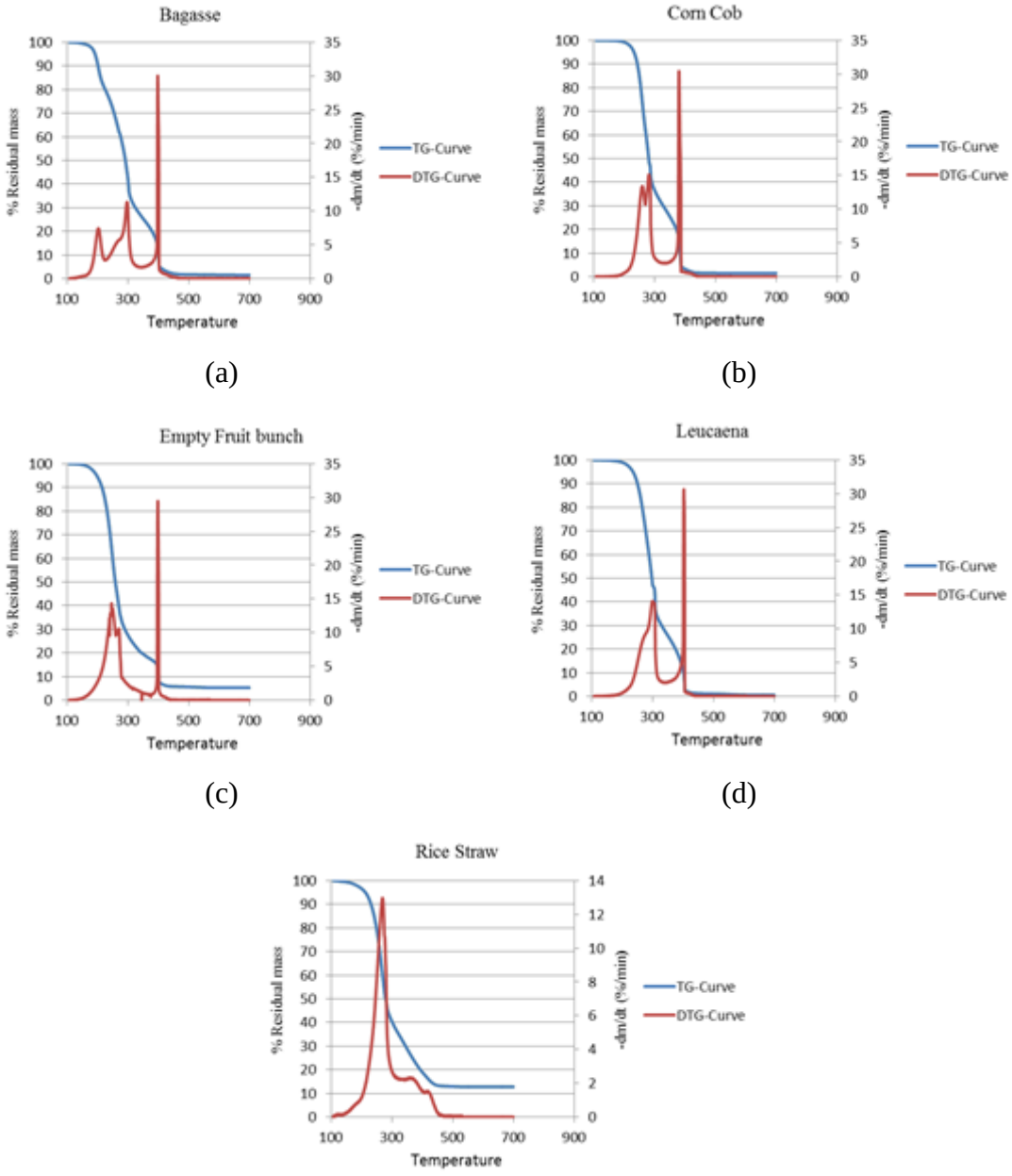

Figure 6.4 TG-DTG curves of biomass combustion at heating rate 10 ^{o}C/min; (a) Bagasse, (b) Corn cob, (c) Empty fruit bunch, (d) Leucaena , (e) Rice straw.

TG-DTG curves of biomass samples in atmospheric air environment a shown in Fig 6.4. Thermal behavior during combustion of biomass can be classified into two main stages. First staged, which high mass degradation, descript volatile matter combustion

(decomposition of hemi-cellulose and cellulose), and another one is main combustion of lignin and char combustion stage. However, both of volatilization and char combustion cannot separate completely.[23, 33, 59] For pure components, hemi-celluose star decompose at low temperature (147-335) and char combustion at 350 – 550 ^{o}C, cellulose decompose at 253 ^{o}C and char celluloses combust at 335- 482 ^{o}C. For lignin, first stage degradation occur at 287 - 306 ^{o}C) and char lignin decompose at 306- 449 ^{o}C. [23] This result confirms that high DTG peak at high temperature represent co-degradation of holo-cellulose (cellulose + hemi-cellulose) and lignin char combustion.

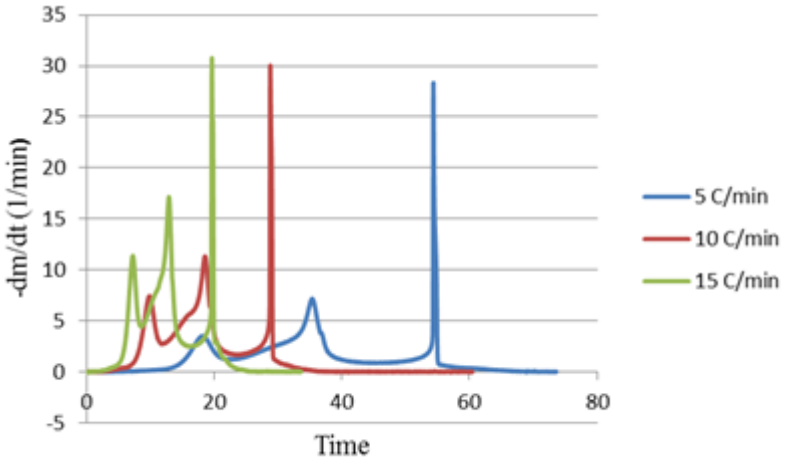

(a)

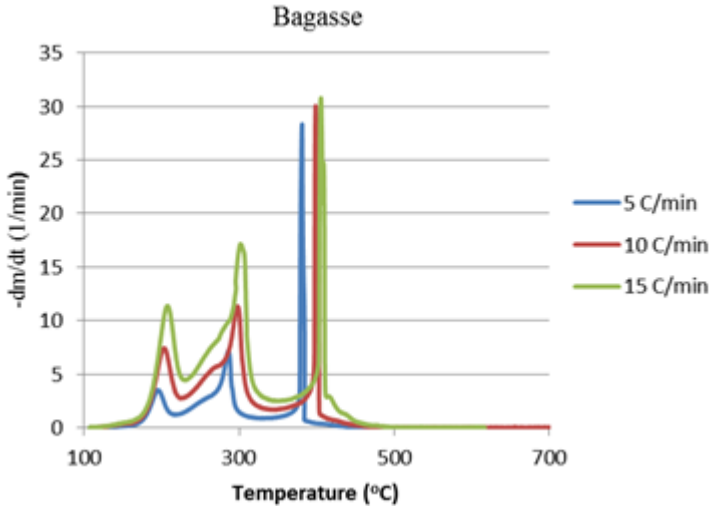

(b)

Figure 6.5 Compare thermal behavior of bagasse combustion at different heating rates: (a) DTG-curve in function of time, (b) DTG-curve in function of temperature.

Thermal behavior of bagasse combustion at different heating rate is shown in Fig 6.5. From this figure, step degradation of biomass tends to occur at higher temperature and DTG peak increase when increase heating rate which similar degradation behavior of biomass pyrolysis. The decomposition behavior of biomass combustion versus time when increased heating rate is clearly shown in Fig 6.5 (a) which decomposition of each pseudo-component occurs at specific temperature and extended conversion.

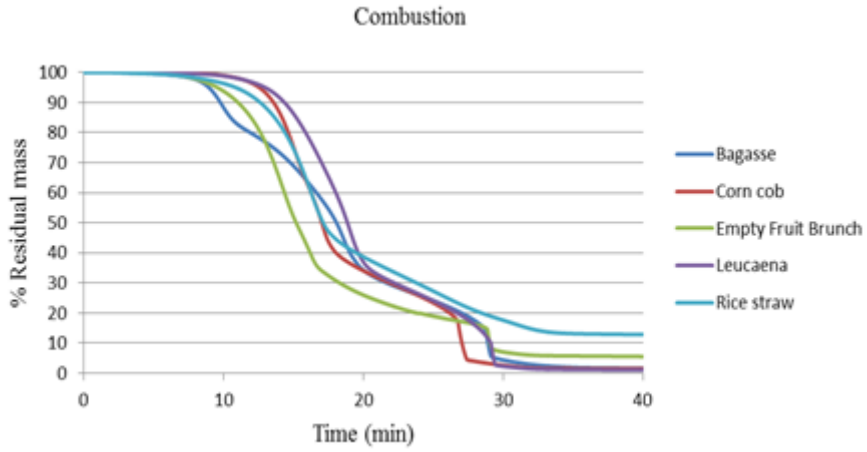

(a)

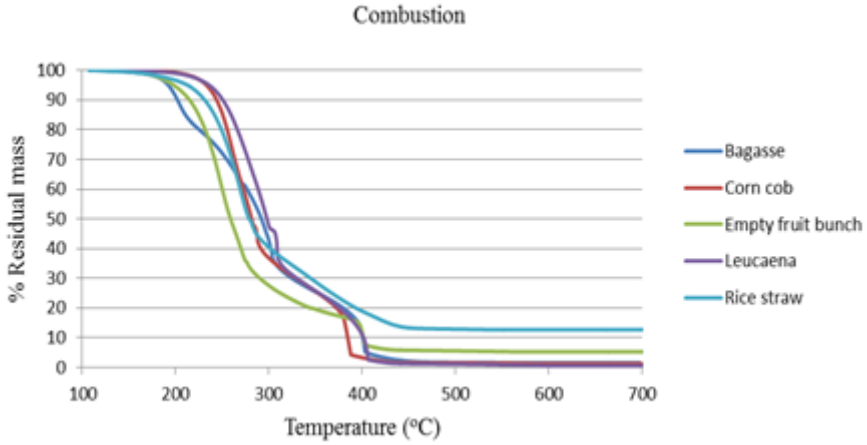

(b)

Figure 6.6 Compare thermal behavior of biomass samples combustion at heating rate 10 ^{o}C/min: (a) TG-curve in function of time, (b) TG-curve in function of temperature.

In Fig 6.6, the first stage of biomass combustion occurs at temperatures higher than 120 ^{o}C and the second stage occurs in temperature around 300 ^{o}C. Rice straw shows first start volatile highest decomposition but required highest combustion time for complete

char combustion. Empty fruit bunch showed lowest time required for volatilization combustion stage, contrast from first stage degradation of empty fruit brunch pyrolysis which slowest time required for volatile degradation. Bagasse showed slowest complete combustion process at 475 ^{o}C.

Morphology has high effect in biomass combustion. Gani and Naruse (2007), [60] performed morphology of cellulose, lignin and biomass. They results showed cellulose chemical fibrous and porous structure. In contrast, morphology of lignin is lumpy solid. Morphology of the actual biomass is still to be fibrous and porous and oxygen can diffuse easily inside the particle during combustion.

Ignition temperature, temperature of the surface at the time of ignition, of each sample was calculated from separated point when plot TG-curve during pyrolysis versus combustion as show in Fig 6.7. [61] Bagasse shows highest ignition temperature and lowest ignition temperature is empty fruit bunch.

Compare thermal behavior of biomass during pyrolysis and combustion as shown in Fig 6.7. In volatilization stage, degradation behaviors of biomass combustion likely close to degradation behavior of pyrolysis but initial reaction temperature tend to shift to occur at lower temperature. Primary DTG-peak decreased by about 5 ^{o}C , 20 ^{o}C, 38 ^{o}C, 20 ^{o}C, 34 ^{o}C of bagasse, corn cob, leucaena, empty fruit bunch, and rice straw, respectively. In second stage, degradation behavior of biomass combustion descripts char and lignin combustion. During combustion process, degradation main pseudo component of biomass are easy to separated, different from pyrolysis which degradation of each individual component overlapped severely.

Table 6.2 Degradation stages of sample Combustion at heating rate 10 ^{o}C/min

Type	First stage					Second stage					
	Temp. range	DTG peak temp.1 (^{o}C)	-dm/dt (% 1/min)	DTG peak temp.2 (^{o}C)	-dm/dt (% 1/min)	Temp. range	DTG peak temp.1 (^{o}C)	-dm/dt (% 1/min)	DTG peak temp.2 (^{o}C)	-dm/dt (% 1/min)	Ignition temp. (C^{o})
Bagasse	140-320	199.29	6.28	295.01	10.66	320-475	398.52	30.02	-	-	245
Corn cob	170-310	256.50	12.05	279.41	14.22	310-445	380.78	30.41	-	-	220
Empty fruit bunch	130-280	246.46	14.33	257.24	10.76	280-441	398.98	29.49	-	-	184
Leucaena	170-320	297.80	13.76	-	-	320-442	403.14	30.65	-	-	232
Rice straw	120-310	267.07	13.80	-	-	310-470	356.26	2.34	413.07	1.47	227

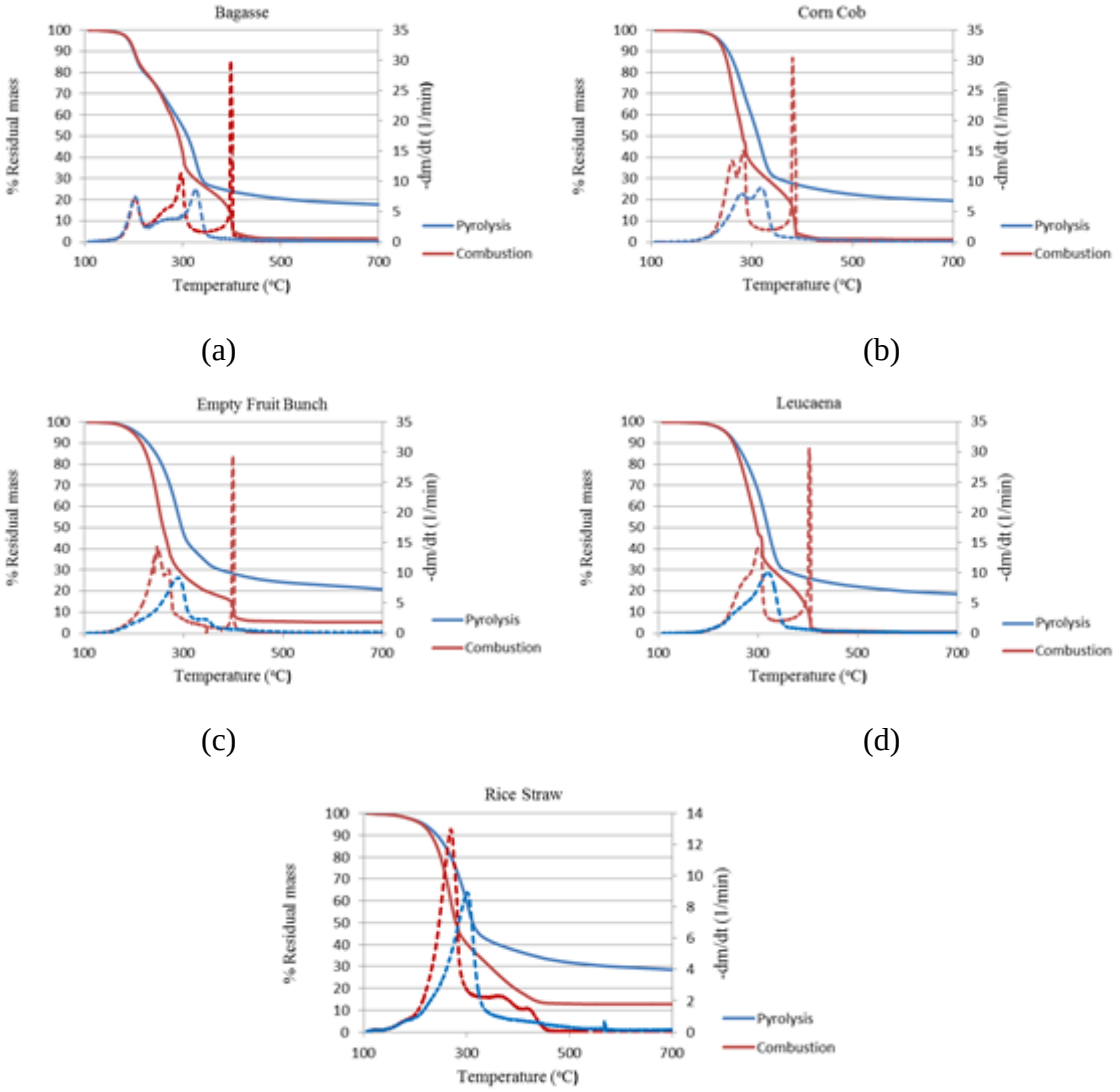

Figure 6.7 Comparison of TG-DTG curves of biomass between pyrolysis and combustion at heating rate 10 ^{o}C/min : (a) Bagasse, (b) Corn cob, (c) Empty fruit bunch, (d) Leucaena, (e) Rice straw.

6.3 Kinetic analysis of biomass

6.3.1 Model fitting method

6.3.1.1 One step global reaction of biomass pyrolysis

Kinetic parameters of biomass samples based on one step global reaction and first order reaction model are shown in Table 6.3 and Fig 6.8 shows the TG-curve of sample form experiment versus mathematical calculation. Activation energy from this model is in the range between 49-89 kJ/mole.

Table 6.3 Kinetic parameter of sample pyrolysis base on one step global reaction model.

Type of biomass	E (kJ/mole)	ln(A)
Bagasse	49.12	6.01
Corn cob	89.00	15.11
Empty fruit bunch	62.72	9.49
Leucaena	75.41	11.67
Rice straw	51.51	6.61

The main thermal behavior that can be explained by this model is degradation in volatilization stage but less to describe in second stage. This can be explained by biomass is non-homogeneous substance and each component has individual degradation behavior. In Fig 6.8 show one step global reaction and first order reaction cannot describe the degradation behavior of biomass overall temperature range.

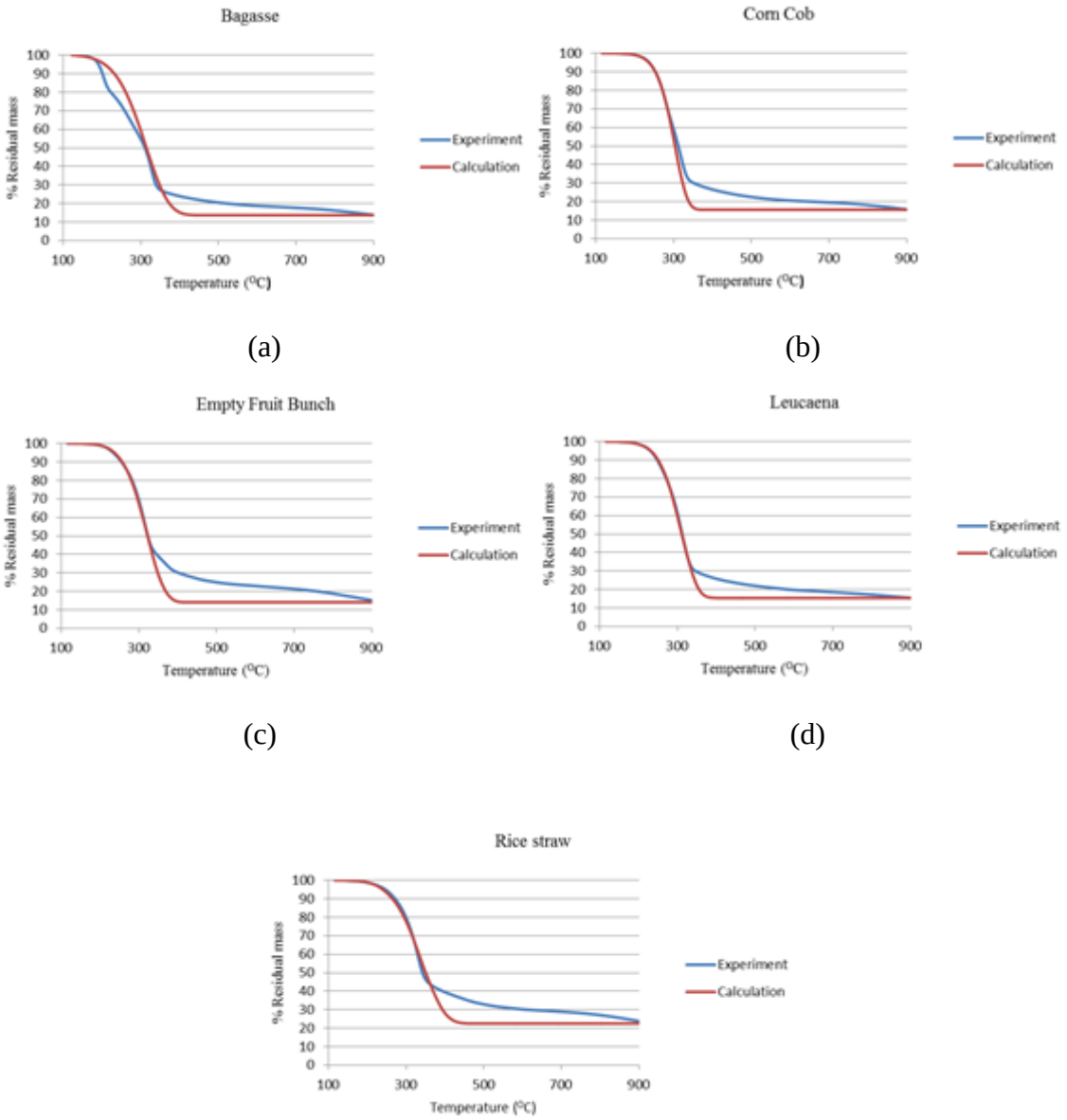

Figure 6.8 Comparison between experiment and calculation of sample pyrolysis at heating rate 10 ^{o}C/min based on one step global reaction model: (a) Bagasse, (b) Corn cob, (c) Empty fruit bunch, (d) Leucaena, (e) Rice straw.

6.3.1.2 One step global reaction of biomass combustion

Kinetic parameters of five samples based on one step global and first order of reaction model as shown in Table 6.4

Table 6.4 Kinetic parameter of sample combustion base on one step global reaction model.

Type	E (kJ/mole)	lnA (1/min)
Bagasse	42.82	4.44
Corn cob	57.24	7.59
Empty fruit bunch	47.62	6.00
Leucaena	64.00	8.92
Rice straw	33.73	2.38

Activation energy of biomass during combustion is lower than pyrolysis. High fixed carbon content in biomass showed low activation energy. In this work, leucaena has highest activation energy (64 kJ/mole) and lowest is rice straw (33.73 kJ/mole). Similarly value which report by Fang et al. (2013) [62] They work showed base on first order of reaction, the activation energy is in the range of 53.6-65.2 kJ/mole for biomass combustion.

Base on one step global reaction model and first order of reaction mechanism, less correlation between experimental and calculation were present both biomass pyrolysis and combustion. Biomass degradation behavior is complex process which depends on temperature and extended conversion. However, the advantage of this method is can be used to find overall degradation rate of biomass and comparison reactivity of each biomass. High value of activation energy represents the decomposition of the less reactive components in biomass.[63]

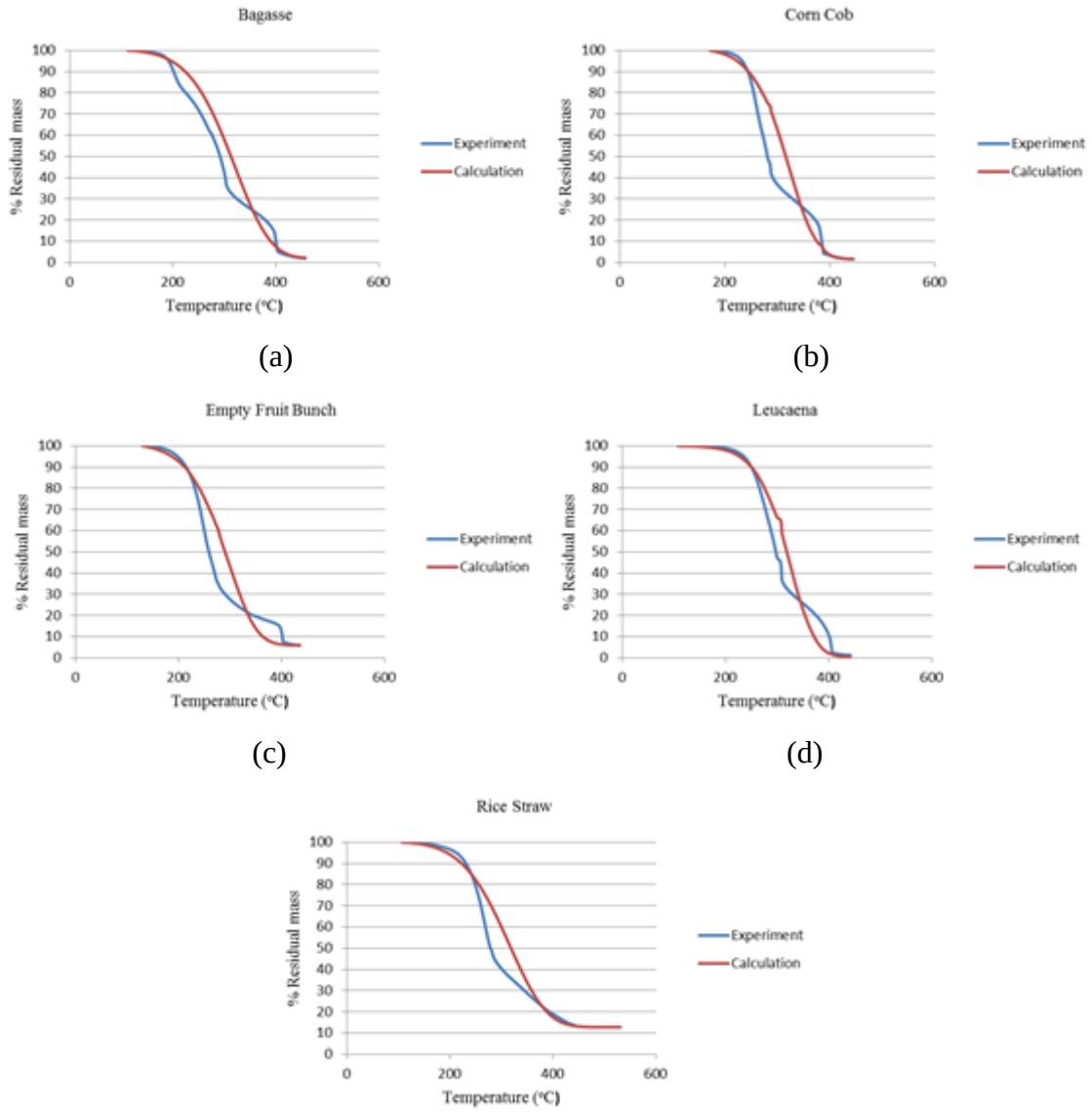

Figure 6.9 Comparison between experiment and calculation of sample combustion at heating rate 10 ^{o}C/min based on one step global reaction model: (a) Bagasse, (b) Corn cob, (c) Empty fruit bunch, (d) Leucaena, (e) Rice straw.

6.3.1.3 Independent parallel reaction model of biomass pyrolysis

Five types of biomass were analyzed by kinetic parameters by independent parallel reaction model. Kinetic parameter of each sample was shown in Table 6.5. Activation energy of lignin, cellulose and hemi-cellulose are 30 – 63 kJ/mole, 107-150 kJ/mole and 66-92 kJ/mole, respectively. This value close to results as reported in [64],

[65], [63]. However, Di blasel (2008), [56] recommended during pyrolysis activation energy of hemi-cellulose, cellulose and lignin are 80 -116 kJ/mole, 195–286 kJ/mole and 18–65 kJ/mole, respectively. This explained by in this work, order of reaction of each component are assume equal 1 (n=1).

Several studies present differences in order of reaction. Aboyade et al (2011), [63] performed reaction orders of pseudo component in biomass. Reaction order of hemi-cellulose is lower than one (0.66-0.88) and cellulose is higher than one (1.16-1.26). Lignin pyrolysis is more complex and reaction order close to 3rd order of reaction. Different from Di blasel (2008), [56] which performed order are comprised between 0.8 and 1.8. Song et al (2007), [64] present order of reactions of biomass base on independent reaction model and *n* order of reaction are 1.00 – 4.00. The fact that different in calculation techniques is case of different in reaction order.

Nonetheless, considering practical utilization, the advantages of independent parallel reaction base of first order reaction are its simple function and well known parameters of reaction scale. [63]

Different type of biomass content different partial pseudo component which case of different in degradation behavior.[9],[22] In Fig. 6.10 experimental and calculation values form independent parallel reaction models are close to. First component is degradation of hemi-cellulose which occurs at temperature around 120 ^{o}C and second is degradation of cellulose which occurs at temperature around 200 ^{o}C. The third component corresponding to the decomposition of lignin appears over a wide temperature range (> 250 ^{o}C). Compare with degradation temperature pure component, hemi-cellulose decomposes at 149 – 315 ^{o}C, cellulose decomposes at 258 – 305 and lignin decomposes at temperature higher than 250 ^{o}C. [23],[56]. Vårhegyi et al (1997), [66]discussed about inorganic salts in biomass effect to degradation of cellulose decompose at lower temperature. Ash has to be diminished by acid washing or hot water washing procedures and test TGA. They results showed degradation behavior of cellulose component is close to degradation of pure cellulose samples.

This result confirmed that the degradation of biomass pyrolysis depended on the degradation behavior of the main pseudo-components and reasonable for apply parallel reaction model to descripted thermal behavior of biomass.

Table 6.5 Kinetic parameters of sample pyrolysis based on independent parallel reaction model

Type of biomass	Component	E (kJ/mole)	ln(A)	%c
Bagasse	lignin	39.00	4.80	0.11
	Cellulose	150.69	29.71	0.39
	Hemi-cellulose	91.50	21.96	0.30
Corncob	lignin	42.00	4.50	0.10
	Cellulose	115.74	23.15	0.34
	Hemi-cellulose	80.16	15.54	0.36
Empty fruit bunch	lignin	47.00	6.28	0.14
	Cellulose	86.54	17.38	0.54
	Hemi-cellulose	66.87	14.05	0.09
Leucaena	lignin	63.08	8.26	0.08
	Cellulose	142.75	28.17	0.56
	Hemi-cellulose	68.50	14.03	0.18
Rice straw	lignin	35.53	3.78	0.15
	Cellulose	107.20	21.90	0.50
	Hemi-cellulose	92.00	21.90	0.10

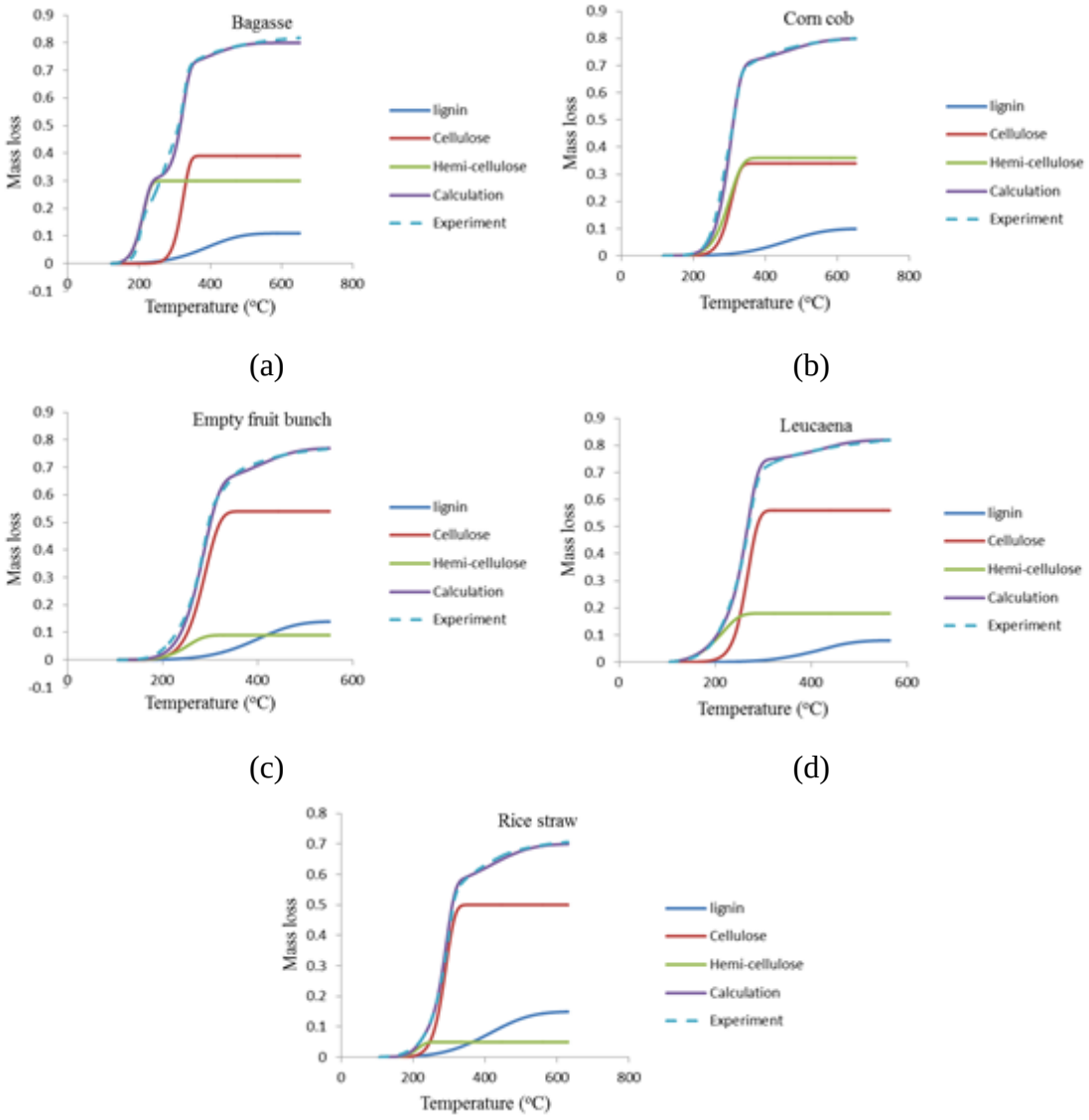

Figure 6.10 Comparison between experimental and calculations of samples pyrolysis at heating rate 10 ^{o}C/min base on independent parallel reaction model: (a) Bagasse, (b) Corn cob, (c) Empty fruit bunch, (d) Leucaena, (e) Rice straw.

6.3.1.4 Biomass combustion models (Barneto et al. (2010) [40])

The results of kinetic parameters from biomass combustion model are shown in Table 6.6. Activation energy of hemi-cellulose is 60 – 100 kJ/mole, cellulose is 111 – 147 kJ/mole and lignin is 27 – 77 kJ/mole. These results are lower than biomass pyrolysis. Corresponding to TG –curve which showed first stage of biomass combustion occurs at

lower temperature compare with biomass pyrolysis, in other words, degradation of pseudo component combustion occur easier than biomass pyrolysis.

Activation energy of helo-cellulose char of samples are 148 – 150 kJ/mole and lignin char are 158 kJ/mole (131 kJ/mole for rice straw). Similar results were presented by Barneto et al (2010).[40] Low activation energy of rice straw were present in this works, this phenomenon may be affected from high mineral matter content in rice straw as mentioned earlier.

Fig. 11 shows the comparison between experimental curve and calculation. High accuracy is present. It can be conclude that biomass combustion model have high efficient to predict degradation behavior of biomass.

Table 6.6 Kinetic parameters of sample combustion base on biomass combustion model.

Type	Component	E (kJ/mole)	ln(A)	%c
Bagasse	Char lignin	158.60	26.87	0.05
	Char holo-cellulose	151.86	26.14	0.19
	Lignin	28.23	4.26	0.12
	Cellulose	111.50	22.676	0.41
	Hemi-cellulose	100.38	23.8	0.22
Corncob	Char lignin	158.6	26.87	0.04
	Char holo-cellulose	148.57	26.14	0.24
	Lignin	65.32	12.6	0.26
	Cellulose	137.69	29.44	0.26
	Hemi-cellulose	95.13	20.27	0.19
Empty fruit bunch	Char lignin	158.6	26.871	0.03
	Char holo-cellulose	152.7	27.8	0.14
	Lignin	27.18	3.37	0.17
	Cellulose	147.37	32.38	0.22
	Hemi-cellulose	100.3	22.52	0.40
Leucaena	Char lignin	158.60	26.87	0.03
	Char holo-cellulose	150.57	26.14	0.17
	Lignin	31.03	3.80	0.20
	Cellulose	113.27	23.32	0.33
	Hemi-cellulose	90.04	19.27	0.27
Rice straw	Char lignin	131.64	22.07	0.10
	Char holo-cellulose	149.55	26.14	0.03
	Lignin	77.11	14.06	0.19
	Cellulose	130.63	28.48	0.50
	Hemi-cellulose	60.00	12.44	0.06

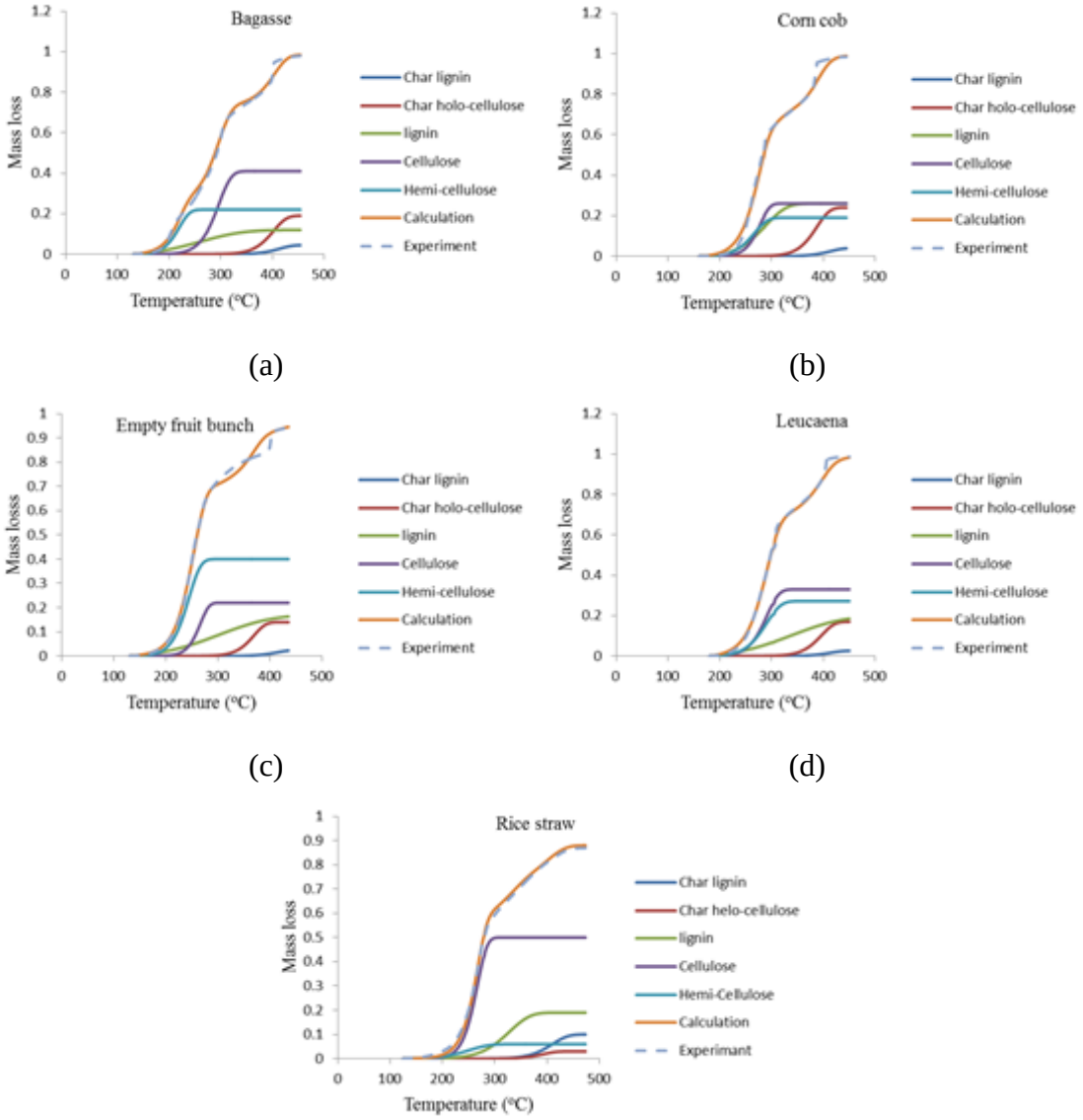

Figure 6.11 Comparison between experiments and calculations of samples combustion at heating rate 10 ^{o}C/min base on biomass combustion model: (a) Bagasse, (b) Corn cob, (c) Empty fruit bunch, (d) Leucaena, (e) Rice straw.

6.3.2 Isoconversional method

6.3.2.1 Isoconversional method of biomass pyrolysis (Ozawa-Fynn-Wall method (ASTM E1641))

Bagasse, Leucaena and rice straw were chosen for the study of the kinetics of the reaction under the Ozawa-Fynn-wall method. Kinetic parameters are shown in Table 6.7. Bagasse showed wide range of activation energy (80.32 -207.73 kJ/mole). Activation energies of bagasse at initial degradation are low and highest at mid of conversion after

that the values are reduced. Activation energies of leucaena vary from highest value (181.39 kJ/mole) at initial stage and lowest value (138.43 kJ/mole) at the end of conversion. Activation energies of rice straw vary between 174.94 kJ/mole at mid of conversion and highest value (201.19 kJ/mole) at initial stage.

Table 6.7 Kinetic parameters of sample pyrolysis base on Ozawa-Fynn-Wall method.

α	E (kJ/mole)	A (1/min)
	Bagasse	
0.1	80.3274	3.43E+07
0.2	91.53046	6.56E+08
0.3	132.081	4.26E+12
0.4	170.1394	8.52E+15
0.5	207.7317	8.52E+18
0.6	206.8579	1.88E+18
0.7	193.4411	5.96E+16
0.8	190.2735	2.22E+16
0.9	158.5504	1.03E+13
	Leucaena	
0.1	181.3879	1.07E+17
0.2	177.6706	1.77E+16
0.3	171.1661	2.04E+15
0.4	176.5109	3.74E+15
0.5	175.9903	2.31E+15
0.6	175.6062	1.65E+15
0.7	176.4745	1.57E+15
0.8	176.9897	1.33E+15
0.9	138.4344	1.46E+11
	Rice straw	
0.1	201.1973	7.56E+19
0.2	198.0104	7.05E+18
0.3	188.4313	3.30E+17
0.4	180.0294	4.44E+15
0.5	174.9414	6.53E+15
0.6	182.0686	2.26E+16
0.7	192.5945	1.53E+17
0.8	191.2313	4.52E+16
0.9	188.2655	5.93E+14

The apparent activation energies of selected biomass obtained from this study were in agreement with other researches. [67-69] Compared between experimental conversion curve and measurement (In Fig 6.12), high accuracy predictions were present.

The low activation energy of bagasse at the initial stage suggests low initial degradation temperature as compared to leucaena and rice straw. Limitation of kinetic analysis from ASTM E1641 is assumed reaction mechanism of sample base on first order of reaction and this method and model develop for homogeneous substance. Complex degradation behavior of biomass as showed in DTG-curve case of various range of activation energy value. Consider value of pre exponential factor of all experiment, it’s cannot be assumed as a constant for the pyrolysis of biomass by using Ozawa-Fynn-Wall method.

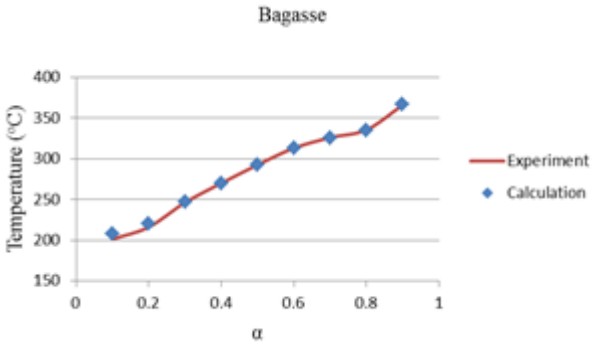

(a)

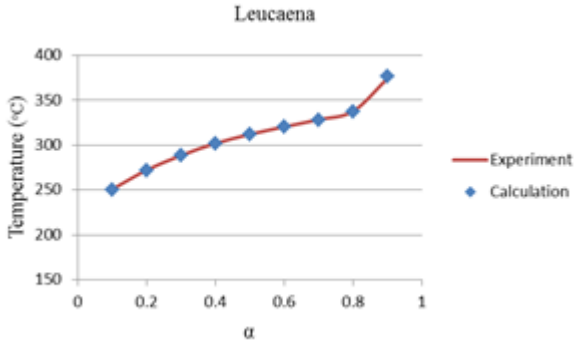

(b)

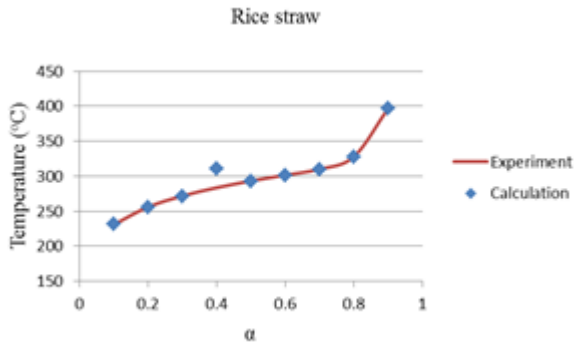

(c)

Figure 6.12 Compare the conversion of simple pyrolysis experiment and Ozawa-Fynn-Wall method of calculation at heating rate 10 ^{o}C/min: (a) Bagasse, (b) Leucaena, (c) Rice straw.

6.3.2.2 Isoconversional method of biomass combustion (Ozawa-Fynn-Wall method (ASTM E1641))

As shown in Table 6.8, the apparent value of activation energy is about 153.41 – 517.17 kJ/mole, 179.61–310.93 kJ/mole and 103.87-200.02 kJ/mole of bagasse, leucaena

and rice straw, respectively. High activation energy value at initial stage of bagasse is case of high ignition temperature compare with leucaena and rice straw. The results showed that the reaction mechanisms are not the same in all conversion and dependent on extended conversion.[70]

Table 6.8 Kinetic parameter of sample combustion based on Ozawa-Fynn-Wall method.

α	E (kJ/mole)	A (1/min)
	Bagasse	
0.1	203.7267	2.54E+22
0.2	517.1719	8.90E+54
0.3	335.1086	1.86E+33
0.4	294.0939	6.91E+27
0.5	205.0374	3.86E+18
0.6	157.0831	4.63E+13
0.7	239.007	3.01E+20
0.8	197.4825	1.06E+15
0.9	153.4112	3.58E+10
	Leucaena	
0.1	217.4711	5.31E+20
0.2	201.4329	5.81E+18
0.3	203.0895	5.42E+18
0.4	205.6564	5.31E+18
0.5	217.2162	4.40E+19
0.6	200.0858	6.32E+17
0.7	224.1521	3.24E+19
0.8	179.6057	3.04E+14
0.9	310.933	2.45E+24
	Rice straw	
0.1	200.0163	7.27E+19
0.2	178.0611	1.73E+17
0.3	164.9959	5.82E+15
0.4	156.4522	6.82E+14
0.5	145.6694	6.42E+13
0.6	138.7138	1.62E+13
0.7	116.8238	4.93E+10
0.8	104.0331	4.56E+08
0.9	103.871	1.76E+08

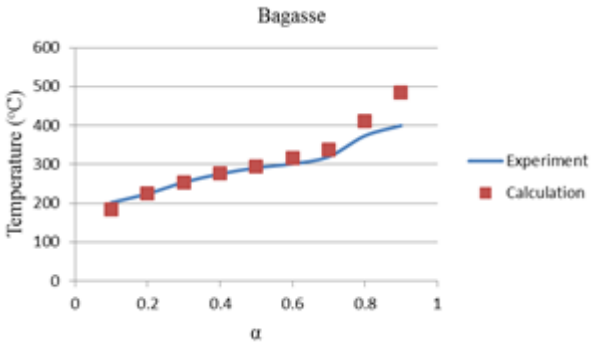

(a)

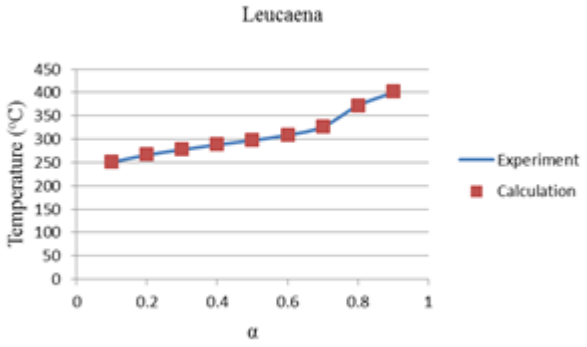

(b)

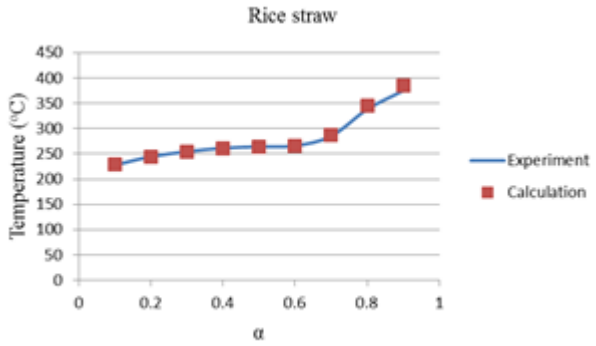

(c)

Figure 6.13 Compare conversion of simple combustion experiment and Ozawa-Fynn-Wall method calculation at heating rate 10 ^{o}C/min: (a) Bagasse, (b) Leucaena, (c) Rice straw.

The advantages when calculating activation energy from isoconversion method are it can be used to describe degradation behavior at any heating rate, high accuracy and can be calculated activation energy without assuming reaction mechanism before. However, of this method are require more data (at less 3 run at different heating rate) for calculated and cannot be explained degradation phenomena (i.e. one step reaction, parallel reaction, two step consecutive reaction, etc.) of biomass.

Each kinetic method used to describe the thermal behavior of biomass both pyrolysis and combustion process give different results. Biomass fuels are heterogeneous substance and sensitive to experimental condition, material characteristics and kinetic models. To compare kinetic parameter of biomass should be comparative in same kinetic method. [39]

CHAPTER 7
CONCLUSION

7.1 Thesis Summary

Biomass has low heating value (13 – 22 kJ/kg) when compared with fossil fuels. High oxygen and low sulfur contain in chemical composition are characterized of biomass. From proximate analysis, biomass has high volatile (volatile of hemi-cellulose and cellulose) matter and low fixed carbon deposition. Correlation between HHV and biomass characteristic showed estimate value from ultimate analysis has highest accuracy and estimate value from chemical structure are very poor, because variation of the biomass components properties as well as the biomass chemical composition.

Cellulose, hemi-cellulose, and lignin are main pseudo component contain in biomass. Different in pseudo deposition in various type of biomass and each pseudo has owned individual degradation behavior. However, thermal behavior of biomass can't descript by chemical structure only. Alkali/ alkaline earth play significant effect (inert catalytic) on thermal behavior during thermal process.

Ash is the impurities which content in biomass. Element concentrations in biomass consist Si, Al, Fe, Ca, Mg, Mn, Na, K, P, S and Cl. Slagging indices are widely used for predict ash behavior in biomass. However, slagging indices develop for coal industrial and each index consider in different element composition. Used of multiple indices will make the assessment more accurate. In addition, boiler technology has direct correlation with ash formation and have to consider when predict ash behavior.

The TGA experiment showed that when increasing the heating rate both pyrolysis and combustion showed each step degradation of biomass sample tend to broader in temperature range and degradation rate (dm/dt) increase when heating rate increased. For pyrolysis process of biomass can be classify into two stages. First stage, which high mass degradation rate, is main volatilization of hemi-cellulose and cellulose and second stage is main degradation of lignin. In combustion experiment showed two stages combustion. First staged, which high mass degradation, describe main volatile combustion of hemi-cellulose and cellulose anther one is main combustion of lignin char combustion stage. Differential of thermal decomposition of each type of biomass required different suitable

operation condition. The use of biomass fuel for effective energy utilization had to consider suitable operation condition of each biomass.

Kinetic of reaction of biomass can be calculated by both isoconversional method and model fitting method. Both pyrolysis and combustion experiment base on one step global reaction base on first order of reaction mechanism show high error when apply for explain degradation behavior but can be used to primary prediction material degradation lifetime. Parallel reaction model, biomass combustion model and Ozawa-Flynn-wall method can be descripted thermal behavior over all temperature range. However, parallel reaction model and biomass combustion model is not reliable to describe degradation behavior when heating rate change. Each kinetic method which used to describe thermal behavior of biomass both pyrolysis and combustion process give different results, when compare kinetic parameter of biomass should be comparative in same method.

7.2 Recommendation for Future Work

The dissolution of ash deposition during thermal conversion, effect of mineral matter and co-firing behavior of biomass should be studied and discussed.

REFFERENCES

[1]. Grover, V.I., Grover V.K. , and Hogland W. (2002), *Recovering energy from waste: various aspects*.: Science Publishers, Inc., USA.

[2]. Demirbaş, A. (1997), Calculation of higher heating values of biomass fuels. *Fuel*, **76**, 5,pp. 431-434.

[3]. Yin, C.Y. (2011), Prediction of higher heating values of biomass from proximate and ultimate analyses, *Fuel*, **90**, 3, pp. 1128-1132.

[4]. Klass, D.L. (1998), *Biomass for renewable energy, fuels, and chemicals*, Academic press.

[5]. Suwannakhanthi, N. (2004), Overview for Thailand's Renewable Energy focusing on Biomass Energy. *Information for the Commercialisation of Renewables in ASEAN (ICRA*).

[6]. Jenkins B., Baxter L.L., Miles Jr. T.R., Miles T.R., (1998), Combustion properties of biomass, *Fuel processing technology*, **54**, 1, pp. 17-46.

[7]. Gaur, S. and Reed T.B. (1998), *Thermal data for natural and synthetic fuels*.

[8]. Vassilev S.V., Baxter D., Andersen L.K., Vassileva C.G., (2010), An overview of the chemical composition of biomass. *Fuel*, **89**, 5, pp. 913-933.

[9]. Grønli, M.G. (1996), A theoretical and experimental study of the thermal degradation of biomass.

[10]. Wang L., Hustad J.E., Skreiberg Ø., Skjevrak G., Grønli M., (2012), A critical review on additives to reduce ash related operation problems in biomass combustion applications. *Energy Procedia*, **20**, pp. 20-29.

[11]. Bryers, R.W. (1996), Fireside slagging, fouling, and high-temperature corrosion of heat-transfer surface due to impurities in steam-raising fuels. *Progress in energy and combustion science*,**22,** 1, pp. 29-120.

[12]. Miles T.R., Miles Jr. T.R., Baxter L.L., Bryers R.W., Jenkins B.M., Oden L.L. (1995), Alkali deposits found in biomass power plants: A preliminary investigation of their extent and nature. Vol 1. National Techrucd Momation Service (NTIS), U.S.

[13]. Shao Y., Wang J., Preto F., Zhu J., Xu C.C. (2012), Ash deposition in biomass combustion or co-firing for power/heat generation, *Energies*, **5** ,12, pp. 5171-5189.

[14]. Sonobe T. and Worasuwannarak N. (2008), Kinetic analyses of biomass pyrolysis using the distributed activation energy model. *Fuel*, **87**, 3, pp. 414-421.

[15]. Vamvuka D., Troulinos S., Kastanaki E. (2006), The effect of mineral matter on the physical and chemical activation of low rank coal and biomass material, *Fuel*, **85,** 12, pp. 1763-1771.

[16]. BISYPLAN (2012), The ash composition, in *The Bioenergy System Planners Handbook*.

[17]. López, Ch., Unterberger S., Maier J., Hein K.R.G. (2003), Overview of Actual Methods for Characterization of Ash Depostion, in ECI Conference on Heat Exchanger Fouling and Cleaning: Fundamentals and Applications, Art, *Engineering Conferences International*, New Mexico, USA.

[18]. Gulyurtlu, I., et al. (2008), Prediction of slagging and fouling tendency of biomass co-firing in fluidized bed combustion. in *Proceedings of Proceedings of 9th International Conference on Circulating Fluidized Beds*.

[19]. MUNIR S. (2010), Potential slagging and fouling problems associated with biomass-coal blends in coal-fired boilers. *Journal of the Pakistan Institute of Chemical Engineers*, **38,** 1.

[20]. Plaza P. (2013), *The development of a slagging and fouling predictive methodology for large scale pulverised boilers fired with coal/biomass blends*., Cardiff University.

[21]. Goethem D.V., (2010)," Promising Biofuel Resources: Lignocellulose and Algae". Available from: http://www.nature.com/scitable/topicpage/promising-biofuel-resources-lignocellulose-and-algae-14255919.

[22]. Skreiberg A., Skreiberg Ø. Sandquist J. Sørum L. (2011), TGA and macro-TGA characterisation of biomass fuels and fuel mixtures, *Fuel*, **90**, 6, pp. 2182-2197.

[23]. Cheng K., Winter W.T., Stipanovic A.J. (2012), A modulated-TGA approach to the kinetics of lignocellulosic biomass pyrolysis/combustion. *Polymer Degradation and Stability*,. **97**, 9, pp. 1606-1615.

[24]. Basu P. (2013), *Biomass gasification, pyrolysis and torrefaction: practical design and theory*. Academic press.

[25]. EI-Wakil M.M.,(1984), *Power plant Technology*., McGraw-Hill, Inc. Singapore.

[26]. Jenkins B.M., Ebeling J.M. (1985), Thermochemical properties of biomass fuels. *California Agriculture*,. **39**, 5/6, pp. 14-16.

[27]. Department of Energy, U.S. (2010), ″Technologies – Gasification". Available from: http://physics.oregonstate.edu/~hetheriw/energy/topics/doc/elec/biomass/Options%20for%20Producing%20Biocrude%20Oils.htm.

[28]. Indus industries (2010), "Biomass Gasification Power Plant". Available from: http://www.mrindus.com/157-biomass-gasification-power-plant.html

[29]. Department of Energy, U.S. (2010), ″Biomass Energy - Biopower". Available from: http://www1.eere.energy.gov/tribalenergy/guide/biomass_biopower.html.

[30]. GOLD A. (2014), "Biomass".; Available from: http://acgoldenergy.co.uk/biofuel.

[31]. Stevens C. and Brown R.C. (2011), *Thermochemical processing of biomass: conversion into fuels, chemicals and power*, Vol. 12, John Wiley & Sons.

[32]. Brown M.E. (2001), *Introduction to thermal analysis: techniques and applications*, Vol. 1, Springer.

[33]. Vuthaluru H. (2004), *T*hermal behaviour of coal/biomass blends during co-pyrolysis. *Fuel Processing Technology*, **85**, 2, pp. 141-155.

[34]. Raveendran K., Ganesh A., Khilar K.C. (1996), Pyrolysis characteristics of biomass and biomass component, *Fuel*, **75**, 8, pp. 987-998.

[35]. Yang H., Yan R., Chen H., Lee D.H., Zheng C. (2007), Characteristics of hemicellulose, cellulose and lignin pyrolysis, *Fuel*, **86**, 12, pp. 1781-1788.

[36]. Raman P., Walawender W.P., Fan L.T., Howell J.A., (1981), Thermogravimetric analysis of biomass. Devolatilization studies on feedlot manure. *Industrial & Engineering Chemistry Process Design and Development*, **20**, 4, pp. 630-636.

[37]. Vyazovkin S., Burnham A.K, Criado J.M., Pérez-Maqueda L.A., Popescu C., Sbirrazzuoli N (2011), ICTAC Kinetics Committee recommendations for performing kinetic computations on thermal analysis data. *Thermochimica Acta*, **520**, 1, pp. 1-19.

[38]. Weerachanchai P., Tangsathitkulchai C., Tangsathitkulchai M. (2010), Comparison of pyrolysis kinetic models for thermogravimetric analysis of biomass, *Suranaree JSci Technol*, **17**, pp. 387-400.

[39]. Kok M.V. and Özgür E. (2013), Thermal analysis and kinetics of biomass samples. *Fuel Processing Technology*, **106**, pp. 739-743.

[40]. Barneto A.G., Carmona J.A., Conesa Ferrer J.A., Díaz Blanco M.J. (2010), Kinetic study on the thermal degradation of a biomass and its compost: Composting effect on hydrogen production, *Fuel*, **89**, 2, pp. 462-473.

[41]. Standard, A., E1641-07 (2012), *Standard test method for Decomposition Kinetics by Thermogravimetry*, ASTM, International, West Conshohocken.

[42]. Jenkins B. (1989), Physical properties of biomass. *Biomass handbook*, pp. 860-891.

[43]. Sheng C. and Azevedo J. (2005), Estimating the higher heating value of biomass fuels from basic analysis data. *Biomass and Bioenergy*, **28**, 5, pp. 499-507.

[44]. Jiménez, L. and González F. (1991), Study of the physical and chemical properties of lignocellulosic residues with a view to the production of fuels. *Fuel*, **70**,8, pp. 947-950.

[45]. Cordero T., Marquez F., Rodriguez-Mirasol J., Rodriguez J.J. (2001), Predicting heating values of lignocellulosics and carbonaceous materials from proximate analysis. *Fuel*, **80**, 11, pp. 1567-1571.

[46]. Nhuchhen D.R. and Abdul Salam P. (2012), Estimation of higher heating value of biomass from proximate analysis: A new approach. *Fuel*, **99**, pp. 55-63.

[47]. Tillman D.A., (1978), *Wood as an energy resource*, New York: Academic Press.

[48]. Annamalai K., Sweeten J., Ramalingam S. (1987), Estimation of gross heating values of biomass fuels. *Trans ASAE*, **30**, pp. 1205-1208.

[49]. Technology., I.o.G. (1978), *Coal conversion systems technical data book*, VA: Available from NTIS,Springfield.

[50]. Graboski M. and Bain R. (1979), Properties of biomass relevant to gasification. *A Survey of Biomass Gasification*, **2**, pp. 21-65.

[51]. Channiwala S. and Parikh P. (2002), A unified correlation for estimating HHV of solid, liquid and gaseous fuels. *Fuel*, **81**, 8, pp. 1051-1063.

[52]. Jenkins, B. and Ebeling J. (1985), Correlation of physical and chemical properties of terrestrial biomass with conversion, *Proceedings of 1985 Symposium Energy from Biomass and Waste IX IGT*, California. p. 371.

[53]. Shafizadeh F., Sarkanen K.V., Tillman D.A., (1976), *Thermal uses and properties of carbohydrates and lignins*, Acadamic press , Inc.

[54]. Demirbaş A. (2001), Relationships between lignin contents and heating values of biomass, *Energy conversion and management*, **42**, 2, pp. 183-188.

[55]. Reina J., Velo E., Puigjaner L. (1998), Thermogravimetric study of the pyrolysis of waste wood. Thermochimica acta, **320,** 1, pp. 161-167.

[56]. Di Blasi C. (2008), Modeling chemical and physical processes of wood and biomass pyrolysis, *Progress in Energy and Combustion Science*, **34**, 1, pp. 47-90.

[57]. Ounas A., Aboulkas A., Bacaoui A., Yaacoubi A. (2011), Pyrolysis of olive residue and sugar cane bagasse: Non-isothermal thermogravimetric kinetic analysis, *Bioresource technology*, **102**, 24, pp. 11234-11238.

[58]. Slopiecka K., Bartocci P., Fantozzi F. (2012), Thermogravimetric analysis and kinetic study of poplar wood pyrolysis, *Applied Energy*, **97**, pp. 491-497.

[59]. Magdziarz A. and Wilk M. (2013), Thermogravimetric study of biomass, sewage sludge and coal combustion, *Energy Conversion and Management*, **75**, pp. 425-430.

[60]. Gani A. and Naruse I. (2007), Effect of cellulose and lignin content on pyrolysis and combustion characteristics for several types of biomass, *Renewable Energy*, **32**, 4, pp. 649-661.

[61]. Mortari DA., Avila I., dos Santos A.M., Crnkovic P.M., (2010), Study of thermal decomposition and ignition temperature of bagasse, coal and their blends. *Thermal Engineering*, **9**, 1, pp. 81-88.

[62]. Fang X., Jia L., Yin L. (2013), A weighted average global process model based on two− stage kinetic scheme for biomass combustion. *Biomass and Bioenergy*, **48**, pp. 43-50.

[63]. Aboyade A.O., Hugo T.J., Carrier M., Meyer E.L., Stahl R., Knoetze J.H., Görgens J.F. (2011), Non-isothermal kinetic analysis of the devolatilization of corn cobs and sugar cane bagasse in an inert atmosphere. *Thermochimica Acta*, **517**, 1, pp. 81-89.

[64]. Hu S., Jess A., and Xu M., Kinetic study of Chinese biomass slow pyrolysis: Comparison of different kinetic model, *Fuel*, 2007. **86**(17): p. 2778-2788.

[65]. Orfao, J., F. Antunes, and J. Figueiredo, *Pyrolysis kinetics of lignocellulosic materials—three independent reactions model*, Fuel, 1999. **78**(3): p. 349-358.

[66]. Varhegyi, G., et al. (1997), Kinetic modeling of biomass pyrolysis. *Journal of analytical and Applied Pyrolysis*, **42,** 1, pp. 73-87.

[67]. Min F.F., Zhang M.X., Chen Q.R. (2007), Non-isothermal kinetics of pyrolysis of three kinds of fresh biomass. *Journal of China University of Mining and Technology*, **17,** 1, pp. 105-111.

[68]. Guerrero M.R., Marques da Silva Paula M., Zaragoza M.M., Gutiérrez J.S., Velderrain V.G., Ortiz A.L., Collins-Martínez V. (2014), Thermogravimetric study on the pyrolysis kinetics of apple pomace as waste biomass. *International Journal of Hydrogen Energy*.

[69]. Mishra, G. and Bhaskar T. (2014), Non isothermal model free kinetics for pyrolysis of rice straw. *Bioresource technology*, **169**, pp. 614-621.

[70]. Idris S.S., Rahman N.A., Ismail K. (2012), Combustion characteristics of Malaysian oil palm biomass, sub-bituminous coal and their respective blends via thermogravimetric analysis (TGA). *Bioresource technology*, **123**, pp. 581-591.

[71]. Kuprianov V.I., Janvijitsakul K., Permchart W. (2006), Co-firing of sugar cane bagasse with rice husk in a conical fluidized-bed combustor. *Fuel*, **85**, 4, pp. 434-442.

[72]. Bernardo E.C., Egashira R., Kawasaki J. (1997), Decolorization of molasses' wastewater using activated carbon prepared from cane bagasse. *Carbon*, **35,** 9, pp. 1217-1221.

[73]. Garcìa-Pèrez M., Chaala A., Roy C. (2002), Vacuum pyrolysis of sugarcane bagasse. *Journal of Analytical and Applied Pyrolysis*, **65,** 2, pp. 111-136.

[74]. Tsai W.T., Lee M.K., Chang Y.M. (2006), Fast pyrolysis of rice straw, sugarcane bagasse and coconut shell in an induction-heating reactor. *Journal of Analytical and Applied Pyrolysis,* **76**, 1–2, pp. 230-237.

[75]. Aboyade, A.O., Carrier M., Meyer E.L., Knoetze J.H., Görgens J.F. (2012), Model fitting kinetic analysis and characterisation of the devolatilization of coal blends with corn and sugarcane residues. *Thermochimica Acta*, **530**, 0, pp. 95-106.

[76]. Phichai K., Pragrobpondee P., Khumpart T., Hirunpraditkoon S. (2013), Prediction Heating Values of Lignocellulosics from Biomass Characteristics, *International Journal of Chemical, Nuclear, Metallurgical and Materials Engineerin,* **7**, 7, pp. 214-217

[77]. Pattiya A. and Suttibak S. (2012), Production of bio-oil via fast pyrolysis of agricultural residues from cassava plantations in a fluidised-bed reactor with a hot vapour filtration unit. *Journal of Analytical and Applied Pyrolysis*, **95**, pp. 227-235.

[78]. Pattiya A., Titiloye J.O., Bridgwater A.V. (2009), Fast Pyrolysis of Agricultural Residues from Cassava Plantation for Bio-oil Production. *Carbon*, **51**, pp. 51-59.

[79]. Sirijanusorn S., Sriprateep K., Pattiya A. (2013), Pyrolysis of cassava rhizome in a counter-rotating twin screw reactor unit. *Bioresource Technology*, **139,** 0, pp. 343-348.

[80]. Liu Z., Quek A., Kent Hoekman S., Balasubramanian R. (2013), Production of solid biochar fuel from waste biomass by hydrothermal carbonization. *Fuel*, **103,** 0, pp. 943-949.

[81]. Srihirun T., Chayasakulviwat P., *Development of Coconut Shell Briquetted Charcoal: Apparatus and Combustion Characterization,"*Department of Chemical Engineering. King Mongkut's University of Technology North Bangkok: Thailand.

[82]. Garivait, S., Chaiyo U., Patumsawad S., Deakhuntod J. (2006), Physical and chemical properties of Thai biomass fuels from agricultural residues, *the second international conference on "Sustainable Energy and Environment*.

[83]. Conesa J.A., Urueña A., Díez D. (2014), Corn stover thermal decomposition in pyrolytic and oxidant atmosphere. *Journal of Analytical and Applied Pyrolysis*, **106,** 0, pp. 132-137.

[84]. Sulaiman F. and Abdullah N. (2011), Optimum conditions for maximising pyrolysis liquids of oil palm empty fruit bunches, *Energy*, **36,** 5, pp. 2352-2359.

[85]. Guerrero, M.R., Marques da Silva Paula M., Zaragoza M.M., Gutiérre J.S., Velderrain V.G., Ortiz A.L., Collins-Martínez V. (2005), Pyrolysis of eucalyptus at different heating rates: studies of char characterization and oxidative reactivity. *Journal of analytical and applied pyrolysis*, **74,** 1, pp. 307-314.

[86]. Pidtasang B., Udomsap P., Sukkasi S., Chollacoop N., Pattiya. (2013), Influence of alcohol addition on properties of bio-oil produced from fast pyrolysis of eucalyptus bark in a free-fall reactor. *Journal of Industrial and Engineering Chemistry*, **19,** 6, pp. 1851-1857.

[87]. Kongsuwan A., Patnukao P., Pavasant P. (2009), Binary component sorption of Cu(II) and Pb(II) with activated carbon from Eucalyptus camaldulensis Dehn bark. *Journal of Industrial and Engineering Chemistry*, **15,** 4, pp. 465-470.

[88]. Chakritthakul S. and Kuprianov V.I. (2011), Co-firing of eucalyptus bark and rubberwood sawdust in a swirling fluidized-bed combustor using an axial flow swirler. *Bioresource Technology*, **102,** 17, pp. 8268-8278.

[89]. Almeida G., Brito J.O., Perré P. (2010), Alterations in energy properties of eucalyptus wood and bark subjected to torrefaction: The potential of mass loss as a synthetic indicator. *Bioresource Technology*, **101,** 24, pp. 9778-9784.

[90]. Wongsiriamnuay T. and Tippayawong N. (2010), Non-isothermal pyrolysis characteristics of giant sensitive plants using thermogravimetric analysis. *Bioresource Technology*, **101,** 14, pp. 5638-5644.

[91]. Lee M.K., Tsai W.T., Tsai Y.L., Lin S.H. (2010), Pyrolysis of napier grass in an induction-heating reactor. *Journal of Analytical and Applied Pyrolysis*, **88,** 2, pp. 110-116.

[92]. Khan Z., Yusup S., Ahmad M.M., Rashidi N.A. (2014), Integrated catalytic adsorption (ICA) steam gasification system for enhanced hydrogen production using palm kernel shell. *International Journal of Hydrogen Energy*, **39**, 7, pp. 3286-3293.

[93]. Kim S.-J.,. Jung S.-H, Kim J.-S. (2010), Fast pyrolysis of palm kernel shells: Influence of operation parameters on the bio-oil yield and the yield of phenol and phenolic compounds, *Bioresource Technology*, **101**, 23, pp. 9294-9300.

[94]. Daud, W.M.A.W., Ali W.S.W., Sulaiman M.Z. (2000), The effects of carbonization temperature on pore development in palm-shell-based activated carbon, *Carbon*, **38**, 14, pp. 1925-1932.

[95]. Hussain, A., Ani F.N., Darus A.N., Ahmed Z. (2006), Thermogravimetric and thermochemical studies of Malaysian oil palm shell waste. *Jurnal Teknologi A*, 45A, pp. 43-53.

[96]. Abnisa, F., Daud W.M.A.W., Husin W.M.W., Sahu J.N. (2011), Utilization possibilities of palm shell as a source of biomass energy in Malaysia by producing bio-oil in pyrolysis process. *Biomass and Bioenergy*, **35,** 5, pp. 1863-1872.

[97]. Haykiri-Acma, H., Yaman S., and Kucukbayrak S. (2013), Co-combustion of low rank coal/waste biomass blends using dry air or oxygen. *Applied thermal engineering*, **50**, 1, pp. 251-259.

[98]. Kaewluan S. and Pipatmanomai S. (2011), Gasification of high moisture rubber woodchip with rubber waste in a bubbling fluidized bed. *Fuel Processing Technology*, **92,** 3, pp. 671-677.

[99]. Ghani, W.A.W.A.K., Mohd A., da Silva G., Bachmann R.T., Taufiq-Yap Y.H., Rashid U., Al-Muhtaseb A.H. (2013), Biochar production from waste rubber-wood-

sawdust and its potential use in C sequestration: Chemical and physical characterization, *Industrial Crops and Products*, **44**, 0, pp. 18-24.

[100]. Ikeda M., Makino H., Morinaga H., Higashiyama K., Kozai Y. (2003), Emission characteristics of NO_x and unburned carbon in fly ash during combustion of blends of bituminous/sub-bituminous coals. *Fuel*,. **82**, 15–17, pp. 1851-1857.

[101]. Suksankraisorn K., Patumsawad S., and Fungtammasan B. (2010), Co-firing of Thai lignite and municipal solid waste (MSW) in a fluidised bed: Effect of MSW moisture content. *Applied Thermal Engineering*, **30**, 17–18, pp. 2693-2697.

[102]. Sonobe T., Worasuwannarak N., and Pipatmanomai S. (2008), Synergies in co-pyrolysis of Thai lignite and corncob. *Fuel Processing Technology*, **89,** 12, pp. 1371-1378.

[103]. Sun R. and Tomkinson J. (2000), Essential guides for isolation/purification of polysaccharides. *Encylopaedia Sep. Sci*, **6**, pp. 4568-4574.

[104]. Sangnark A. and Noomhorm A. (2003), Effect of particle sizes on functional properties of dietary fibre prepared from sugarcane bagasse. *Food Chemistry*, **80**, 2, pp. 221-229.

[105]. Hon, D.N.-S. (1995), *Chemical modification of lignocellulosic materials*, CRC Press.

[106]. Haghighi Mood S., Hossein Golfeshan A., Tabatabaei M., Salehi G.J., Najafi G.H., Gholami M., Ardjmand M. (2013), Lignocellulosic biomass to bioethanol, a comprehensive review with a focus on pretreatment. *Renewable and Sustainable Energy Reviews*, **27**, pp. 77-93.

[107]. Menon V. and Rao M. (2012), Trends in bioconversion of lignocellulose: Biofuels, platform chemicals & biorefinery concept, *Progress in Energy and Combustion Science*, **38**, 4, pp. 522-550.

[108]. Pattiya, A., Titiloye J.O., Bridgwater A.V. (2010), Evaluation of catalytic pyrolysis of cassava rhizome by principal component analysis. *Fuel*, **89,** 1, pp. 244-253.

[109]. Panyakaew S. and Fotios S. (2011), New thermal insulation boards made from coconut husk and bagasse. *Energy and Buildings*, **43,** 7, pp. 1732-1739.

[110]. Aboyade, A.O., Görgens J.F., Carrier M., Meyer E.L., Knoetze J.H. (2013), Thermogravimetric study of the pyrolysis characteristics and kinetics of coal blends with corn and sugarcane residues. *Fuel Processing Technology*, **106**, 0, pp. 310-320.

[111]. Palamae, S., Palachum W., Chisti Y., Choorit. (2014), Retention of hemicellulose during delignification of oil palm empty fruit bunch (EFB) fiber with peracetic acid and alkaline peroxide. *Biomass and Bioenergy*, **66,** 0, pp. 240-248.

[112]. Park Y.C. and Kim J.S. (2012), Comparison of various alkaline pretreatment methods of lignocellulosic biomass. *Energy*, **47**, 1, pp. 31-35.

[113]. Parajó, J.C., Garrote G., Cruz J. M., Dominguez H. (2004), Production of xylooligosaccharides by autohydrolysis of lignocellulosic materials. *Trends in Food Science & Technology*,. **15**, 3–4, pp. 115-120.

[114]. Wannapeera J., Fungtammasan B., and Worasuwannarak N. (2011), Effects of temperature and holding time during torrefaction on the pyrolysis behaviors of woody biomass. *Journal of Analytical and Applied Pyrolysis*, **92**, 1, pp. 99-105.

[115]. Reddy, K.O., Maheswari C.U., Shukla M., Rajulu A.V. (2012), Chemical composition and structural characterization of Napier grass fibers. *Materials Letters*, **67**, 1, pp. 35-38.

[116]. Jin, S. and Chen H. (2007), Near-infrared analysis of the chemical composition of rice straw. *Industrial Crops and Products*, **26,** 2, pp. 207-211.

[117]. Williams P.T. and Nugranad N. (2000), Comparison of products from the pyrolysis and catalytic pyrolysis of rice husks. *Energy*, **25**, 6, pp. 493-513.

[118]. Yang, H.S., Wolcott M.P., Kim H.S., Kim S., Kim H.J. (2007), Effect of different compatibilizing agents on the mechanical properties of lignocellulosic material filled polyethylene bio-composites. *Composite Structures*, **79,** 3, pp. 369-375.

[119]. Chin, K.L., H'ng P.S., Wong L. J., Tey B.T., Paridah M. T. (2011), Production of glucose from oil palm trunk and sawdust of rubberwood and mixed hardwood. *Applied Energy*, **88**, 11, pp. 4222-4228.

[120]. Vamvuka D. and Kakaras E. (2011), Ash properties and environmental impact of various biomass and coal fuels and their blends. *Fuel Processing Technology*, **92**, 3, pp. 570-581.

[121]. Chaivatamaset P., Sricharoon P., Tia S. (2011), Bed agglomeration characteristics of palm shell and corncob combustion in fluidized bed. *Applied Thermal Engineering*, **31**, 14, pp. 2916-2927.

[122]. Elizabeth O.C. (2013), Strength properties of coconut fiber ash concrete. *Journal of Research in Architecture and Civil Engineering*, **1,** 1, pp. 1-4.

[123]. Mohammed, M.A.A., Salmiaton A., Wan Azlina W., Mohamad Amran M.S. (2012), Gasification of oil palm empty fruit bunches: a characterization and kinetic study, *Bioresource technology*, **110**, pp. 628-636.

[124]. Thy P., Jenkins B. M., Grundvig S., Shiraki R., Lesher C.E., (2006), High temperature elemental losses and mineralogical changes in common biomass ashes. *Fuel*, **85**, 5–6, pp. 783-795.

[125]. Vassilev S.V., Baxter D., Vassileva C.G. (2014), An overview of the behaviour of biomass during combustion: Part II. Ash fusion and ash formation mechanisms of biomass types, *Fuel*, **117**, pp. 152-183.

[126]. Pipatmanomai, S., Fungtammasan B., Bhattacharya S. (2009), Characteristics and composition of lignites and boiler ashes and their relation to slagging: The case of Mae Moh PCC boilers. *Fuel*, **88**, 1, pp. 116-123.

[127]. Luan, C., You C., Zhang D. (2014), Composition and sintering characteristics of ashes from co-firing of coal and biomass in a laboratory-scale drop tube furnace, *Energy*, **69**, pp. 562-570.

APPENDIX A
BIOMASS PRPERTIES

A. 1 Proximate and ultimate analysis of biomass

Type	Proximate analysis (%db.)			Ultimate analysis (%d.a.f.)						HHV	Local	Ref
	Volatile matter	Fix Carbon	Ash	C	H	O	N	S	Cl	(MJ/kg)		
Acacia mangium	88.47	11.24	0.29	42.93	6.17	50.05	0.26	<0.1	-	17.8	Thailand	This work
Bagasse	86.32	11.89	1.79	44.61	6.1	49.05	0.24	<0.1	-	17.9	Thaiand	This work
	73.63	22.17	4.2	42.64	6.62	50.48	0.19	0.07	-	a	Thailand	[71]
	72.22	25.85	1.93	-	-	-	-	-	-	-	Thailand	[72]
	82.1	16.3	1.6	49.6	6	43.8	0.5	<0.1	-	-	Florida	[73]
	-	-	5.17	58.14	6.05	34.57	0.69	0.19	0.36	18.61	Taiwan	[74]
	82.25	7.72	10.03	48.05	6.35	44.93	0.33	0.33	-	16.6	South African	[75]
Bamboo	76.52	16.32	2.29	47.97	5.71	45.87	0.45	<0.1	-	19.61	Thailand	This work
Bamboo leaf	71.67	8.31	20.02	49.78	7.1	39.16	4.08	-	-	17.76	Thailand	[76]
Cassava rhizome	81.5	14.9	3.6	51.4	7.3	40.2	1	<0.1	-	20.3	Thailand	[77]
	78.07	18.26	4.02	51.59	6.69	40.45	1.27	<0.1	-	23.67	Thailand	[78]
	81.9	10.7	7.3	53.4	7.6	38	1.1	<0.1		21.7	Thailand	[79]
Cassava stalk	81.2	13.8	5.2	55.8	8.1	34.7	1.3	<0.1	-	21.5	Thailand	[77]
	79.9	14.09	6.01	51.12	6.87	41.34	0.67	< 0.1	-	17.58	Thailand	[78]
Coconut husk	68.32	26.35	5.33	51.3	5.84	42.42	0.44	<0.1	-	19.85	Thailand	This work
	79.23	17.85	2.92	47.72	3.85	46.93	1.5	-	-	19.08	Thailand	[76]
	80.9	11	8.1	47.75	5.61	45.51	0.9	0.23		18.4	Singapore	[80]
Coconut leaf	80.75	12.92	6.33	51.13	6.61	40.49	1.77	-	-	20.83	Thailand	[76]
Coconut shell	70.72	21.22	0.9	48.53	7.75	44.08	0.56	-	-	19.42	Thailand	[81]
	-	-	3.81	63.45	6.73	28.27	0.43	0.17	0.95	22.83	Taiwan	[74]
Corn cob	84.38	15.16	0.46	46.58	6.3	46.65	0.47	<0.1	-	18.23	Thailand	This work
	88.25	9.51	2.23	44.76	4.78	49.26	1.2	-	-	18.76	Thailand	[76]
	76.77	17.59	5.73	46.89	6.15	46.14	1.38	<0.01	-	14.36	Thailand	[82]
	82.95	15.45	1.6	46.44	6.1	46.95	0.2	0.33	-	18	South African	[75]
Corn stover	79.1	12.8	8.1	44.6	6	48.07	0.73	0.1	0.5	18.27	Spain	[83]
	63.83	11.67	24.5	49.9	7.1	42.1	0.9	0.3	-	13.2	South Africa	[75]
Empty fruit bunch	85.79	11.31	2.9	52.73	7.2	39.42	0.65	<0.1	-	19.15	Thailand	This work
	83.86	10.78	5.36	49.07	6.48	38.29	0.7	<0.10	-	19.35	Malaysia	[84]
Eucalyptus wood	83.47	15.41	1.12	51.67	6.43	41.64	0.24	<0.1	-	20.12	Thailand	This work
	82.6	16.4	1	48.7	6.2	44.8	0.3	-		18.6	Spain	[85]

A. 1 Proximate and ultimate analysis of biomass (cont')

Type	Proximate analysis (%db.)			Ultimate analysis (%d.a.f.)						HHV	Local	Ref
	Volatile matter	Fix Carbon	Ash	C	H	O	N	S	Cl	(MJ/kg)		
Eucalyptus bark	76.1	19.7	4.2	38.7	4.5	54.9	0.3	<1.6	-	15.7	Thailand	[86]
	83.85	14.63	1.52	41.36	4.67	-	-	-	-	-	Thailand	[87]
	79.05	12.57	8.38	53.63	6.03	39.88	0.42	0.04	-	19.38	Thailand	[88]
	81.6	12.2	6.2	-	-	-	-	-	-	17.1	Brazil	[89]
Eucalyptus leaf	79.2	10.3	10.5	46.96	6.22	44.82	1.23	0.77	-	18.9	Singapore	[80]
Leucaena leucocephala	84.62	14.98	0.4	47.63	5.86	46.09	0.42	<0.1	-	21.22	Thailand	This work
Melaleuca alternifolia	84.99	13.54	1.47	51.59	6.45	41.67	0.28	<0.1	-	20.84	Thailand	This work
Mimosa	72.23	23.98	3.76	43.9	6	48.7	1.4	-	-	17.5	Thailand	[90]
Napier grass	82.2	12.34	5.46	46.25	5.94	44.75	3.06	<0.1	-	17.8	Thailand	This work
	80.14	9.17	10.69	42.4	5.96	45.32	1.71	0.09	0.24	-	Taiwan	[91]
Narrow leaf cattail	79.19	10.39	10.42	44.27	5.78	48.91	1.04	-	-	16.27	Thailand	[76]
Palm shell	80.92	14.67	4.31	49.74	5.68	43.36	1.02	0.27	-	18.46	Malaysia	[92]
	91.06	1.55	7.4	44.56	5.22	49.77	0.4	0.05	-	15.6	Malaysia	[93]
	78.74	20.32	1.2	50.1	6.85	41.15	1.9	-	-	-	Malaysia	[94]
	74.2	23.38	2.33	48.64	6.33	44.31	0.72	-	-	19.1	Malaysia	[95]
	75.51	22.14	2.36	49.74	5.32	44.86	0.08	0.16	-	-	Malaysia	[96]
Rice straw	72.79	15.62	11.59	46.56	6	46.67	0.77	<0.1	-	15.7	Thailand	This work
	63.61	6.88	29.51	49.38	6.25	42.66	1.72	-	-	15.07	Thailand	[76]
	62.86	11.89	25.24	59.39	6.69	41.42	0.8	0.13	-	11.54	Thailand	[82]
	-	-	11.04	50.93	6.04	41.61	0.83	0.23	0.36	16.35	Taiwan	[74]
Rice husk	66.2	10	23.8	44.8	6.3	47.9	0.9	0.1	-	13.9	Turkey	[97]
	58	18.01	12.99	44.99	6.39	48.15	0.42	0.05	-	15.57	Thailand	[71]
	65.24	14.29	20.47	40.69	5.06	53.75	0.4	0.1	-	13.23	Thailand	[82]
	59.55	19.43	21.02	38.2–55.8	0.2–0.31	29.9–31.7	1.7–1.9	0.07–0.12	-	12.12–19.0	Malaysia	[95]
Rubber wood	88.9	10	1.1	46.4	5.7	47.7	0.2	-	-	17.1	Thailand	[98]
	65.84	28.05	6.1	53.25	6.5	38.15	2.05	0.05	-	19.88	Thailand	[88]
	51.39	14.29	22.67	53.4	6.7	36.8	3.1	0	-	18.3	Malaysia	[99]
Bituminous	26.6	58	15.4	82.23	5.67	9.69	1.89	0.54	-	28.2	Australia	[100]
Thai lignite	42.78	41.11	16.11	58.41	4.65	30.16	1.67	5.13	-	23.72	Thailand	[101]
	49.1	32.6	18.3	58.7	5	33.4	2	0.9	-	-	Thailand	[102]

A. 2 Chemical structure of biomass

Type	Chemical structure (% dry basis) (d.a.f. a)					Ref
	Lignin	Hemi-Cellulose	Cellulose	Extractive	Ash	
Bagasse	19.4	28.7	39.2	1.6	5.1	[103]
	18.65	26.68	45.25	-	-	[104]
	20.76	-	42.41	-	1.6	[73]
	20.09	21.34	39.64	8.7	10.3	[75]
	20a	30a	40a	10a	-	[105]
	11.4	31.1	43.1	-	-	[106]
Bamboo	23	18–20	49–50	-	-	[107]
Cassava rhizome	20.84	38.1	26.68	10.36	4.03	[108]
Coconut husk	36.73	-	51.12	-	-	[109]
	43-49a	10-20a	32-43a	4.5a	-	[105]
Corn cob	14.6	31.8	43.2	3.9	2.2	[103]
	16.43	37.49	35.33	9.35	1.6	[75]
	15a	35a	45a	5a	-	[105]
	18.8	31.3	34.4	15.5	1.3	[11]
	6.7–13.9	39.8	32.3–45.6	-	-	[107]
	6.1	31.9	33.7	-	-	[106]
Corn stover	17.4	25.8	38.3	-	-	[106]
	35a	25a	35a	5a	-	[105]
	1.0–19.1	20.7–24.6	35.1–39.5	-	-	[107]
	14.81	19.75	25.05	14.15	26.32	[110]
Empty fruit bunch	13-37	17-33	43-65	-	-	[111]
	18.1	22.1	59.7	0.1	5.36	[84]
Eucalyptus	30.10a	18.70a	41.80a	-	-	[112]
	22.9	16.6	46.6	13.9	0.2	[113]
	29	11–18	45–51	-	-	[107]
Leucaena leucoce	27.1a	31.8a	33.10a	8.00a	-	[114]
Napier grass	20.60a	33.67a	45.66a	-	-	[115]
	26.72	-	-	6.69	9.68	[91]
Mimosa	32.64	-	-	-	3.7	[90]
Palm shell	42.21	22.06	30.6	9.89	7.4	[93]
	44	21.6	27.7	-	2.36	[96]
Rice straw	12.3	27.7	36.5	3.8	13.3	[103]
	7.2–12.8	19.8–31.6	30.3–38.2	-	7.8–15.(	[116]
	17–19	23–25.9	29.2–34.7	-	-	[107]
Rice husk	19.2	29.3	34.4	-	17.1	[117]
	20.6	-	-	6.5	13.2	[118]
	21.3	15.6	36.7	-	14.3	[113]
	15.4–20	11.96–29.3	28.7–35.6	-	-	[107]
Rubber wood	27.6	-	55.6	-	1.98	[119]

A. 3 Element analysis of biomass

Type	% Ash (db.)	% Cl (db.)	HHV (MJ/kg)	Element composition (% Ash oxide)									Ref
				SiO2	Al2O3	TiO2	Fe2O3	CaO	MgO	Na2O	K2O	P2O5	
Bagasse	2.44	0.03	19.4	46.61	17.69	2.63	14.14	4.47	3.33	0.79	4.15	2.72	[12]
	-	-	-	54	15.3	3.5	14.8	1.9	2.2	0.9	3.5	-	[120]
Bamboo whole	0.9	0.08	-	9.92	0.67	0.08	0.67	4.46	6.57	0.44	53.38	20.33	[8]
Corn cob	2.1	0.06	17.6	36.6	0.56	-	5.08	0.91	9.23	0.23	33.08	12.41	[121]
Corn straw	7.7	-	19	49.95	5.06	0.29	2.53	14.3	4.49	0.16	18.53	2.42	[8]
Coconut husk	-	-	-	14.34	35.61	-	0.18	33.27	19.86	0	1.03	-	[122]
Coconut shell	3.2	-	-	66.75	8.48	0.01	6.16	2.41	1.54	4.62	8.48	1.54	[8]
Empty Fruit Bunch	3.63	-	17.2	10.83	1.22	-	3.6	12.5	8.75	1.54	53.73	1.84	[123]
Eucalyptus	4.3	-	-	41	-	-	-	18	4.2	1.9	8.7	-	[97]
	8.1	-	-	41	-	-	-	22	2.9	1.2	4.7	-	[97]
Eucalyptus bark	13.64	-	18.47	10.04	3.1	0.12	1.12	57.74	10.91	1.86	9.29	2.35	[8]
Rice straw	18.67	0.58	15.15	74.67	1.04	0.09	0.85	3.01	1.75	0.96	12.3	1.41	[12]
	22.1	0.648	-	75.38	0.09	0.01	0.1	1.6	1.64	0.14	11.95	0.61	[124]
	13.1	-	-	51	-	-	-	8.9	3.5	2.8	16	-	[97]
Rice husk	18	-	-	89.86	1.04	0.02	0.41	1.4	0.49	0.23	4.16	0.6	[125]
	18	-	-	94.48	0.21	0.02	0.22	0.97	0.19	0.16	2.29	0.54	[8]
Thai Lignite	32.3	-	-	31.6	7.5	0.3	14.7	19	2.6	1.1	1.6	0.2	[126]
Bituminous	8.62	0.08	28.99	48.08	36.41	1.97	6.57	4.01	1.22	0.65	0.45	0.11	[127]
	15.2	-	28.2	48–68	22–35	1–2.2	0.8–10	0.4–6	0.3–1.8	0.1–1.7	0.3–2.8	-	[120]